universität wien

MASTERARBEIT / MASTER'S THESIS

Titel der Masterarbeit / Title of the Master's Thesis

„Morphological assessment of modern human upper and lower first molars“

verfasst von / submitted by

Vanda Halász B.Sc.

angestrebter akademischer Grad / in partial fulfilment of the requirements for the degree of

Master of Science (MSc)

Wien, 2019 / Vienna 2019

Studienkennzahl lt. Studienblatt / degree programme code as it appears on the student record sheet:	UA 066 827
Studienrichtung lt. Studienblatt / degree programme as it appears on the student record sheet:	Masterstudium Anthropologie
Betreut von / Supervisor:	Univ.-Prof. Dr. Gerhard Weber
Mitbetreut von / Co-Supervisor:	Cinzia Fornai, PhD

Contents

Abstract

First permanent molars are the most well studied tooth types of the human dentition. Most of the previous dental studies used the outer enamel surface (OES) and traditional, linear measurements to capture their morphological differences. Such kind of investigations can be limited by various factors, including the abrasion of the occlusal surface or partial destruction of the enamel layer. The contact area between the dentin and the enamel is called the enamel-dentin-junction (EDJ). The EDJ is defined in an early development stage and serves as a blueprint of the OES. Owing to its anatomically deeper location, the EDJ is less affected by damage and wear than the OES. Although many studies have focused on molars, there has been no previous comprehensive study on dental crown morphological variability according to geographical origin. The main purpose of this work is to provide a morphological description of upper and lower molars across different populations, to assess the degree of covariance between upper first molars (uM1) and lower first molars (lM1) and to see if there exists an influence of size on shape variation. To this end, two different approaches were compared: Geometric Morphometrics (GM) and the analysis of the discrete traits.

For this study the EDJ of 80 teeth (45 uM1s and 35 lM1s) were examined. The sample consisted of groups differing in terms of geographical origin and subsistence strategy, namely: Avars, Bedouins, Europeans, South Americans, South-East Asians and Sub-Saharan Africans. The teeth were scanned in the Vienna µCT Lab, Vienna, Austria. Afterwards, the sample was examined through statistical methods and techniques proper to Virtual Anthropology, which combined the manipulation of 3D image datasets to landmarks- and semilandmarks. The use of virtual image techniques allowed us to investigate the inner dental structures without destructing valuable human remains. For the GM approach, landmarks and curve semi landmarks were placed on the 3D surface models of the EDJ. The spatial coordinates were later converted into Procrustes shape coordinates by means of General Procrustes Analysis. Multivariate statistical methods were used to assess the shape variance, covariance, size and allometry. For the descriptive analysis, we examined 10 qualitative traits of the molars (4 for uM1s and 6 for lM1s) based on the Arizona State University Dental System (ASUDAS).

All results showed a wide overlap between the sample groups. Our interpretation is that variation in dental morphology is not driven by genetic drift nor is it the result of an adaptation to diet. Modern human molars show stronger shape variation in their distal aspects than in their mesial regions. According to the findings of this study a clear distinction among anatomically modern human populations based only on dental gross morphology or the manifestation of discrete traits is not possible.

Zusammenfassung

Erste Dauermolaren sind die bestuntersuchten Zähne des menschlichen Gebisses. Eine Großzahl der wissenschaftlichen Studien beschäftigt sich mit permanenten Backenzähnen, jedoch wurde bis dato noch keine vergleichende Studie über die Kronenmorphologie auf Populations- oder auf einer geografischen Ebene durchgeführt. Unser Ziel ist es, eine morphologische Beschreibung der oberen und unteren ersten Molaren (uM1 + lM1) vorzulegen, ihre mögliche Co-Variation abzubilden und den Einfluss von Größe in Bezug auf die Form zu untersuchen. In dieser Studie wurden zwei Herangehensweisen angewendet: Geometric Morphometrics (GM) und die Analyse von diskreten Zahneigenschaften. Um Unterschiede in der jeweiligen Stichprobe zu erfassen, beschrieben vorhergehende Studien die äußere Zahnoberfläche (OES) mittels traditionellen, linearen Messungen. Solche Untersuchungen werden von mehreren Faktoren limitiert, wie etwa eine abgenutzte oder eine beschädigte Zahnoberfläche. Die Form der Kontaktfläche zwischen den Materialien Zahnschmelz und Dentin – die sogenannte Schmelz-Dentin-Grenze (EDJ) – wird während der frühen Zahnentwicklung bestimmt. Aufgrund ihrer tiefen Lage wird die EDJ von solch externen Einwirkungen weniger stark beeinflusst und eignet sich deshalb hervorragend für morphologische Studien. Nicht invasive Methoden, wie µCT Scans und Methoden der virtuellen Anthropologie erlauben uns den Zugriff auf tiefergelegene Strukturen, ohne dabei das wertvolle Forschungsmaterial zu zerstören.

Für diese Studie wurden insgesamt 80 Dauermolaren (45 uM1 und 35 lM1) untersucht. Die Stichprobe umfasst Individuen verschiedener geographischer Herkunft: Afrikaner, Asiaten, Beduine, Awaren, Südamerikaner und Europäer. Alle Zähne wurden im µCT Lab der Universität Wien gescannt und mit Hilfe von virtuellen Techniken untersucht. Für den GM Ansatz wurden Landmarks und Semilandmarks entlang der 3D-Oberflächen platziert und anschließend durch multivariate Analysen ausgewertet. Der traditionelle Ansatz basiert auf der Beschreibung der qualitativen Zahnmerkmale mithilfe des Arizona State University Dental Systems (ASUDAS).

Alle Analysen zeigen eine weitgehende Überlappung der Gruppen. Unsere Interpretation besagt, dass die Variation der Zahnmorphologie nicht durch genetisches Driften oder durch Ernährungsadaptation entstanden ist. Die Varianz triff häufiger in den hinteren als in den vorderen Bereichen der Backenzähne auf. Unsere Studie bestätigt, dass eine eindeutige Zuordnung auf Basis der Form und Gestalt der ersten Molaren nicht möglich ist.

Introduction

Owing to their chemical composition, teeth are the most durable part of the human body and thus tend to be better preserved than other human remains. In fact, the enamel consists of 95% inorganic material. Teeth convey information about human biology, diet, development, and taxonomy. Therefore, they are well studied using variable approaches. The types of investigation possible on teeth are very divers and span from clinical studies (Yoshimura et al., 2008; Moynihan et al., 2009; Gaewkhiew et al., 2017), over the application of geographic databases such as GIS (Geographic information system) (Bartling and Schleyer, 2003; Pereira et al., 2010; Panda et al., 2019) or OFA (https://www.ofa.org), to approaches in the field of anthropology, where we can distinguish between genetic / biomolecular (Handt et al., 1994; Pääbo et al., 2004), isotopic (Stahl, 1968; Kodama et al., 2019; Plomp et al., 2019) and morphological studies. Based on the morphological aspect of teeth, we can differentiate between traditional, qualitative or descriptive approaches and studies using geometric morphometrics (GM) - all in 2D or 3D. Classical studies have used traditional methods examining mostly the outer aspect of the crown. This can be carried out either through classic 2D measurements (e.g.: mesiodistal and buccolingual crown diameters or crown outlines) (Moorrees and Chadha, 1962; Wood and Zuckerman, 1981; Bernal, 2007; Brook et al., 2009; Fiorin et al., 2017), or through descriptive methods such as discrete trait evaluation (Dahlberg, 1963; Turner et al., 1991; Ortiz et al., 2012; Carter et al., 2014; Martin et al., 2017). The description of dental wear (Molnar, 1971; Clement et al., 2012; Delezene et al., 2013) and the analysis of the macro- and microwear of the occlusal surface (Walker et al., 1978; Mahoney, 2006; Mahoney et al., 2016; Peterson et al., 2018) consider also the outer aspect of the dental crown. Working with the previous methods on the outer enamel surface (OES) requires a good preservation of the outermost tooth surface when wear is not the focus of the study. However, dental wear is a ubiquitous phenomenon, which increases with the individual's age. To overcome this difficulty, the morphology of the enamel-dentin junction (EDJ) can be studied instead of the OES (e.g. Martin, 1985; Schwartz et al., 1998; Bailey, 2004; Skinner et al., 2008a; Smith et al., 2012; Skinner et al., 2015; Fornai et al., 2015; Weber et al., 2016; Zanolli et al., 2018; Krenn et al., 2019). The EDJ can reveal crucial information about crown morphology, where the strong correlation between the structures detectable on the EDJ and OES were shown by numerous studies (Olejniczak et al., 2007; Skinner et al., 2008b; Bailey et al., 2011; Ortiz et al., 2012; Morita et al., 2014; Fornai et al., 2015; Martin et al., 2017).

The morphogenesis of teeth or odontogenesis is mainly regulated by the expression of specific genes and morphogenetic factors (Thesleff and Sharpe, 1997; Tucker and Sharpe, 1999). In addition to the individual's phylogenetic background, different parameters such nutrition or

pathogens can influence tooth odontogenesis (e.g. enamel hypoplasia) especially in early stages of development (Ash et al., 2003; Bei, 2009; Townsend et al., 2003). Once formed, the shape of the teeth is determined and does not change other than by mechanical or chemical events, such as wear, erosion or trauma (Deter, 2009; Forshaw, 2014). Odontogenesis starts intra-uterine and can be divided into four stages: initiation, morphogenesis, differentiation and eruption (1998). The amelogenesis, the formation of the enamel starts after the cells for the prevailing substance of the tooth (i.e., dentin) were formed in the dentinogenesis. After reaching the bell stage, the cells of the tooth start to differentiate. Along the *membrana praeformativa* (or basal lamina) the cells of the inner epithelium turn into ameloblasts and the cells on the other side of the lamina turn into odontoblasts. The odontoblasts start to move towards the centre of the papilla thereby forming dentin. Shortly after the ameloblasts become active and start enamel formation. This process generates an exact copy of the *membrana praeformativa*, which is conveyed in the adult stage as the EDJ (Hillson, 1996). Given that enamel production only happens during this stage, the EDJ serves as an exact image of the *membrana praeformativa.* The final crown configuration is product of a repetitive activation and silencing of the embryonic signalling centres or e*namel knots* (Jernvall and Thesleff, 2000; Salazar-Ciudad and Jernvall, 2002). These knots regulate the development of the inner epithelium and molecularly prohibit the formation of new, nearby knots (Jernvall and Thesleff, 2000). The primary enamel knot appears at the tip of the first dentin horn and controls the formation of the second knot. The second knot controls the formation of the third knot, and so on. This process is called the patterning cascade model and entails that molar cusp expression is determined by the connection between the timing and spacing of the enamel knots initiation and the growth period before mineralization (Jernvall, 2000; Salazar-Ciudad and Jernvall, 2002; Polly and Mock, 2018; Ortiz et al., 2018). Ortiz et al. (2018) showed that a small intercuspal distance between previously initiated enamel knots more likely results in an additional cusp on the crown periphery, while a great intercuspal distance is an indicator for additional cusps between two adjacent and early initiated cusps. Previous studies on the shape covariation between the EDJ and the OES shown a general morphological covariance, although the OES varies more owing to higher variation in enamel deposition than in dentin formation (Bailey, 2002; Morita, 2016; Morita et al., 2014; Ortiz et al., 2012; Schwartz et al., 1998; Skinner et al., 2008b, 2009).

First permanent molars erupt at the age of six and therefore remain only a short period of time in the alveolar cavity of the bone during the life time of an individual (Kondo et al., 2005; Townsend et al., 2009). Owing to stronger genetic control the shape of first molars is more stable than in second or third molars (Dahlberg, 1971; Morita, 2016; Ortiz et al., 2018). The latter develop later in ontogeny and tend to have more variation in size and shape due to the influence of sexual hormones with growing age (Gingerich, 1974).

The ancestral mammalian dental formula (3 incisors – 1 canine – 4 premolars – 3 molars) describes the original composition of the mammal dentition in one quadrant. Due to diet specialization, teeth underwent evolutionary modifications, both in morphology and number. In hominins the ancestral dental formula is 2 – 1 – 2 – 3 (Weiss and Mann, 1985). The different dental types are specialized for various functions. The main function of the incisors is cutting of food, while canines are specialized in both cutting and ripping food. Premolars have an intermediate role between ripping and grinding and the main purpose of molars is crushing and grinding food efficiently. The upper molars are composed by the trigon and the talon. The protocone (mesiolingual), the paracone (mesiobuccal) and the metacone (distobuccal) are the cusp forming the trigon, which is the evolutionary oldest part of upper molars (Fig.1). The talon is placed distolingually to the trigon. Its cusp is called hypocone and it is the evolutionary more recent addition to the main cusps (Hunter and Jernvall, 1995).

The evolution of lower molar anatomy is more complicated. The mesial part is called trigonid and is formed by the protoconid (mesiobuccal) and the metaconid (mesiolingual) (Fig. 1). Similar to the upper molars, the primordial primate trigonid exhibited a third cusp, the paraconid, placed between the two anterior cusps but it reduced during evolution. The distal part of lower molars is called talonid and was originally formed by the hypoconid (distobuccal) and the entoconid (distolingual). The hypoconulid is the latest evolutionary addition and is placed distally between the hypoconid and the entoconid.

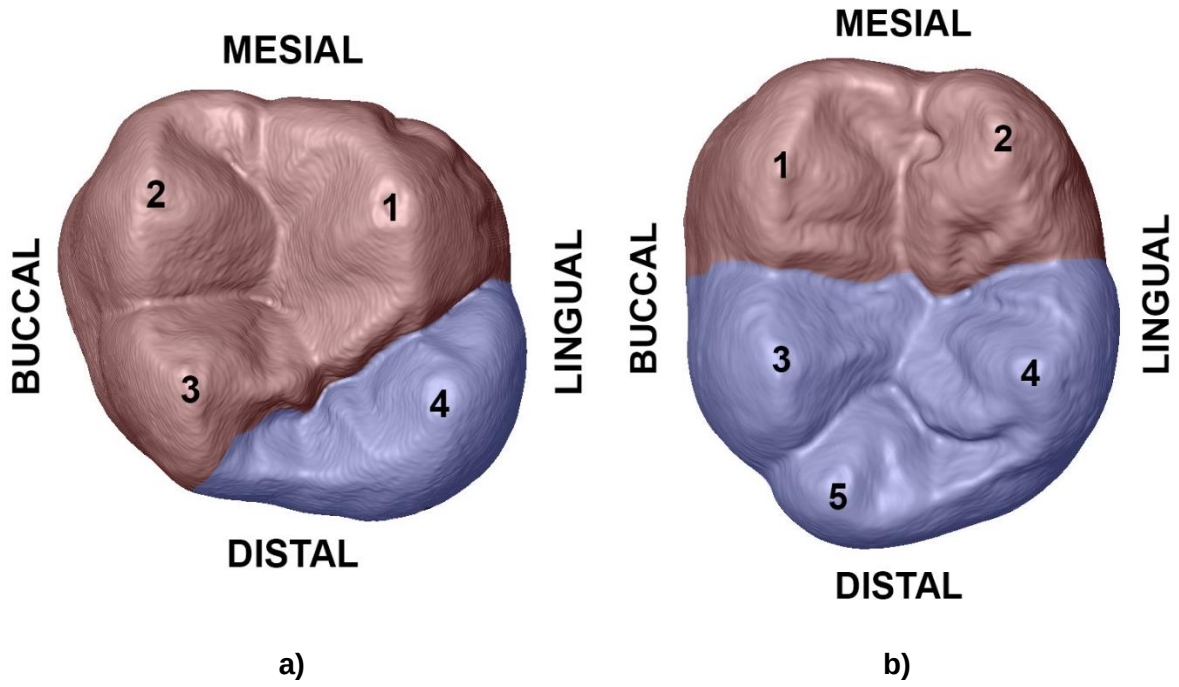

Fig. 1 – Left (mirrored) uM1 and left lM1 of individual CS654 displaying the main cusps, the trigon/id areas shadowed in red and the talon/id areas shadowed in blue.
a) uM1 – (1) protocone; (2) paracone; (3) metacone; (4) hypocone; **b)** lM1 – (1) protoconid; (2) metaconid; (3) hypoconid; (4) entoconid; (5) hypoconulid.

This study on first permanent molars is part of a series at the Department of Evolutionary Anthropology / University of Vienna that investigates the 3D morphology of human and ape teeth (Buchegger (2015) – upper premolars; Krenn (2015) – lower premolars; Teplanova (2015) – upper second molars; L. Liu (ongoing work) – upper and lower canines; P. Šimková (ongoing work) – second deciduous molars; N. Oberklammer (ongoing work) – upper premolars of apes). These projects use previously established protocols (Benazzi et al., 2012; Fornai et al., 2015; Weber et al., 2016; Hershkovitz et al., 2018), taken into consideration the morphological differences between the different tooth classes. They examine teeth combining virtual imaging and geometric morphometric techniques, which present several advantages with respect to traditional methods (Weber and Bookstein, 2011):

- inner structures are accessible (e.g. roots of in situ teeth or pulp cavity),
- in a non-destructive way;
- virtual data are permanently available;
- great range of options for virtually handling the data (which means also higher degree of safety for the original objects);
- easy data exchange, facilitating discussion of the results within the scientific community.

The first aim of the current study is to provide information about first permanent upper and lower molar morphology, and to explore the variability in terms of shape and size within modern humans. The individuals of the sample differed in terms of ethnicity, and diet. Among the sample there are hunter-gatherers, nomads and agriculturalists originating from four continents (Africa, Europe, Asia and South America). Additionally, the covariation between different crown regions and the general covariation between corresponding uM1 and lM1 were analyzed. Our intention is to provide data for further studies on permanent first molars and to contribute the research about the evolution of the genus *Homo.*

Materials

For this project, 3D image datasets from micro-CT scans of 45 upper and 35 lower first permanent molars (uM1 and lM1, respectively) from recent modern humans were virtually prepared and analyzed (Table 1 and Fig. 2). The sample is composed of individuals representing different geographical groups, i.e. Avars (n = 11), Central Europeans (n = 15), Khoisan (n = 7), Near East (n = 9), Papuans (n = 8), Central Africans (n = 8), South East Asians (n = 9), and South Americans (n = 13) (Fig. 2). For 18 individuals both upper and lower teeth could be included. Sex was known only for 38 individuals (23 males and 15 females).

The Avars, European horse-riding, nomadic people with Asian background, are represented by individuals from the burial site "Csokorgasse", Vienna, Austria and are dated to the 7th and 8th century A.D. The Middle European, South American and parts of the Central African material was made available by the Anatomical Institute of the Medical University of Vienna and the Pathological-Anatomical Museum Narrenturm in Vienna. The Near-East Bedouin molars were provided by the University of Tel Aviv (Israel). The Papuan, Khoisan and parts of the Central African teeth are part of the Rudolf Pöch collection at the Department of Evolutionary Anthropology of Vienna.

Official ethical statement of the Department of Evolutionary Anthropology, University of Vienna: *'The Papuan, Khoisan and Central African teeth were collected at the end of the 19th and beginning of the 20th century and are part of the Rudolf Pöch collection. The Department of Evolutionary Anthropology of the University of Vienna is fully aware of the highly problematic acquisition circumstances regarding Indigenous remains procured by the Austrian anthropologist Rudolf Pöch (1870–1921) during his Oceania and South Africa expeditions between 1904 and 1909. These collections held by the Department of Evolutionary Anthropology have since been closed for a thorough provenance research as to contexts of colonial injustice.'*

In a first repatriation effort, Australian Indigenous remains (not used in this study) were formally returned in 2011 under the patronage of the Austrian Academy of Sciences.

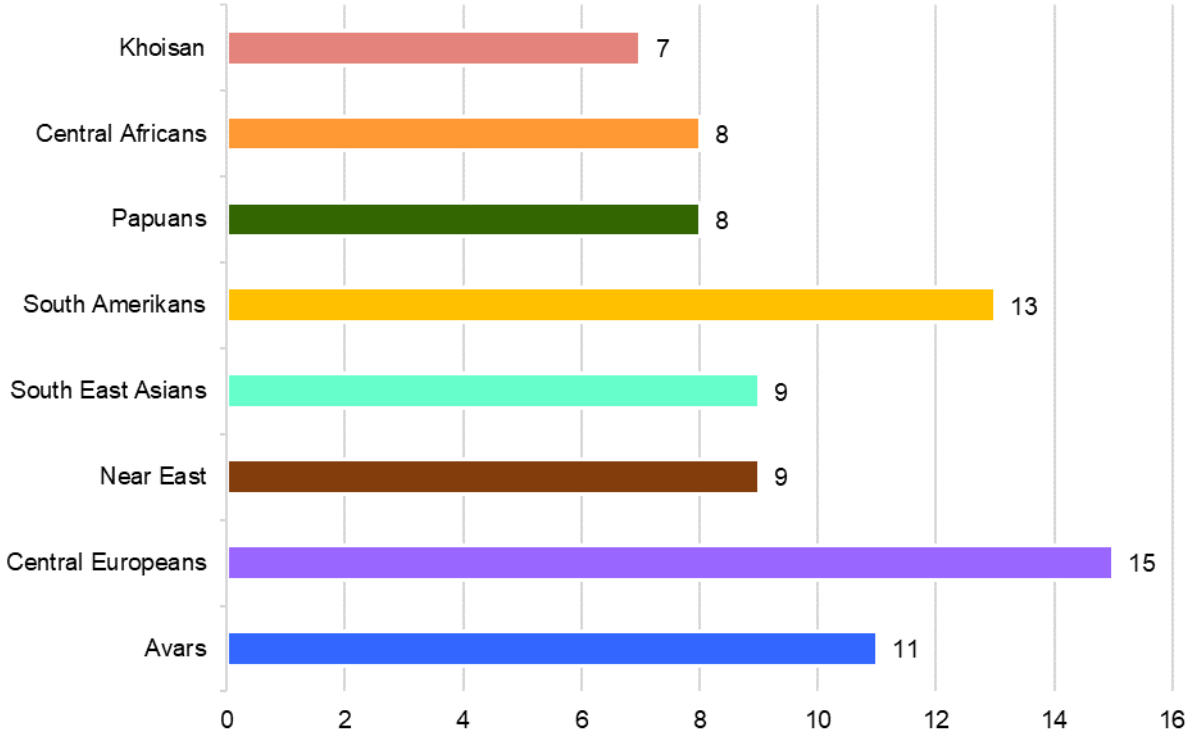

Fig. 2 – Sample composition - 80 teeth in total (45 u M1s and 35 lM1s) from different ethnical and geographical backgrounds.

The sample size of this study was limited by the fact that the uM1 and lM1 erupt early in the lifespan of an individual (Ash et al., 2003), and thus, dental collection show mostly moderate to heavy degree of wear. Only complete teeth without dental pathologies and with a wear stage lower than four (Molnar, 1971) were included. Heavier wear - implying major loss of dentinal material, would have prevented landmark collection on the EDJ. Left teeth were preferred while gathering the sample, but if a left tooth was unusable or absent, the right M1 was selected instead and was virtually mirrored for standardization. The investigation of asymmetry was not part of this study. Since there are no hints in the literature pointing to the existence of directional asymmetry in human dentitions, the selection of prevailingly left molars should not bias the outcome of this study. More importantly, we initially aimed for a balanced sample of upper and lower teeth. However, there were more upper teeth available for this study than lower ones, because mandibles were often missing in the collections, while the crania or at least the maxillae were still preserved. From an overall amount of 78 uM1s available in the collections considered, 45 (57.7%) could be included, while 35 out of 55 lower molars (63.6%) were suitable.

Table 1 – Sample composition // U = upper M1, L = lower M1 // f = female, m = male // "+" = tip reconstruction was necessary, "-" = tip reconstruction was not necessary.

Population	Collection No.	Jaw	Age	Sex	Degree of wear (Molnar, 1971)	Tip reconstruction (U / L)
African *(including Khoisan and hybrids with Xhosa)*	S23	U+L	15-20	f	1 / 2	- / +
	S29	U	30-40	m	2	+
	S46	L	14-18	f	2	+
	S61	U	25-30	m	2	+
	S68	U	25-30	m	4	+
	S81	U+L	adult	?	2 / 2	- / -
	S85	U	adult	?	2	+
	S87	U	adult	?	2	+
	S111	L	20-30	m	2	+
	S118	L	7-8	?	1	-
	S138	U+L	adult	?	2 / 2	+ / +
	C333	U	adult	?	2	-
Avar	CS495	U+L	7-8	?	2 / 2	+ / +
	CS498	U	25-30	f	2	+
	CS502	U+L	13-15	?	2 / 3	+ / +
	CS541	U	19-30	f	3	+
	CS569	U+L	16-18	m	2 / 2	+ / +
	CS582	U	19-25	f	2	+
	CS654	U+L	3-5	?	1 / 1	- / -
European	120_074_711	U	6	m	1	-
	120_080_717	U+L	10	m	1 / 1	- / -
	120_120_997	L	7	f	2	-
	120_123_1043	U	10	m	2	-
	122_199_961	L	20	m	2	+
	122_510_1554	U+L	22	m	2 / 2	+ / +
	122_511_1555	L	adult	f	2	+
	125_011_1072	U+L	adult	m	2 / 2	+ / +
	125_213_1015	U	46	f	2	+
	125_415_1124	U	6	m	1	-
	127_622_1200	U	24	m	2	+
	300_510_578	U	11	f	2	-
Near East	BED_RCEH_036	U	juvenile	?	1	-
	BLZ_004	L	?	?	1	-
	BLZ_014	L	?	?	4	+
	BLZ_037	L	?	?	3	+
	BLZ_273	L	?	?	4	+
	BLZ_407	U	?	?	1	-
	BLZ_441	U	?	?	1	-
	BLZ_483	U	?	?	3	+
	BLZ_506	U	?	?	3	+
Papua New Guinea	CN5	U	adult	m	2	-
	CN220	U+L	mature	m	2 / 2	- / +
	CN223	U	adult	?	2	+
	CN230	L	adult	m	2	-
	CN232	U+L	adult	m	2 / 3	+ / +
	CN236	U	mature	m	2	+
South America	793	L	adult	?	4	+
	806	U+L	adult	m	2 / 2	- / +
	964	U+L	juvenile	f	2 / 2	+ / +
	1169	U	juvenile	?	2	-
	1525	L	adult	?	2	+
	2286	U	adult	f	2	+
	5443	U+L	juvenile	f	2 / 2	- / +
	5385	L	adult	?	3	+
	5389	U	infantile	?	2	-
	5758	L	adult	?	2*	+
South East Asian	1365	U+L	adult?	f	2 / 2	- / -
	1368	U+L	adult?	f	2 / 3	+ / +
	1370	U+L	adult?	f	2 / 3	+ / +
	1376	L	36	m	2	+
	1383	L	28	m	2	+
	2583	U	?	f	1	-

Methods

Geometric Morphometrics (GM)

GM is an approach for the study of shape variation using Cartesian landmark coordinates. GM entails several steps starting from data acquisition, processing, and analysis until the display of results (Weber and Bookstein, 2011). The main advantage of GM versus "traditional" methods is that all spatial relationships among landmarks are preserved and can be mapped back into physical space. This allows us to visualize results such as shape differences within and between groups (Slice, 2005). Slice (2005, page 3) defines shape as *"… geometric properties of an object, that are invariant to location, scale and orientation"*.

First of all, the biological object is represented by landmark spatial coordinates. Landmarks can be 2D or 3D points and must be identified following specific rules (Bookstein, 1997; Weber and Bookstein, 2011). Each of the collected landmarks must be selected following the rule of homology. This means they represent the morphology of topologically equivalent elements, which are in the same spatial relationship with the surrounding elements. Homology can be "primary", where the homology is based on structural and topological similarity, or "secondary" when the homology is bases on common ancestry. In GM the concept of "computed homology" also applies, where the homology is obtained by interpolations driven by the landmarks (Bookstein, 1992; Palci and Lee, 2019). This methodology makes the study of semilandmarks (namely landmarks without a clear and identifiable location) possible, by sliding them along curvatures or surfaces until the difference to the template configuration is minimized (Mitteroecker and Gunz, 2009). The position and number of landmarks also have to be consistent for all specimen within a study. Landmarks can be classified as Type I, II, III, IV, V, VI (Bookstein, 1997; Weber and Bookstein, 2011).

- **Type I** landmarks are anatomical points, where the homology is provided by biologically unique patterns or forms (e.g. juxtaposition of two tissues).
- **Type II** landmarks are points provided by geometrical and not histological criteria (e.g. extreme of a curvature). In 3D these are usually the maxima or minima of plane curvatures (e.g. deepest or highest points on a surface i.e. pits, peaks or passes).
- **Type III** landmarks are characterised locally by information from multiple curves and by symmetry (e.g. intersection of 1. ridgecurve / midcurves, 2. observed curve / and midcurve, 3. ridgecurve / observed curve).

- **Type IV** landmarks are semilandmarks on curves. Their number has to be sufficient to represent the curve and consistent through the sample (see below at Landmark configuration)
- **Type V** landmarks semilandmarks on surfaces. They represent inter-landmark surface patches.
- **Type VI** landmarks are geometrically constructed semilandmarks (for example, the midpoint between two landmarks).

A proper comparison of shapes can be achieved by registering landmark configurations through normalization methods such as the General Procrustes Analysis (GPA) (Gower, 1975). This superimposition approach consists of translation, rotation and uniform scaling until the Procrustes distances (PD) between the corresponding landmarks are minimized, where PD are the sum of squared distances between the corresponding points of two configurations. Through GPA the two components of form - shape and size - can be analyzed both separately or jointly, depending on the biological questions to address. Size often dominates the variation between or within groups (Slice, 2005). It can therefore be advantageous to exclude it from the analysis if the focus is pure shape variation. GPA consists of an iterative process in which a template individual is selected at the beginning and its configuration is used for the superimposition of the sample. The remaining individuals are fitted to this reference and the mean is computed iteratively. Thus, the landmark configuration of the initial individual is constantly replaced by the continuously recalculated mean and fitted to the new estimation until the PD reach their minimum (Gower, 1975). Most of the multivariate statistical tools assume a linear, Euclidean space, while Procrustes shape coordinates follow the rules of Kendall's space. To overcome this problem, Procrustes shape coordinates are projected into Kendall's tangent space, where the rules of Euclidean space apply. This makes it possible to apply multivariate statistics such as Principle Component Analysis (PCA). The PCA is one of the main exploratory multivariate tools used in GM studies. It is a tool for dimensional reduction that can be used for reducing a large set of probably correlated variables to a smaller set uncorrelated variables, that still contains most of the information of the original set (Rohlf and Slice, 1990). A PCA can be executed both in shape and form space. It results in a low dimensional space, which is a very useful way for visualizing and processing high-dimensional data sets (Mitteroecker and Gunz, 2009). The final visualization of the results can be carried out in different ways, using vector plots or warping based on Thin-Plate Spline. Using inter- or extrapolated deformation grid is very helpful for interpretations of the shape variance and the deformation along the coordinate axis (Slice, 2005). Thus, GM makes it possible to actually observe and describe differences, associations and variability within the sample (Slice, 2005).

GM methods permit analyzing size separately from shape. For this purpose, the natural logarithm of Centroid Size (lnCS) is calculated and is subtracted from the form, obtaining shape. Centroid size is the square root of summed squared distances of landmarks from their centroid (Slice et al., 1996). Size as represented by the lnCS can be analysed as such or can it be reintegrated into the analysis of shape for the investigation of form.

Digitization, segmentation and realignment of the crown

The teeth were scanned still *in situ* in the Vienna micro-CT Lab, Austria, with the Viscom X8060 NDT scanner using the following parameters: voxel size 21 – 60 µm, 110 – 140 kV, 280 – 410 mA, 1400 – 2000 ms, 0.75 mm copper filter (Fig. 3).

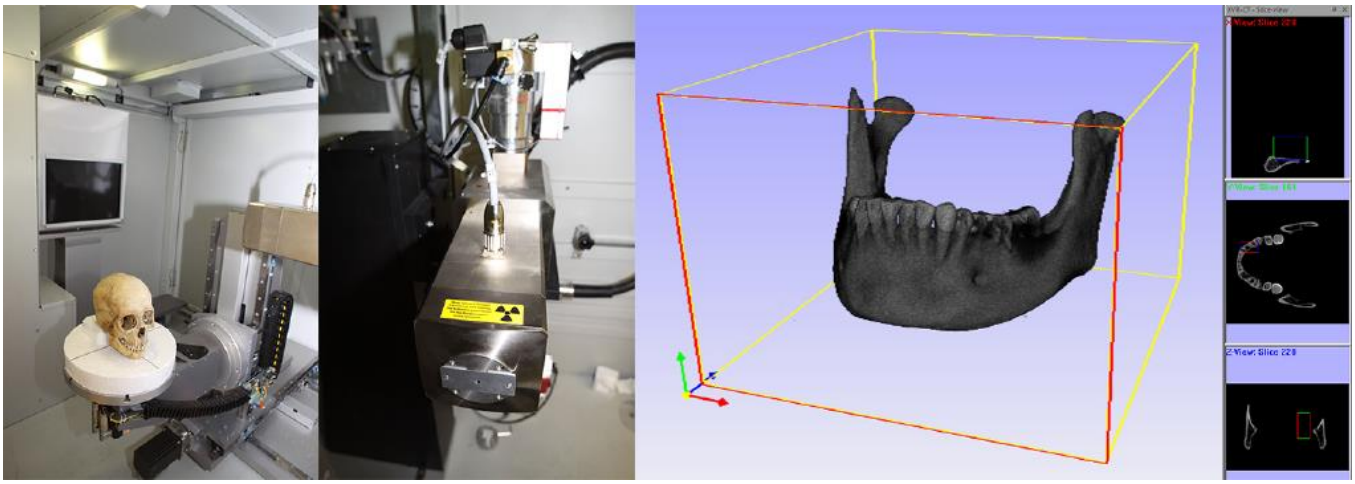

a) **b)** **c)** **d)**

Fig. 3 – a) + b) Scanning the sample material in Viscom X8060 NDT (https://www.micro-ct.at); **c)** raw data of a mandibula; **d)** range of reconstruction (Krenn, 2015).

After reconstruction of the raw images (XVR-CT software) the TIFF images were imported in Amira 6.5 (www.fei.com) to separate the dentin from the enamel and the tooth from the alveolar bone and adjacent teeth (Fig. 4a). For the segmentation the half-maximum-height protocol (Spoor et al., 1993) was followed together with manual intervention. In case of slightly worn dentin horns (namely, only circular abrasion, no parts of the ridge curve visible), the tips were reconstructed by extending the curvature of the dentin profile still present, as seen in 2D. The edges of the still present EDJ were extended until they converged. This procedure was repeated every few slices and the intermediate slices were reconstructed by interpolation in order to create a smooth reconstruction. The process was performed on all planes for the sake of accuracy. Afterwards the reconstructed area was examined as a 3D surface and the reconstructed tip was assigned to the dentin material. After segmentation, 3D models were generated and landmarks were placed tightly along the cervical line in order to align an oblique slice and create the best-fit plane of the cervical margin. Afterwards, the crowns were

separated from the rest using the best fit plane and the surface models of both EDJ and outer enamel surface (OES) were exported (Fig. 4 b-c).

For reorientation of the whole crown and the acquisition of the cervical and crown outlines, the 3D surface models were imported into the program Geomagic Design X64Bit (v2016.1.1, 3D Systems) and the protocol by Benazzi et al. (2011, 2012, 2014) was followed (Fig. 4d). The cropped surface models of the dental crowns were oriented as the cervical plane was parallel to the xy plane. The crowns were further aligned by rotating them along the z-axis. In particular, the crowns were rotated until the mesial margin of the uM1 was parallel to the y axis, and the lM1 until the mesial groove and the lingual margin of the tooth were parallel to the x axis. Afterwards, the profile of the crown and cervical region were captured by using a spline curve. For the crown outline, a polyline representing the silhouette of the oriented outer enamel surface was automatically gathered to ease the placement of the spline. The use of the curve spline made it possible to correct the crown outline in case of damaged enamel caps or interproximal wear. As a next step the cervical outline was created with the help of a second curve spline. Due to large missing parts of the enamel tooth 5758 had to be excluded from the analysis of both outlines. After the adjustments the oriented surfaces and outlines were exported for further analysis. The oriented surfaces and outlines were exported for further data collection.

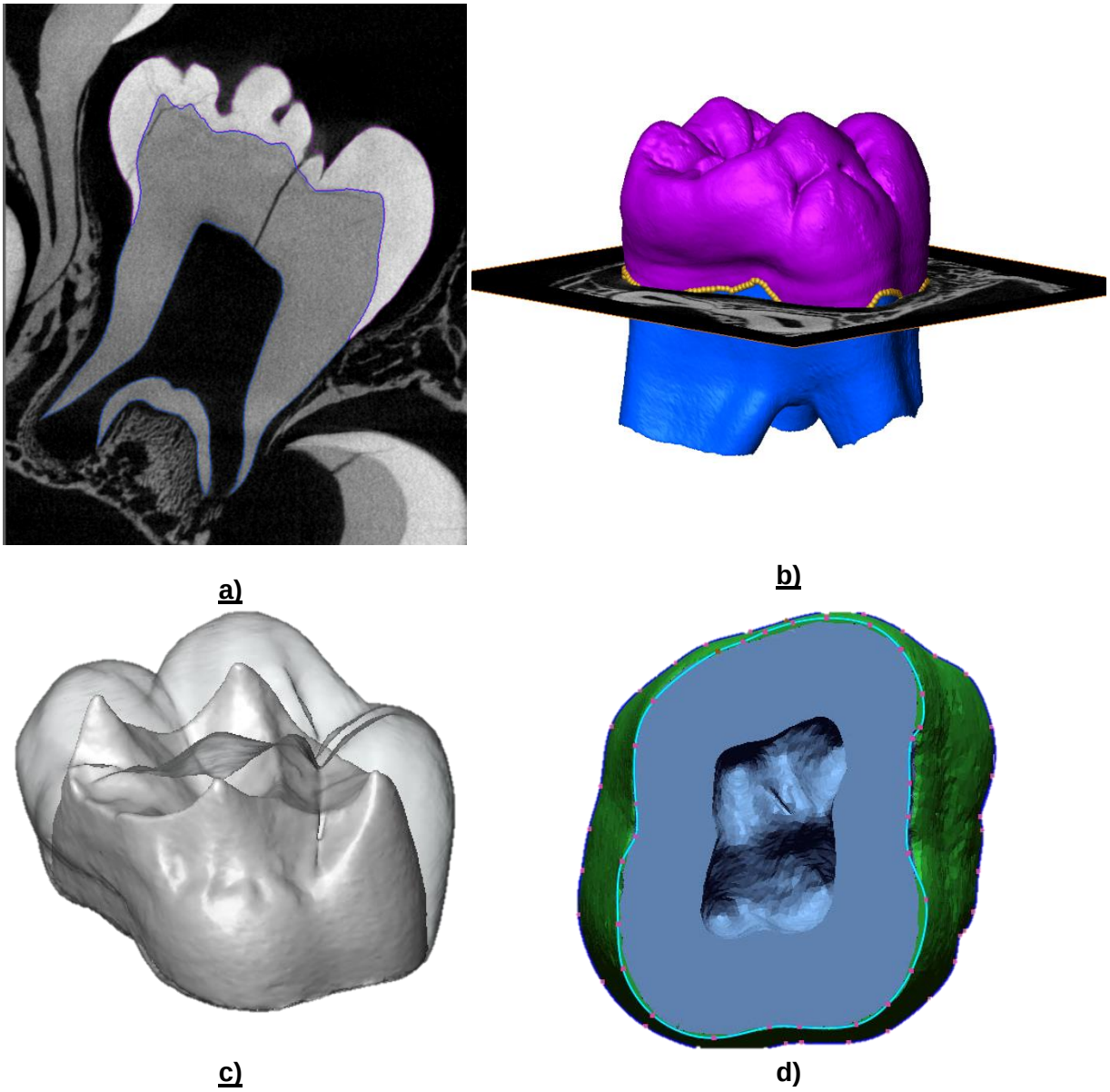

Fig. 4 – a) Showing the separation of enamel and dentin in the segmentation editor of Amira software; **b)** best fit plane of the cervical margin; **c)** cropped uM1 molar crown; **d)** reorientation of the crown and creation of the cervical and crown outlines in Geomagic software.

Landmark configurations

In this study, for each tooth four sets of landmarks (Fig. 5) and semilandmarks were collected and analyzed in Evan Toolbox 1.72 (http://www.evan-society.org):

1. Occlusal aspect of the enamel-dentin junction (EDJ)
2. crown outline
3. cervical outline
4. combined data set including EDJ and cervical outline (COM)

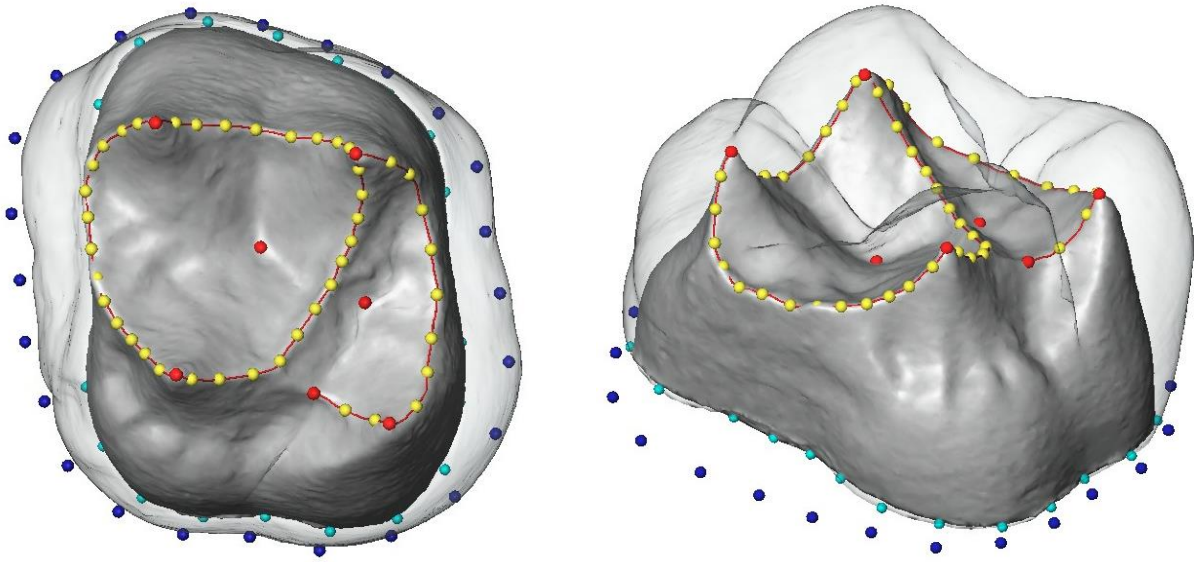

Fig. 5 – Landmarks representing the four data sets: EDJ (yellow and red), cervical outline (turquoise), crown outline (blue) and the combined data set (yellow, red and turquoise together).

Each dental feature (point 1 to 3 above) was analyzed separately. Moreover, the EDJ and cervical landmark configurations (point 4) were merged into a combined data set so as to represent the whole dentinal crown at once.

Both landmarks (red in Fig. 5) and curve semilandmarks (yellow in Fig. 5) were placed to represent the occlusal aspect of the EDJ. For the uM1 four of the seven landmarks were placed on the dentin horn tips and two were placed at the deepest points of the talon and the trigon at the central fovea and the distal fossa, respectively (Fig. 6). The seventh landmark was placed at the lowest point along the marginal ridge between the hypocone and the protocone. On the lM1 four of the eight landmarks used were set on the main horn tips. Two landmarks were placed on the deepest points along the buccal and lingual marginal ridges between the hypoconid and the protoconid and between the entoconid and the metaconid. The deepest point on the occlusal surface, where the buccal and lingual grooves meet the mesial and distal grooves was marked by landmark seven (Fig. 6). Differently from other studies on lower molars (Fornai et al., 2015; Weber et al., 2016) an additional landmark was added on the top of the hypoconulid since it was identifiable on each individual of the sample. For an accurate representation of the occlusal ridge a curve was traced by means of a large number of points (between 150 and 350 landmarks depending on the tooth size). The curve was used as sliding references in Evan Toolbox 1.72.

Afterwards the semilandmarks were collected on the reference specimen or template. For an accurate description of the marginal ridge of uM1, we used 43 semilandmarks (sLMs) as in previous studies (Teplanova, 2015; Weber et al., 2016; Hershkovitz et al., 2018).

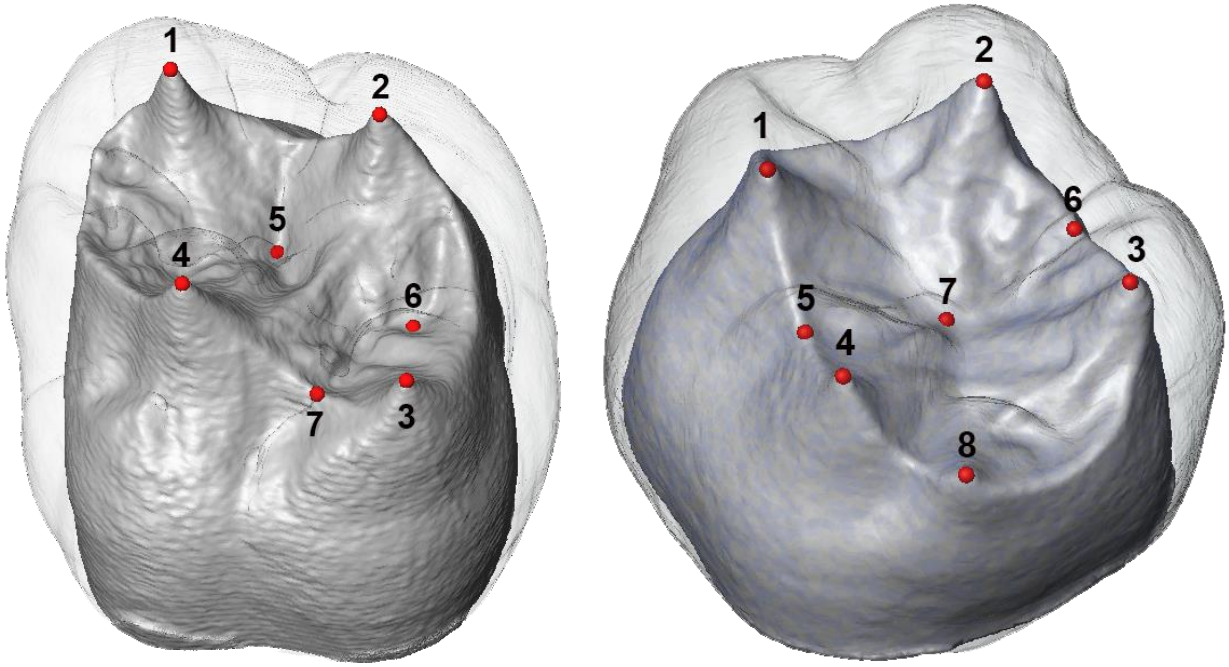

a) **b)**

Fig. 6 – Landmarks representing the occlusal aspect of **a)** uM1s (n = 7), and **b)** lM1s (n = 8).

The semilandmarks were placed on the template uM1 (collection no. 964), and were equidistantly spaced along the curve. Therefore, the number of semilandmarks of the various segments of the curve depended on the length of the segments themselves. For the lower M1s, the edges are longer than those of the upper ones. Thus, a slightly larger number of semilandmarks was necessary. Consequently, 47 semilandmarks were placed in equal distances on the lM1 template (collection no. CN230). The remaining individuals were loaded into Evan Toolbox 1.72 as targets, considering uM1s and lM1s as two distinct samples. The semilandmarks of the template tooth were warped onto the target tooth and the projected semilandmarks were slid to minimize the bending energy (Bookstein, 1997; Mitteroecker and Gunz, 2009).

Sampling of pseudo-landmarks on cervical and crown outlines

The curves previously created in Geomagic (see section 'Digitization, segmentation and realignment of the crown') representing crown and cervical outlines were exported as *.igs objects for further data collection in Rhinoceros 5.0 SR9. After determining the centroid of the area of the outlines, each outline was split into 24 segments by 24 equiangular spaced radial vectors (in 15-degree intervals) with origin corresponding to the centroid (Fig. 7). The first

radius was parallel to the y-axis towards positive values. At the intersection of the outlines and the radii, 24 pseudo-landmarks were collected and exported for GM analysis.

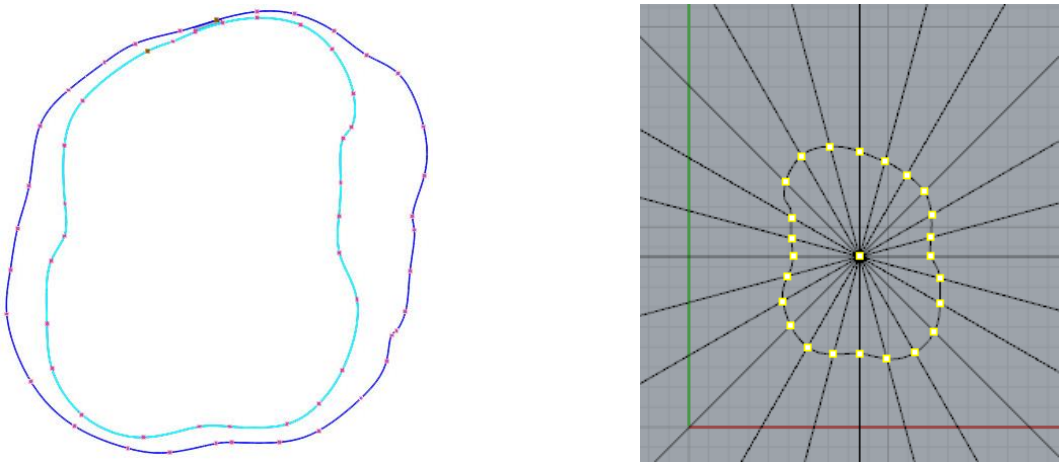

a) **b)**

Fig. 7 – a) Based on the uM1 outlines collected in Geomagic software; **b)** 24 pseudo-landmarks were geometrically constructed along the cervical line in Rhinoceros 5.0.

Analysis of the landmark configurations

First, a General Procrustes Analysis (GPA) was applied to remove all the non-shape related variation and a PCA was carried out. In a later step, the PCA was also carried out in form space, to evaluate the effect of size on shape variation. This study uses Thin-Plate Spline driven warping as a method of visualization. Furthermore, a multiple regression analysis was performed in Evan Toolbox 1.72. The size differences between the ethnical and continental groups were evaluated via a non-parametric test, the Kruskal-Wallis-Test (KW-test). It was performed on the lnCS values with the software SPSS Statistics v25 (IBM Corp.). Owing to the rather small sample size, a Monte Carlo Permutation was performed with 10.000 permutations. Further, for the 18 cases for which both upper and lower M1s were available, a 2-Block Partial Least Square Analysis (2B-PLS) was computed. For the 2B-PLS analysis, two parameters were discussed: the pairwise correlation of latent variables (singular warp value (SV)) 1 left and 1 right, which explain how two data sets (blocks) correlate with respect to each other (e.g. how the upper and lower M1s correlate between individuals), and the total squared covariance, which represented the covariation for the two blocks considered within the whole sample (e.g. how all the lower molars covary with all the upper molars). The two values do not necessarily have to be close to each other. Given that the pairwise correlation considers the covariation between two individually integrated anatomical units, its value is expected to be higher.

Non-metric traits

For this investigation the standards of the Arizona State University Dental Anthropology System (ASUDAS) were used (Turner et al., 1991). Although this system was actually developed for identifying dental traits on the OES, most of these traits can be found on the EDJ as well. During tooth development the major aspects of the crown morphology are predetermined and developed on a membrane called the *membrana praeformativa* (see Introduction). On the outside of this membrane layers of enamel are built over time, therefore the EDJ is a preservation of the basal membrane's original shape (Butler, 1956). Based on Nager's (1960) observations, there are 3 types of metric structures:

- **Type 1** primary-definitive traits: are consistently visible on the EDJ and on the (unworn) occlusal aspect of the OES
- **Type 2** primary-temporary traits: are only visible on the EDJ, but not on the (unworn) outer enamel surface
- **Type 3** secondary traits: are only represented on the outer enamel surface and not on the EDJ

This study considers only Type 1 and 2 traits given that most of the teeth in our sample show worn outer enamel surfaces. Only traits detectable on the crown were rated, while root morphology was not a topic of this study. The qualitative traits considered in this sample are described below and listed in Tables 19 and 20.

Our sample included all seven types of Carabelli's trait expression, therefore we referred to Hunter et al. (2010) and analyzed the influence of the intercuspal distances (ICD) on the Carabelli's trait manifestation in uM1s. To assess whether there exists any correlation between the molar size and the degree of manifestation, we used two different approaches. First, we used our adapted GM data (shape data in form space, not in mm), and second according to Hunter's (2010) pilot study we calculated the absolute distances in mm.

For the first approach, the original GM data set was tested for similar signals as Hunter (2010) described. Yet, the data set had to be slightly adjusted. First, the landmarks of the four main tips were isolated and a GPA was performed. In a next step the ratio between the lnCS values of the main horn tips and the crown outline was calculated in order to produce a unitless measure of the dental uM1 crown. The new variables were then analyzed via Ordinal Regression in combination with the Carabelli ordinal values (ASUDAS) (Table 12). For the second approach, we used the same method as Hunter et. al (2010) dividing the mean intercuspal distance (in mm) by the area of the crown outline. The mean intercuspal distance was calculated of the distances between paracone and metacone, metacone and hypocone,

hypocone and protocone, protocone and paracone. These absolute intercuspal distances were calculated by applying elementary trigonometry to the landmark coordinates representing the tips of the dentinal horns. In addition, the ratios between each intercuspal distance and the area of the crown outline were calculated (Table 13 – 17). As a control approach the Carabelli expressions were merged together in 3 new groups, depending on their manifestation degree (Table 18). Scott and Irish (2017) defined grade 2 as the breakpoint for Carabelli's trait, therefore we lumped teeth without Carabelli's trait and with a grade 1 manifestation in the same category (i.e. "under breakpoint"). In earlier frequency studies Scott and Turner (1997) used only teeth with well pronounced traits (manifestation 5 - 7) to characterize the global variation, thus we classified manifestations higher than 5 as "big". Carabelli's traits showing manifestation from 2 to 4 were classified as "small".

Discrete traits of the upper first molar enamel-dentine junction

Metaconule

The metaconule (Fig. 8) or fifth cusp manifests between the metacone and the hypocone. Its size can vary between a small conule not visible on the OES and a well separated cusp on the distal marginal ridge.

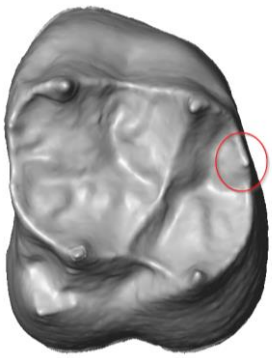

Fig. 8 – showing a grade 4. Metaconule (cat. no. CS569).

Carabelli's cusp

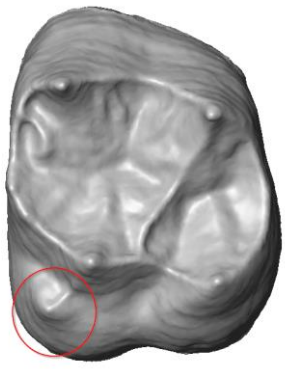

Fig. 9 – showing a grade 6. Carabelli's tubercle (cat. no. CN5).

This trait might occur on the mesiolingual dentine horn (protocone) in upper molars (Fig. 9). The range of expression is wide and varies from a slight groove to a massive, distinct cusp. Carabelli's cusps were used to be interpreted as diagnostic features of European individuals (Carbonell, 1960; Turner, 1967; Alvesalo et al., 1975; Scott, 1980; Marado and Campanacho, 2013), although recent research indicates no difference in its manifestation between populations (Scott and Irish, 2017). Studies by Hunter et al. (2010) suggest that the manifestation of this tubercle can be associated with the intercuspal distances. The closer the four main horn tips are together, the more markedly greater the manifestation of the trait.

Anterior accessory tubercle (AAT)

AATs (Fig. 10) were first classified by Kanazawa et al (1990) and can be found on the mesial ridge (Turner et al., 1991). An AAT is named protoconule if it is proximal to the protocone and paraconule if it is closer to the paracone.

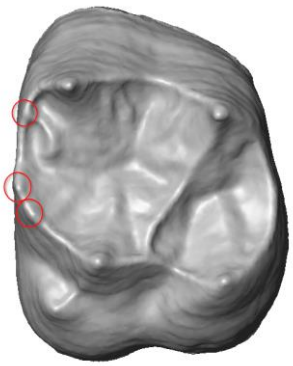

Fig. 10 – showing 3 AATs (cat. no. CN5).

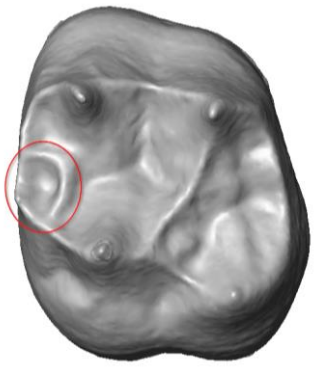

Fig. 11 – showing an ATR (cat. no. 125_510_1554).

Anterior transverse ridge (ATR)

The ATR (Fig. 11) originates at the mesial ridge between the protocone and the paracone and extends towards the central groove. An AAT can be frequently found at the origin of an ATR. The length and degree of manifestation of the ATR vary strongly. For this study only the information about the absence or presence was considered.

Enamel extension (EE)

The EE (Fig. 12) can be variously expressed and can appear like a short extension of the enamel line or a massive enamel pearl reaching the bifurcation of the roots.

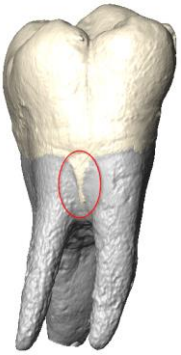

Fig. 12 – showing the only EE in the sample (cat. no. 2583).

Discrete traits of the lower first molar enamel-dentine junction

Hypoconulid

The hypoconulid (Fig. 13) is a phylogenetically recent trait addition to the basic 5-cusp blueprint of lower molars (similarly to the hypocone in the upper molars). During the later stages of hominin evolution, it has gone through reduction. A reduction or absence of this trait is more frequent in M2s than M1s. The peculiarity can varies between slightly to strongly expressed (Turner et al., 1991).

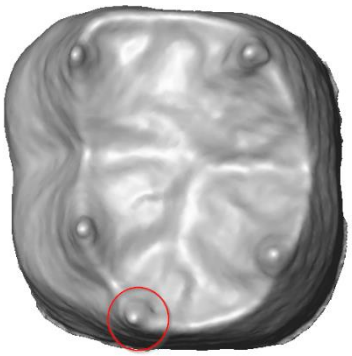

Fig. 13 – showing the Hypoconulid (cat. no. CN230).

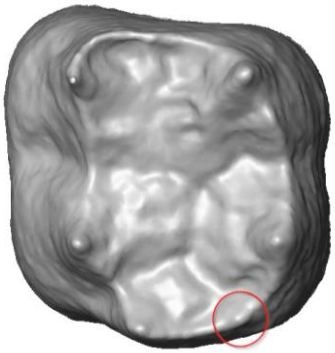

Fig. 14 – showing a grade 2 Entoconulid (cat. no. S111).

Entoconulid

The entoconulid (Fig. 14), also called cusp 6, can be found on the distal area of lower molars between the hypoconulid and the entoconid. Its classification requires the presence of the hypoconulid.

Metaconulid

The metaconulid (Fig. 15), or cusp 7, can be expressed on the lingual side of lower molars between the metaconid and the entoconid. It is often not visible on the OES but can be scored on the EDJ.

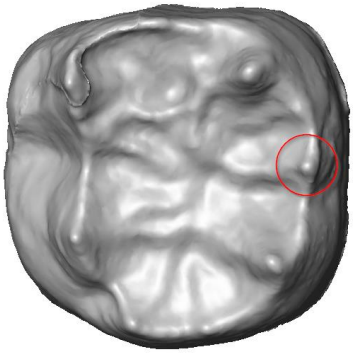

Fig. 15 – showing a grade 4 Metaconulid (cat. no. 5758).

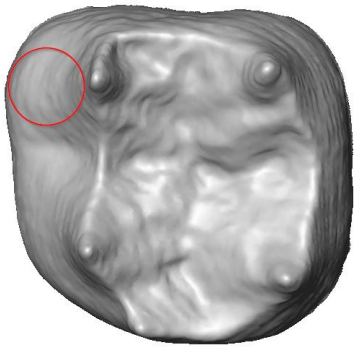

Fig. 16 – showing a grade 4 Metaconulid (cat. no. 5758).

Protostylid

The protostylid (Fig. 16) is a cingular derivative of the mesiobuccal area in lM1s. It was quite common in early humans but is less present in modern samples. The expression can vary between absent to a separated tubercle.

Midtrigonid crest (MC)

MC (Fig. 17) is a crest that can connects the protoconid and the metaconid. Six different types of trigonid crests can be scored, depending on their position and being either continuous or interrupted by the sagittal sulcus (Korenhof, 1982; Martínez de Pinillos et al., 2014). This study reports whether the MC is absent, discontinues or continuous.

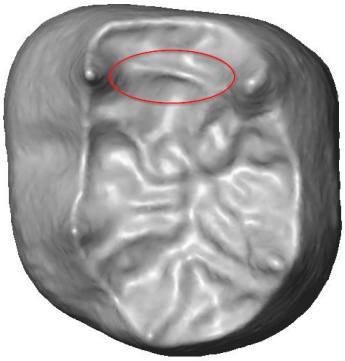

Fig. 17 – showing a MC (cat. no. BLZ_004).

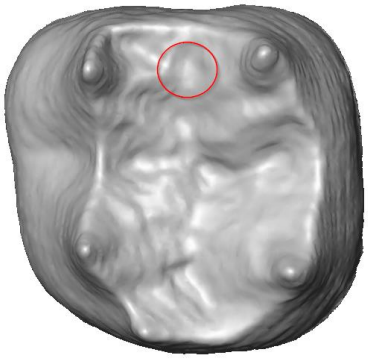

Fig. 18 – showing an AF (cat. no. 120_080_717).

Anterior fovea (AF)

An AF (Fig. 18) is a polymorphic trait in the mesial region of lM1's occlusal aspect. The AF is a depression visible when both a MC and a mesial ridge are present.

Groove Pattern

The pattern of the occlusal surface on lower molars (Fig. 19) can be classified based on how the 4 main cusps relate to each other:

y: contact between Metaconid and Hypoconid

x: contact between Protoconid and Entoconid

+: contact between all cusps at central sulcus.

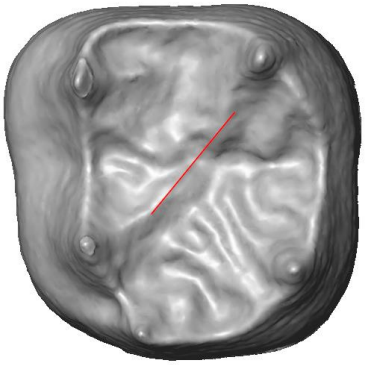

Fig. 19 – showing a "Y" pattern (cat. no. BLZ_037).

Results

Geometric Morphometrics

The main result of all geometric morphometric analyses performed was the large overlap of the different populations in the PC plots for both uM1s and lM1s (Fig. 20 - 27, and Table 2). The first two PCs covered around 45% of the variance in the combined, EDJ and outlines analyses. Percentages of explained variance are given for the first 6 PCs in Table 2. In all data sets the first two PCs showed gross shape variation and every further PC reflected progressively more localized shape differences. Shape variation is described below for the PCs explaining more than 5% of variation.

Table 2 – Percentage of variance explained by the PCs for the various analyses for uM1s and lM1s (EDJ = enamel-dentin junction, CER = cervical outline, COM = combined data set, CRO = crown outline). Only values higher than 5% are reported for 3D datasets. For 2D datasets, only the values for the first two PCs are indicated.

	uM1				lM1			
PC	**EDJ**	**CER**	**COM**	**CRO**	**EDJ**	**CER**	**COM**	**CRO**
PC1	24.54	31.72	29.27	33.52	20.03	45.77	29.19	48.99
PC2	19.21	22.48	16.68	16.35	14.80	22.21	15.4	13.46
PC3	10.6	11.39	9.74	13.44	12.56	11.69	12.01	9.04
PC4	7.68	9.60	7.72	9.49	9.04	6.36	7.33	6.65
PC5	6.91	6.40	5.68	6.69	7.48	3.67	6.49	4.55
PC6	4.75	5.32	5.18	5.13	5.19	2.76	4.34	3.86

Shape variation in upper first molars

EDJ

The EDJ analysis (Fig. 20) explains shape variance for the apical third of the dental crown, therefore the description that follows refers only to this portion of the dentinal crown. Variation along PC1 (24.54% of total variance explained) was driven by the relative size of the trigon to the talon in mesiodistal direction. The greater the relative distance between the protocone and hypocone is, the further distolingually located is the talon with respect to the trigon. Larger trigon areas correspond with lower dentine horns and vice versa. The warping along PC2 (19.21%) represents the relative shape variation of the talon compared to the trigon along with the relative distance between the mesial horns (protocone and paracone) versus the distal horns (meta- / hypocone). The decreasing buccolingual width of the distal aspect results in a

buccolingually proportionally wider mesial aspect. Along PC3 (10.6%), the hypocone varies in its mesiodistal extent. A bulging hypocone is associated with a small and narrow trigon surface and centrally bent horn tips, while a narrow hypocone corresponds to a wider trigon and straight horn tips. PC4 (7.68%) reflects the change in the relative distance between the lingual and buccal horn pairs, where either the buccal horns (paracone and metacone) are closer to each other than the lingual horns (hypocone and protocone) or vice versa. A general buccolingual and mesiodistal elongation of the occlusal area can be observed along PC5 (6.91%).

Cervical outline

Along PC1 (31.72%), shape variation occurs at the distolingual aspect of the outline (Fig. 21), reflecting the relative expansion of the hypocone. An expanded distolingual region is associated with a rounded and smaller shape of the remaining outline in proportion to the hypocone area. Therefore, a reduced distolingual area results in a buccolingually elongated overall shape. Along PC2 (22.48%), the variance occurs around the middle sections of the mesial and distal aspects of the outline, ranging from constricted (as in an hourglass) to bulging.

Crown outline

The first PC (33.52%) for the crown outline describes the relative mesiodistal to buccolingual widths (Fig. 22). Crown outlines vary from rounded with a slightly enlarged mesiobuccal aspect to mesiodistally elongated. Shape variation in the hypocone area can be observed along PC2 (16.35%), and consists in the relative expansion of the distolingual aspect.

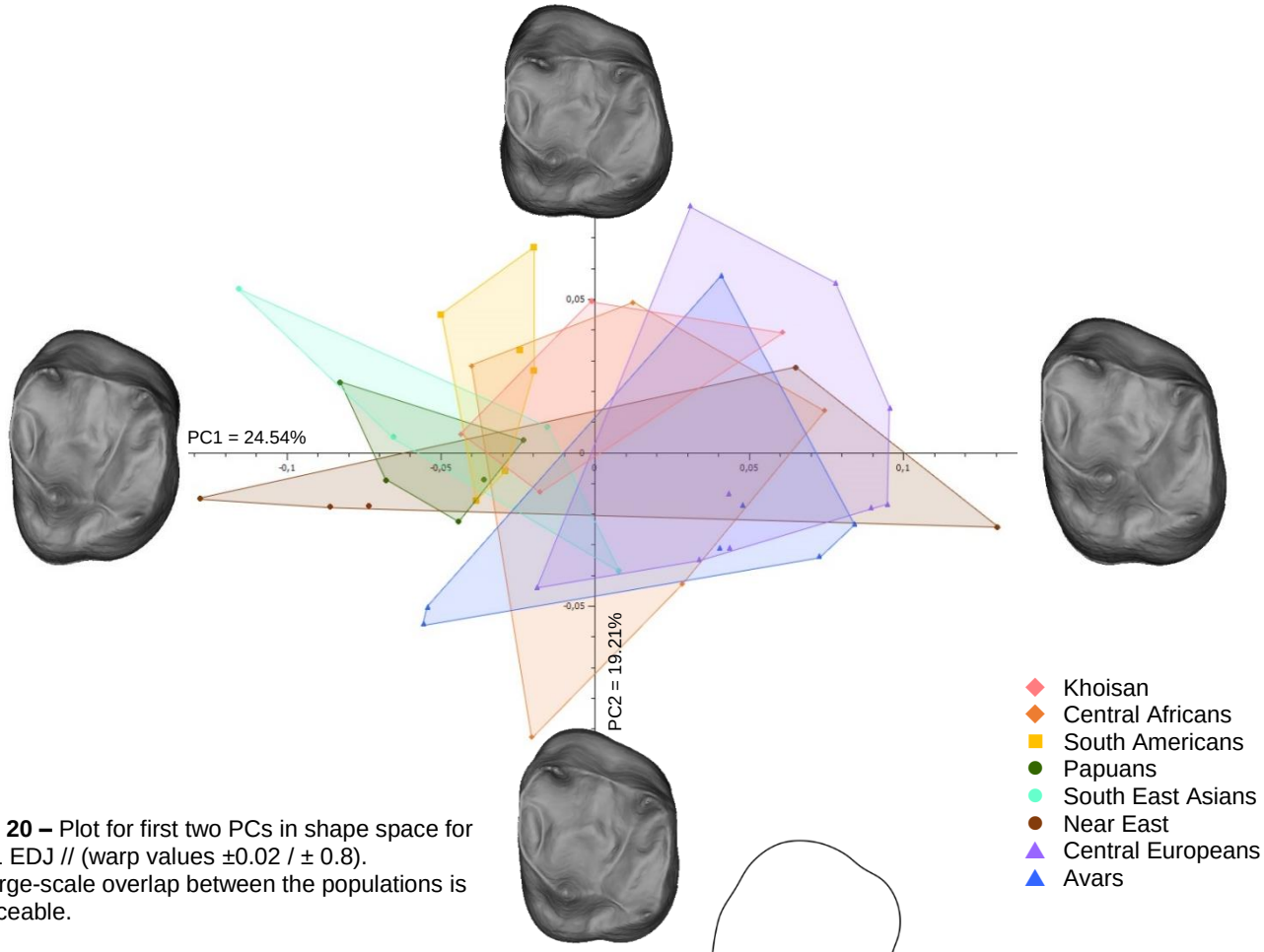

Fig. 20 – Plot for first two PCs in shape space for uM1 EDJ // (warp values ±0.02 / ± 0.8).
A large-scale overlap between the populations is noticeable.

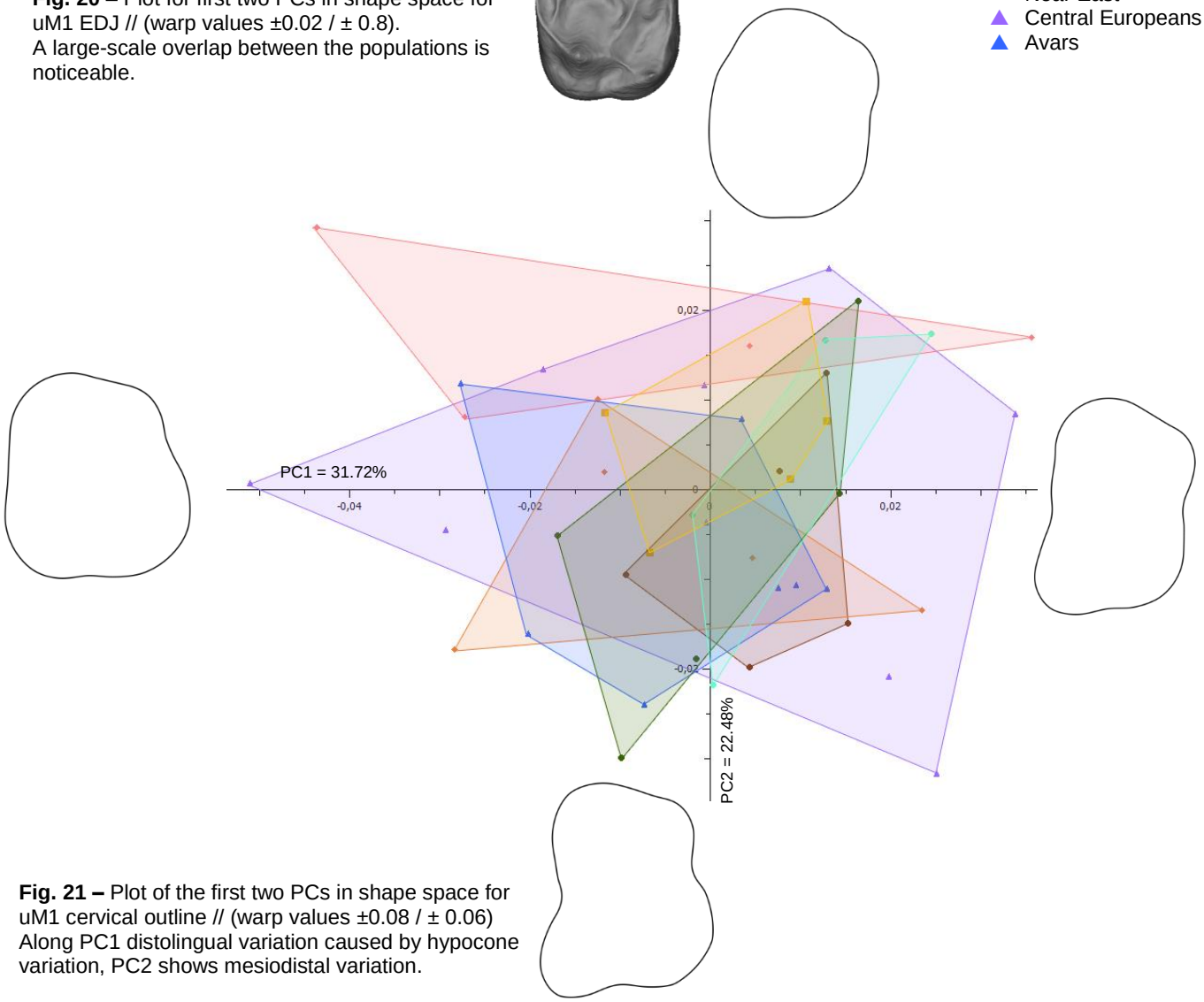

Fig. 21 – Plot of the first two PCs in shape space for uM1 cervical outline // (warp values ±0.08 / ± 0.06)
Along PC1 distolingual variation caused by hypocone variation, PC2 shows mesiodistal variation.

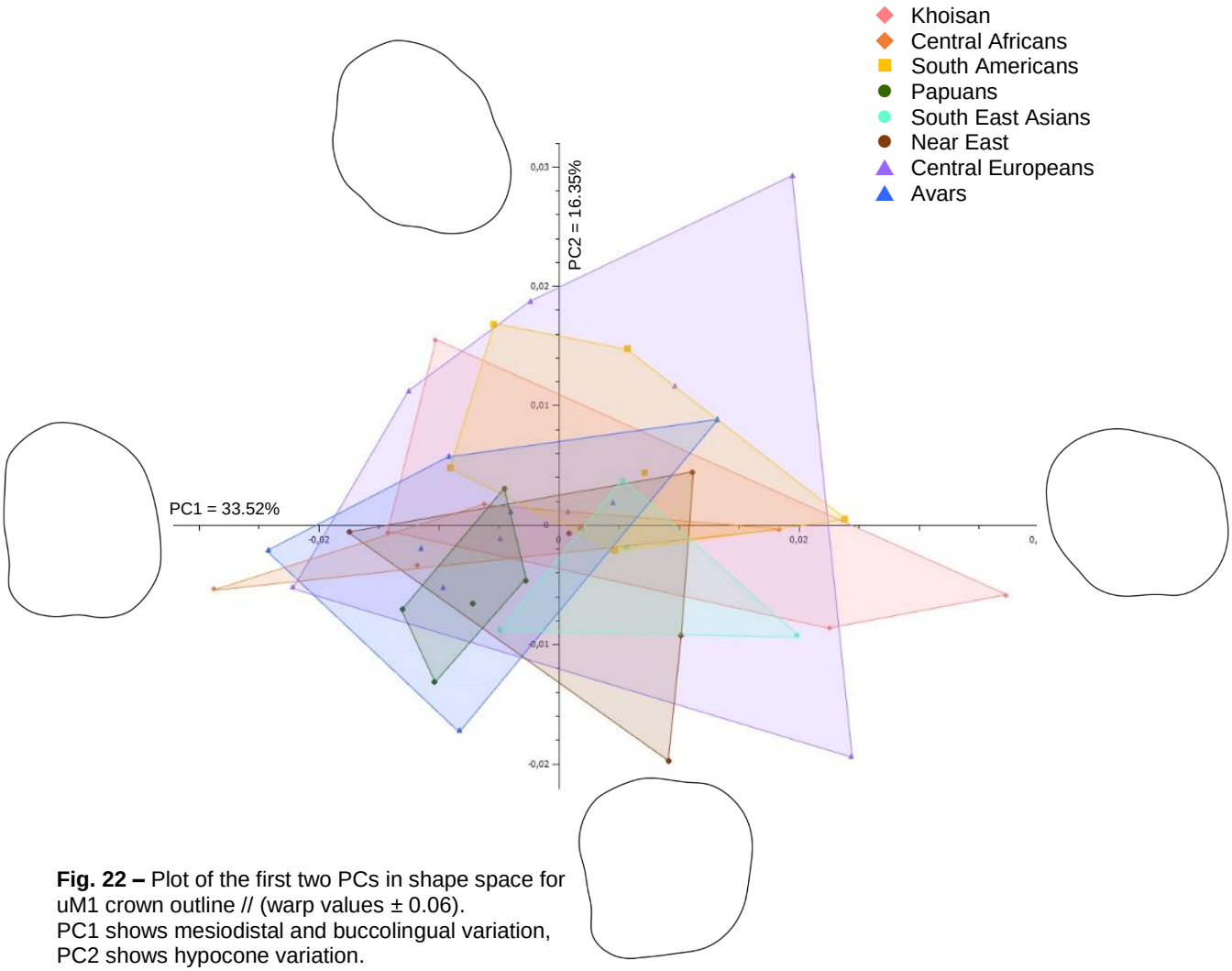

Fig. 22 – Plot of the first two PCs in shape space for uM1 crown outline // (warp values ± 0.06).
PC1 shows mesiodistal and buccolingual variation, PC2 shows hypocone variation.

Combined EDJ and cervical outline datasets

The combined dataset included both EDJ and CER data sets, thus representing the entire dentinal crown. Along PC1 (29.27%), the combined variation of crown height and the relative size of the trigon to the talon can be observed (Fig. 23). Low-crowned uM1s possess expanded trigons, while high-crowned uM1s show smaller trigons. Similar to PC1 of the EDJ analysis, PC2 (16.68%) in the combined data set shows the variation between the proportions of the talon to the trigon. A buccolingually expanded hypocone results in a narrower trigon and vice versa. A narrower talon is associated with a relatively larger trigon, featuring a larger buccolingual distance between the two mesial dentine horns. Along PC3 (9.74%), a concomitant reduction versus expansion of the hypocone and metacone can be observed. Their change in size results in a reduction or expansion of the whole distal area. PC4 (7.72%) shows relative changes in the size of the trigon to the positioning of the dentine horns. A small trigon area is associated with horn tips pointing towards the occlusal centre of the trigon, while larger trigons show straighter dentine horns. The position of the hypocone with regard to the protocone also changes between distal (large trigon) and distolingual (small trigon). PC5 (5.68%) explains the variation in the general shape of the tooth outline. It varies between buccolingually elongated with mesiodistally small talon and closely positioned hypocone and round with a mesiodistally elongated talon and a larger, distolingually located hypocone. The relative mesiodistal expansion of the talon is represented by PC6 (5.18%).

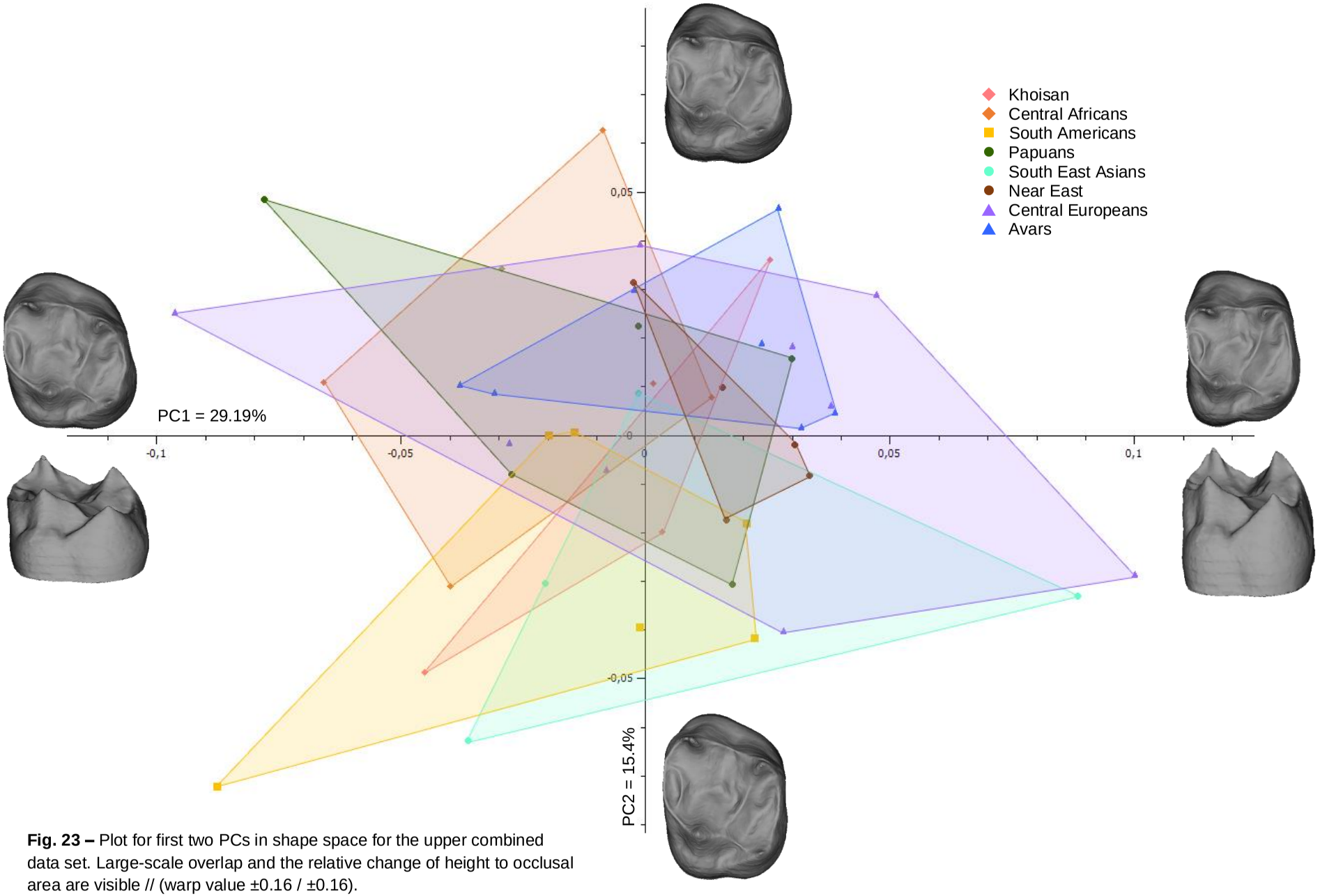

Fig. 23 – Plot for first two PCs in shape space for the upper combined data set. Large-scale overlap and the relative change of height to occlusal area are visible // (warp value ±0.16 / ±0.16).

Shape variation in lower first molars

EDJ

Along PC1 (20.03%), the shape differences in the mesial to distal relative expansion of the occlusal surface can be observed, which varied inversely (Fig. 24). The size of the hypoconulid is related to its relative distance to the entoconid - the closer those tips are, the smaller and lower the hypoconulid is. PC2 (14.80%) accounts for the mesiodistal transition of the hypoconid and entoconid. Their variation also influences the distance between hypoconid and hypoconulid. In addition, if the hypoconid and entoconid are placed further distally, the lingual ridges bulge lingually. The curvature of the buccal and lingual ridges varies between a deep apical curvature and an almost straight line between the two corresponding horn tips. Shape variation along PC3 (6.84%) represents the inverse change in relative size between the occlusal area and the hypoconulid along with the relative height of the dentine horns. A relatively small occlusal surface results in high horns and a pronounced hypoconulid, while a broader surface corresponds in short horns and a reduced hypoconulid. The variation in the position of the hypoconulid relatively to the hypoconid can be observed along PC4 (5.79%). Along this PC, the higher the hypoconulid and the further distal its position are, the shorter the other dentine horns are.

Cervical outline

A general shape variation from a rectangular to a squared cervical outline is visible along PC1 (45.77%) (Fig. 25). PC2 (22.21%) shows the inverse expansion of the mesiolingual and distolingual tooth aspects. In both PC1 and PC2 there is a variation of the constriction in the middle portion of the lateral aspects. The constriction is more distinctive on the lingual side, but also visible when rising the warp values above the extremities of our distribution. An inspection of the original 3D models of the teeth revealed that this effect is related to the shape of the roots. Widely separated roots result in a depression of the buccal and lingual aspect of the cervical outline, while close root branches are associated to straight buccal and lingual outlines.

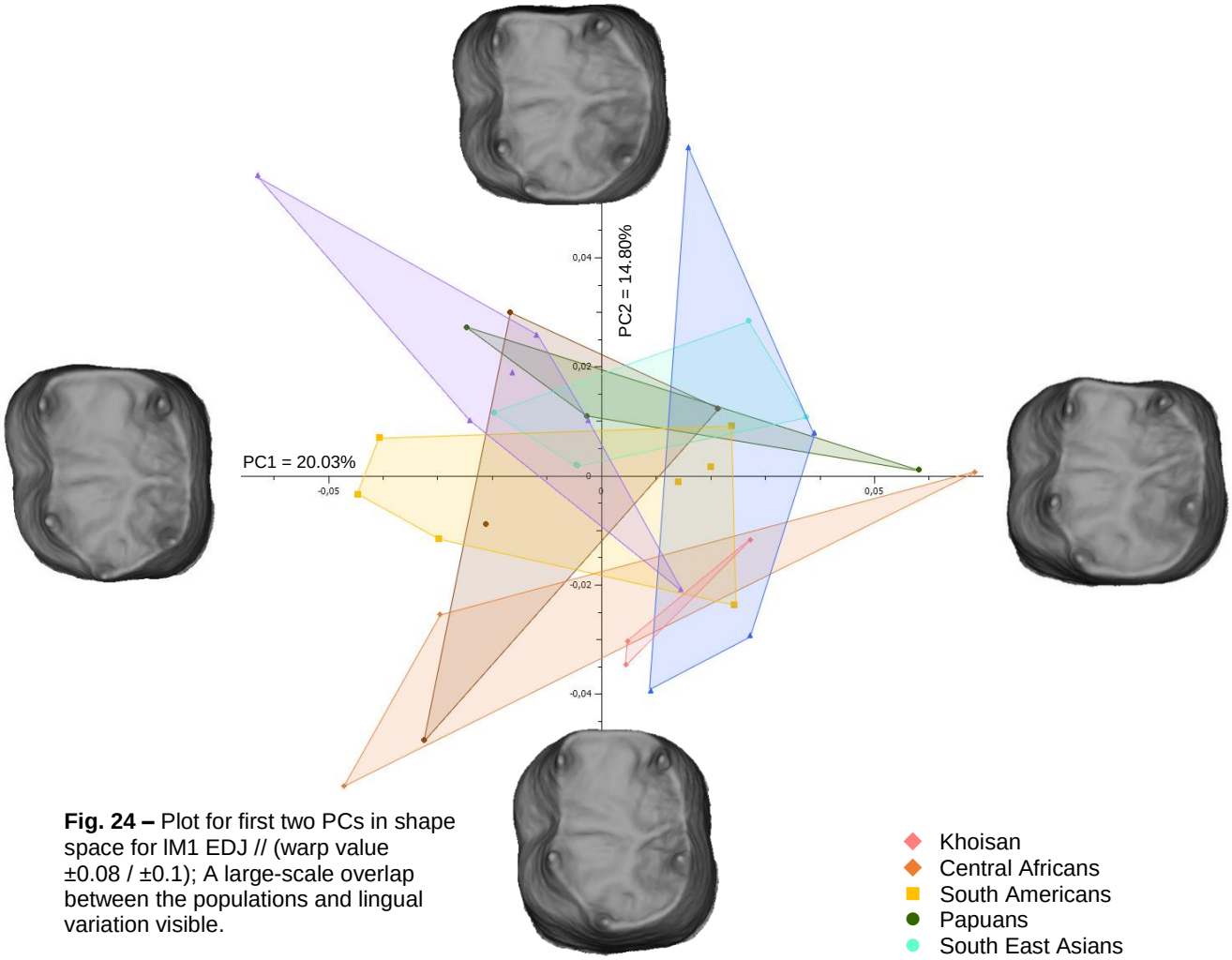

Fig. 24 – Plot for first two PCs in shape space for lM1 EDJ // (warp value ±0.08 / ±0.1); A large-scale overlap between the populations and lingual variation visible.

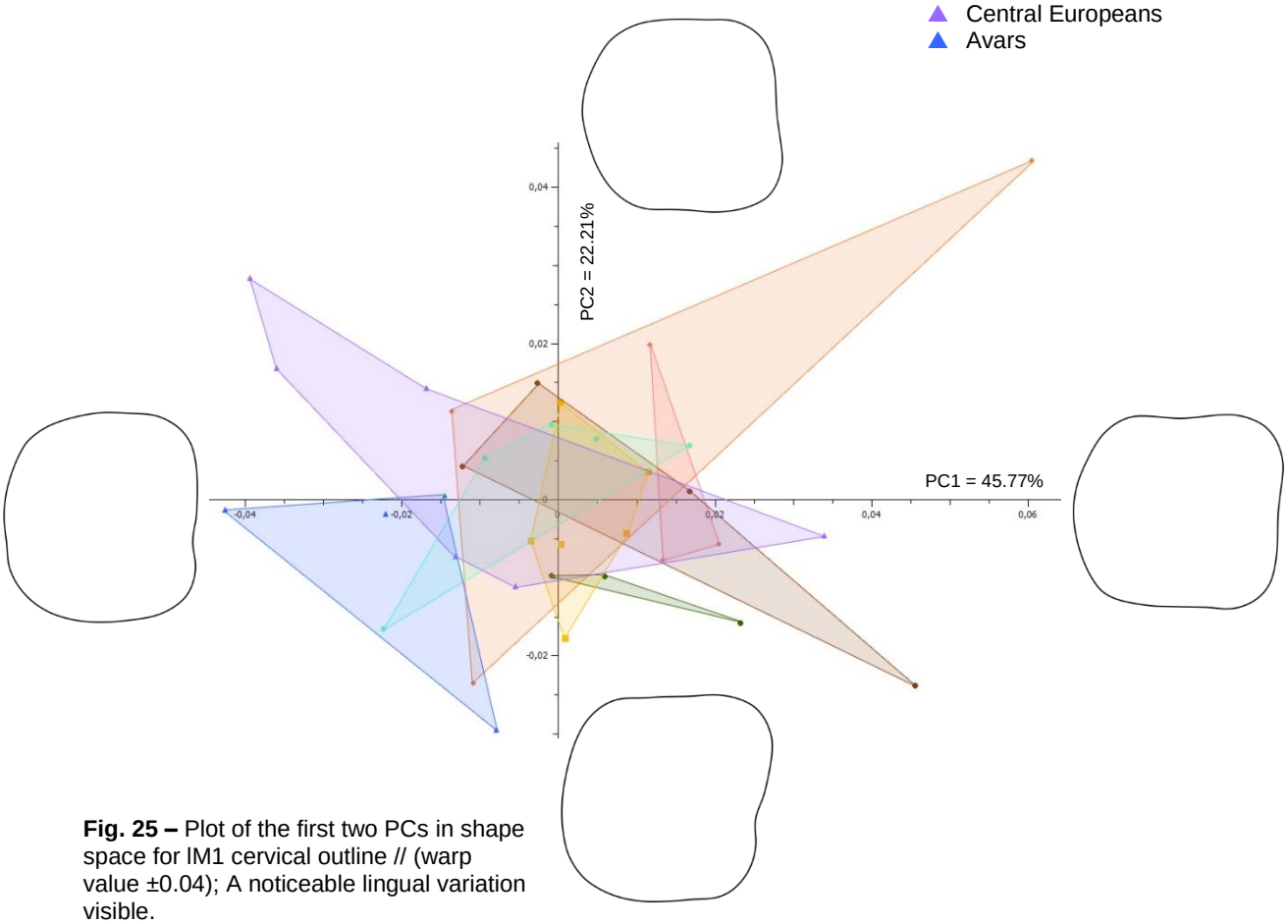

Fig. 25 – Plot of the first two PCs in shape space for lM1 cervical outline // (warp value ±0.04); A noticeable lingual variation visible.

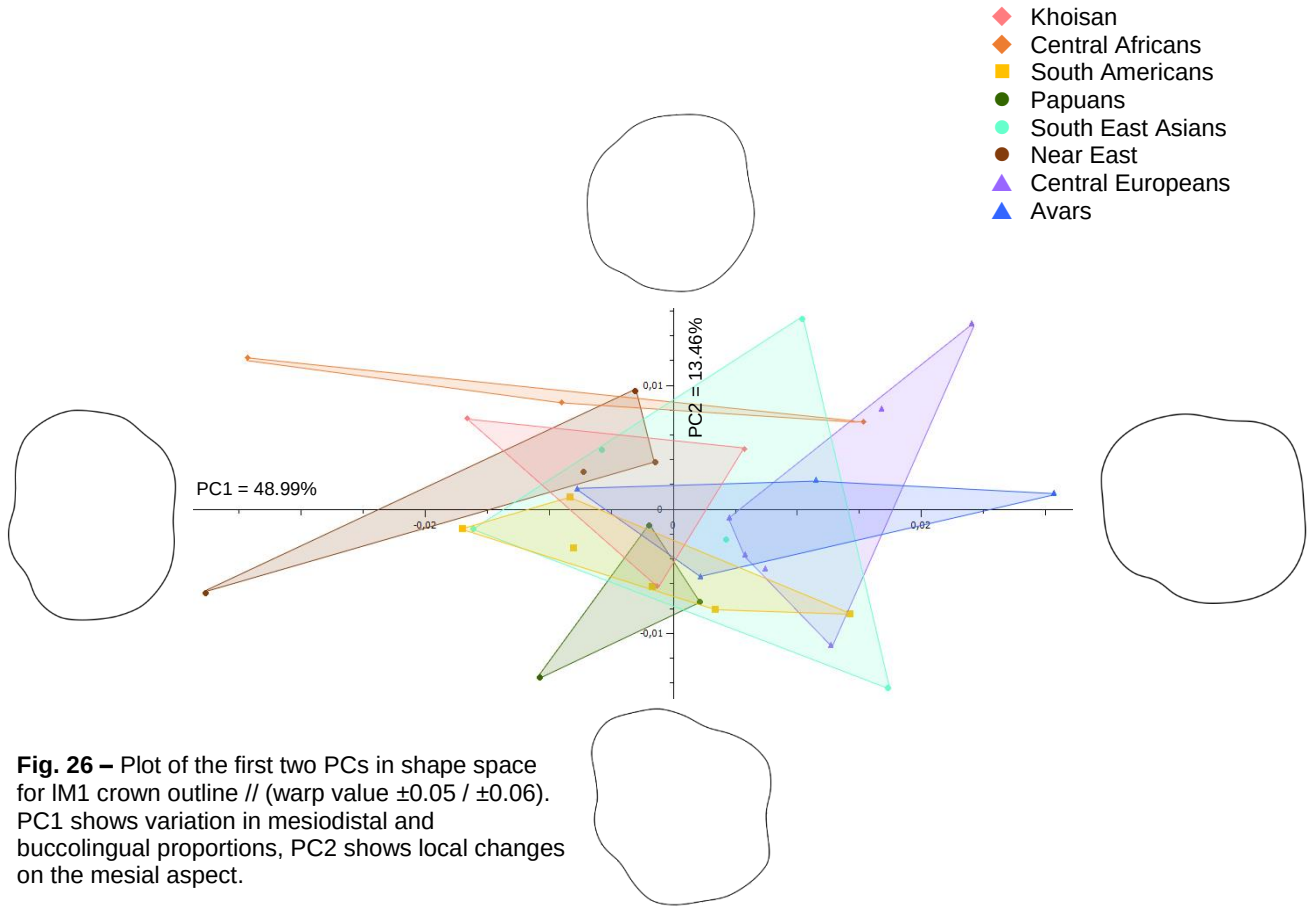

Fig. 26 – Plot of the first two PCs in shape space for lM1 crown outline // (warp value ±0.05 / ±0.06). PC1 shows variation in mesiodistal and buccolingual proportions, PC2 shows local changes on the mesial aspect.

Crown outline

For the lM1, PC1 (48.99%) describes variation of the mesiodistal and buccolingual proportions (Fig. 26). Similar to PC1 of the cervical outline, the crown shape varies from rectangular to square owing to relative mesiodistal expansion. PC2 (13.46%) shows local changes from rounded to irregularly shaped outlines.

Combined EDJ and cervical outline datasets

Similar to the EDJ and the uM1 combined data sets, the greatest variability (PC1 29.19%) is explained by the proportion of the crown height to the expansion of the occlusal aspect (tall and narrow versus short and broad, Fig. 27). Shape variation along PC2 (15.4%) corresponds to the relative proportions between the occlusal surface and the cervical area. A small, mesiodistally elongated occlusal surface results in a buccolingually expanded basal area. Instead, mesiodistally expanded occlusal areas are associated to reduced basal areas. Connected to this are variable degrees of steepness of the buccal and lingual side walls. PC3 (12.01%) shows similar shape variation as EDJ PC1, namely the relative inverse mesial to distal expansion of the occlusal surface. Along PC4 (7.33%), the relative position of the hypoconulid to the hypoconid, and the position of the buccal and lingual tips with respect to each other can be observed (see lM1 EDJ - PC2). PC5 (6.49%) describes the relative position and size of the hypoconulid with respect to the hypoconid, and to the remaining horns. A small hypoconid placed closely to the hypoconid is associated with a wide crown surface and prominent dentine horns, while a distally placed and enlarged hypocone results in a buccolingually narrow occlusal surface and shorter horn tips.

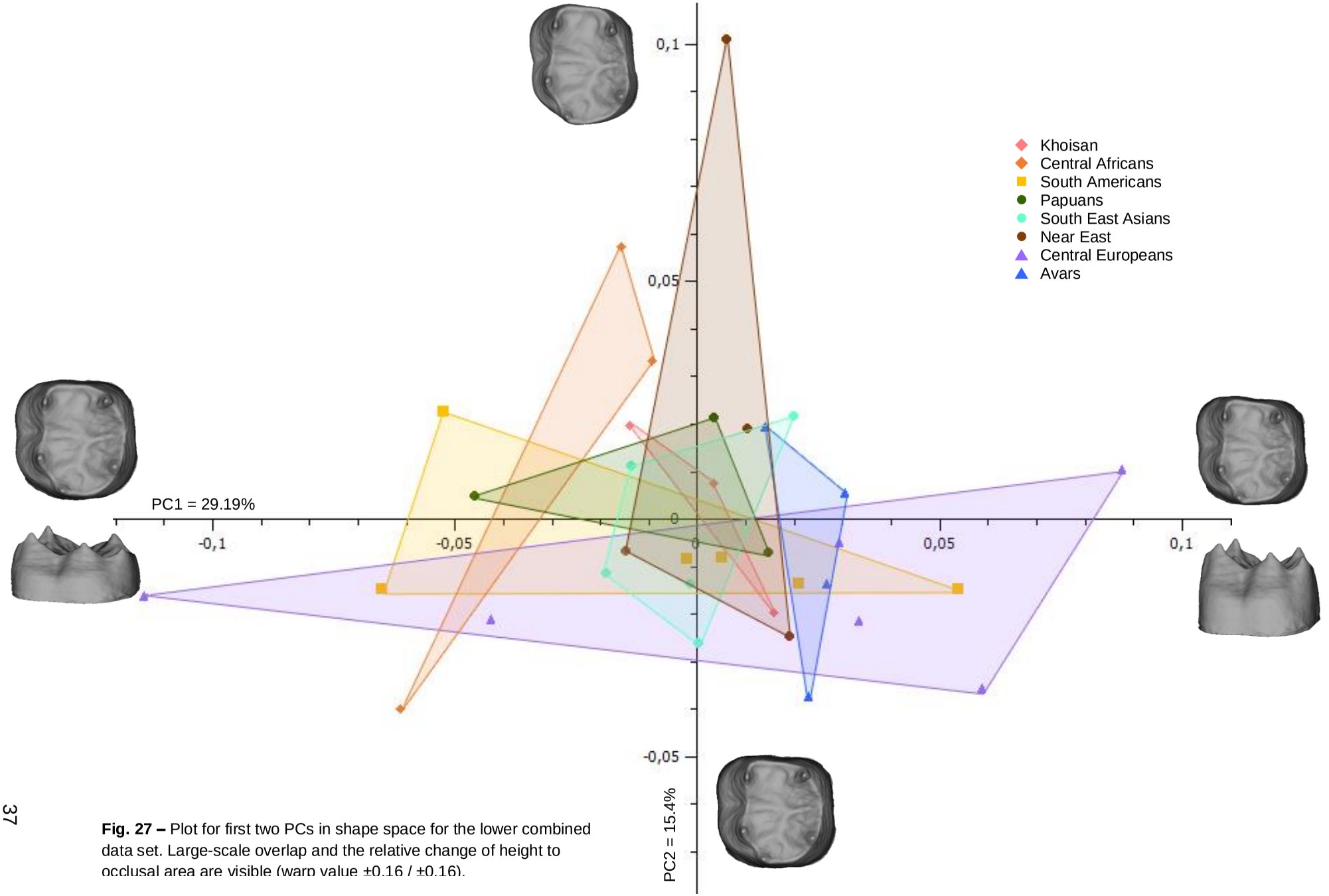

Fig. 27 – Plot for first two PCs in shape space for the lower combined data set. Large-scale overlap and the relative change of height to occlusal area are visible (warp value ±0.16 / ±0.16).

2-Block Partial Least-Squares Analysis (2B-PLS)

The first pair of latent variables represents the gross morphological variation visible in the first PCs. This variation affects both uM1 and lM1 (e.g. crown height change). Table 3 shows the percentage of the total squared covariance and the pairwise correlation between all possible combinations for the 2B-PLS analysis. Values lower than 0.6 show low correlation between the data sets or represent local changes and therefore are not discussed further.

Pairwise correlation between upper and lower molars

The pairwise correlation between the 18 corresponding upper and lower molar pairs (from the same individual) ranges between $r_1 = 0.56$ for the upper and lower cervical line and $r_1 = 0.85$ for the upper and lower EDJ (Table 3). The percentage of the total squared covariance of the antagonistic M1s ranges between 37.9% for the upper EDJ and crown outline and 84.7% for the lower cervical and crown outlines.

In the combined data set, the covariation along SV1 is driven by the following major factors. Both upper and lower M1s vary together between a small base area with high horn tips and a relatively enlarged base area and flat horns (Fig. 28). The highest variation can be observed in the distal aspects both in uM1 and lM1. For the uM1 this variation is mostly driven by the shape variation of the hypocone and for lM1 by the peculiarity and position of the hypoconulid. A distolingually enlarged hypocone results in a mesially shifted and reduced hypoconulid, whereas a reduced hypocone implicates a distinct and rather buccally placed hypoconulid. This strong distal variation is also clearly visible in the EDJ data set ($r_1 = 0.85$; total squared covariance = 50.8%; Fig. 29) and both in the cervical ($r_1 = 0.56$; total squared covariance = 71.2%; Fig. 30) and the crown outline ($r_1 = 0.76$; total squared covariance = 69.9%; Fig. 31).

Pairwise correlation within dental types

The highest pairwise correlations can be found between the outlines CER/CRO in both upper and lower molars (Fig. 32; uM1 $r_1 = 0.71$, lM1 $r_1 = 0.82$), and the lowest values for the EDJ/CRO combination (uM1 $r_1 = 0.64$, lM1 $r_1 = 0.74$). The correlation between the lM1 CER/CRO outlines is driven by the change in buccolingual vs. mesiodistal aspect. Mesiodistally elongated outlines possess a narrower buccolingual aspect and a more pronounced constriction of the middle region. In the uM1 the correlation is driven by the variation of the hypocone expansion.

Table 3 – 2B PLS SV1 results for pairwise correlation and percentages of total covariance in uM1 and lM1 (CER = cervical outline; CRO = crown outline, COM = combined data set).

Pairwise correlation			
	uM1 EDJ	**uM1 CER**	**uM1 CRO**
uM1 EDJ		0.64	0.73
uM1 CER	0.64		0.71
uM1 CRO	0.73	0.71	
	lM1 EDJ	**lM1 CER**	**lM1 CRO**
lM1 EDJ		0.75	0.74
lM1 CER	0.75		0.82
lM1 CRO	0.74	0.82	
	uM1 EDJ	**uM1 CER**	**uM1 CRO**
lM1 EDJ	0.85		
lM1 CER		0.56	
lM1 CRO			0.76
	uM1 COM		
lM1 COM	0.61		
% of total squared covariance			
	uM1 EDJ	**uM1 CER**	**uM1 CRO**
uM1 EDJ		42.2	37.9
uM1 CER	42.2		51.3
uM1 CRO	37.9	51.3	
	lM1 EDJ	**lM1 CER**	**lM1 CRO**
lM1 EDJ		58.7	57.5
lM1 CER	58.7		84.7
lM1 CRO	57.5	84.7	
	uM1 EDJ	**uM1 CER**	**uM1 CRO**
lM1 EDJ	50.8		
lM1 CER		71.2	
lM1 CRO			69.9
	uM1 COM		
lM1 COM	42.9		

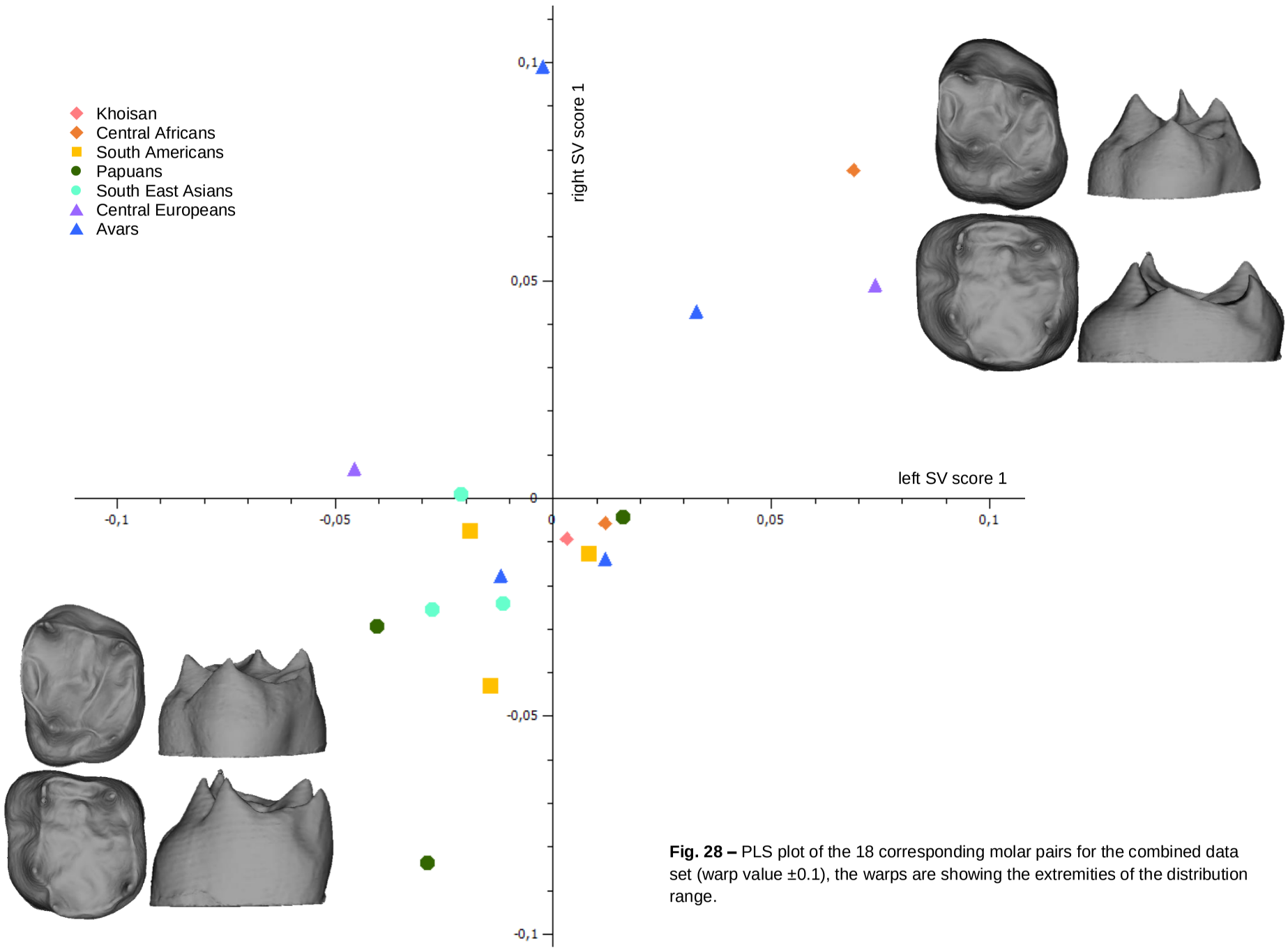

Fig. 28 – PLS plot of the 18 corresponding molar pairs for the combined data set (warp value ±0.1), the warps are showing the extremities of the distribution range.

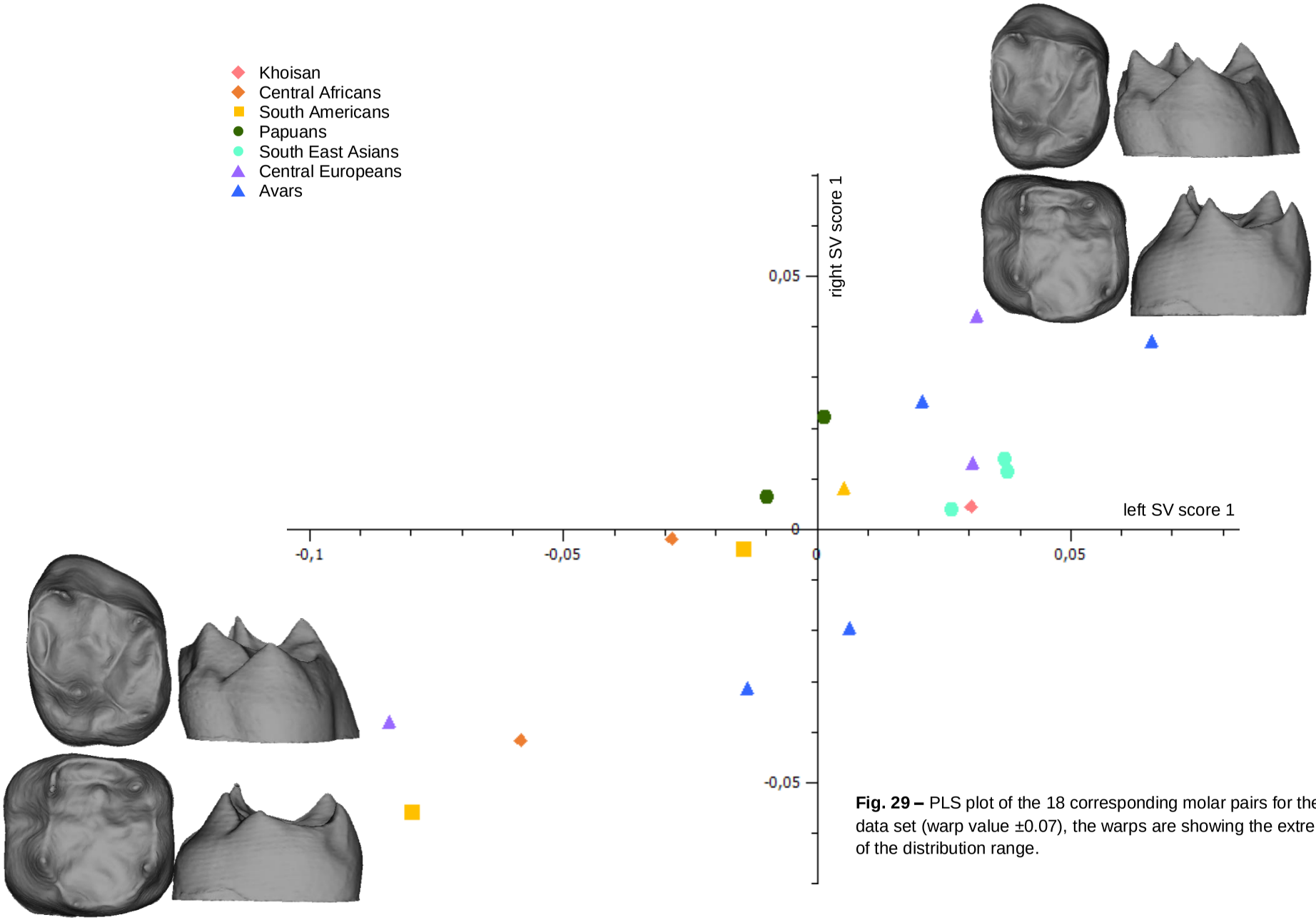

Fig. 29 – PLS plot of the 18 corresponding molar pairs for the EDJ data set (warp value ±0.07), the warps are showing the extremities of the distribution range.

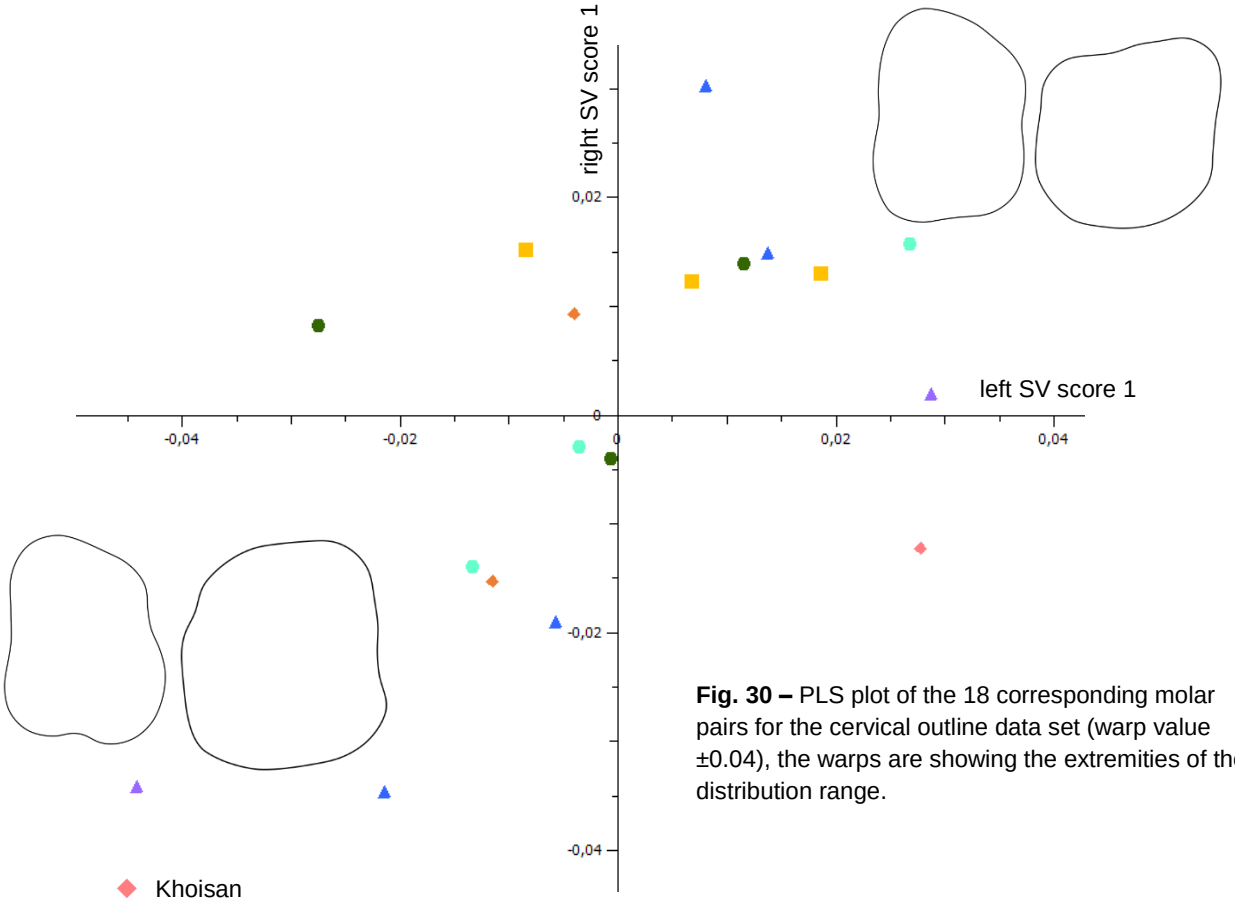

Fig. 30 – PLS plot of the 18 corresponding molar pairs for the cervical outline data set (warp value ±0.04), the warps are showing the extremities of the distribution range.

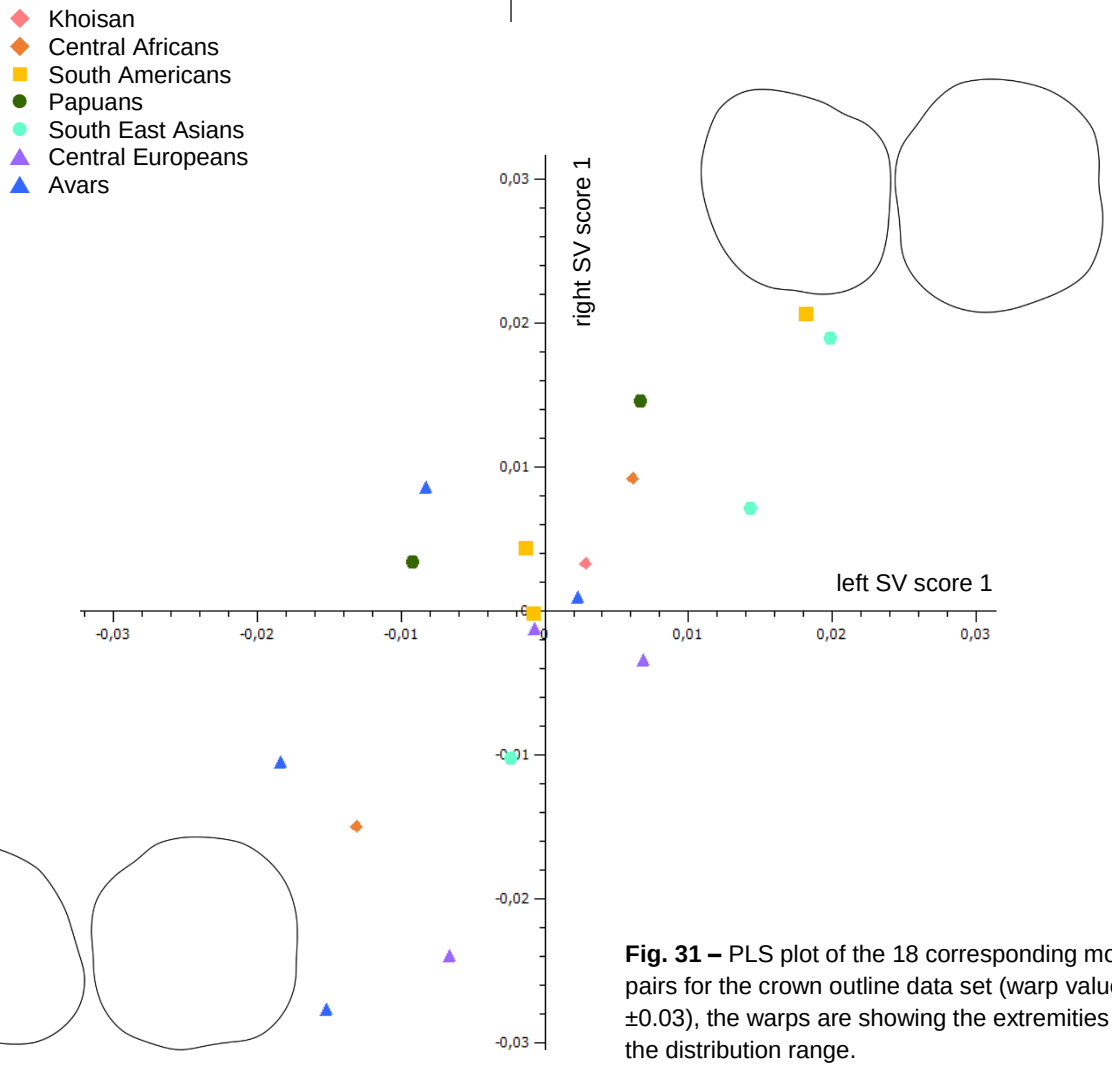

Fig. 31 – PLS plot of the 18 corresponding molar pairs for the crown outline data set (warp value ±0.03), the warps are showing the extremities of the distribution range.

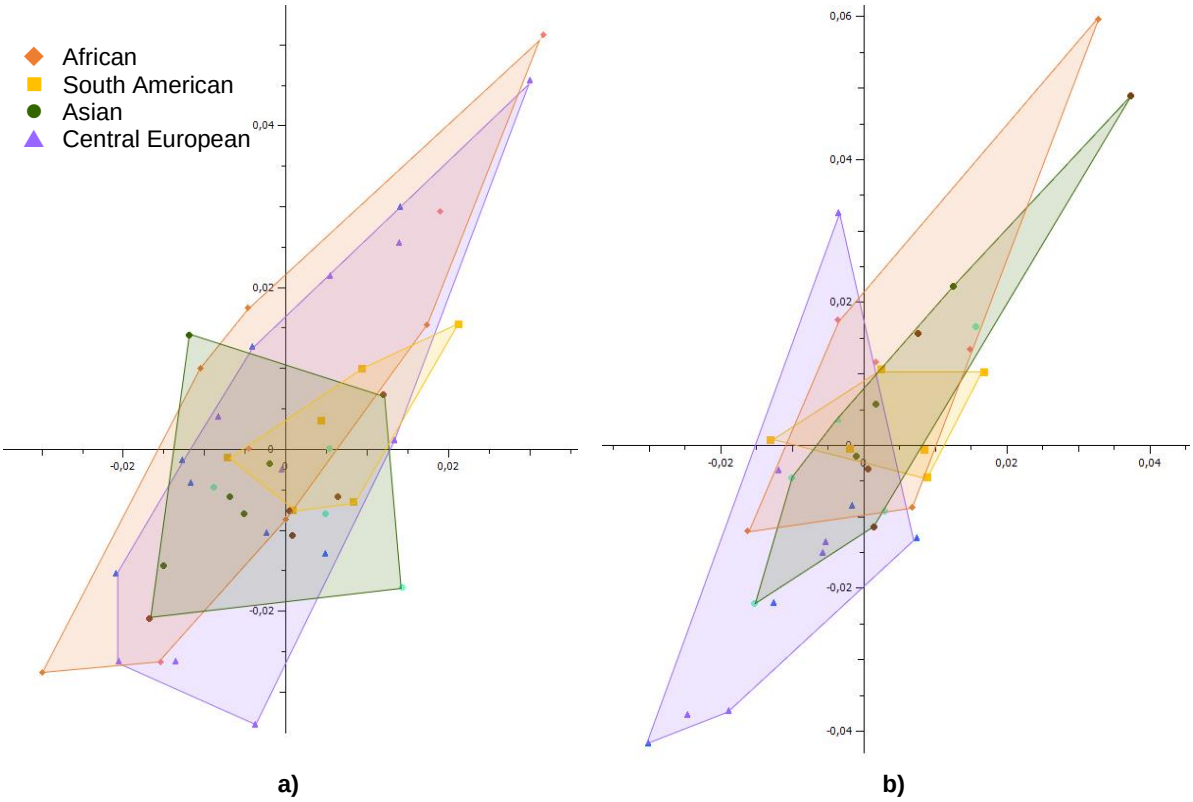

Fig. 32 – PLS plots for **a)** upper and; **b)** lower pairwise correlation between the cervical and crown outlines.

Size

As expected, in form space size dominates the first PC (combined data set uM1 = 41.04% and combined data set lM1 = 54.58% of variance explained). A separation between the ethnical groups still does not occur (Table 4; Fig. 34 and Fig. 38). The variation in form space was examined also on continental level and based on sex (see below), and no grouping can be observed.

Table 9 shows, that Europeans have the smallest upper and lower molars both at continental (Fig. 36) and at population level (Fig. 37). Within the populations, the largest upper molars belong to the Khoisan and, at continental level, to the African. Here, the combined size values are an exception, because the biggest teeth belonged to the Asian populations. A similar size variation can be observed for the lower molars. Based on the EDJ, CER and CRO data sets on a continental level, African specimen show the largest sizes, but the largest size for the combined analysis are shown by the Asian populations.

There is a visible discordance between the upper and lower M1s for the Near East and the Khoisan populations (Fig. 33). When comparing the size difference between the ethnicities, Khoisan have the largest lower molars and the Near East population the second smallest. Conversely, for the uM1 Bedouins are the greatest in size, while Khoisan teeth are classified rather small. The size in all other populations stays quite consistent between the upper and lower jaw.

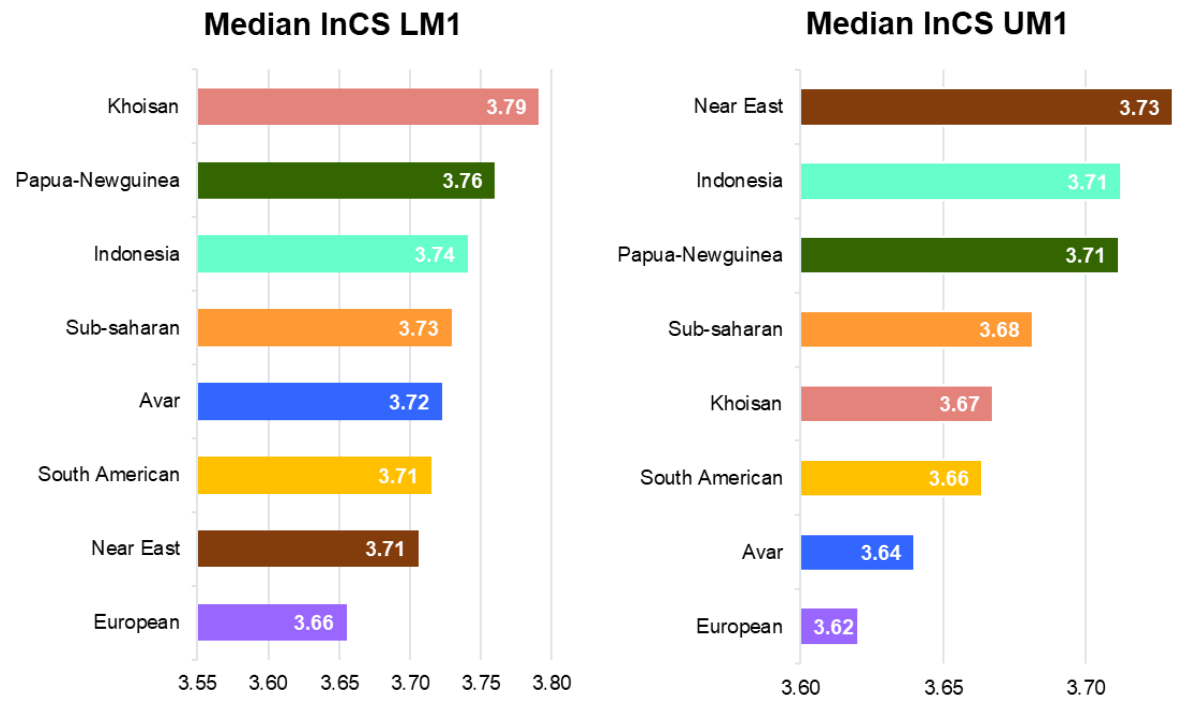

Fig. 33 – Combined data set of uM1s and lM1s showing the median size differences between populations. There is a striking discordance between the upper and lower M1s of Khoisan and Near East sample. This could be an effect of the rather small sample size.

Table 4 – Percentage of variance explained in form space by the PCs.

	uM1				lM1			
PC	**EDJ**	**CER**	**COM**	**CRO**	**EDJ**	**CER**	**COM**	**CRO**
PC1	41.12	31.72	41.04	33.52	54.62	45.77	54.58	48.99
PC2	15.01	22.48	16.50	16.35	9.21	22.21	13.59	13.46
PC3	9.83	11.39	10.29	13.44	6.84	11.69	6.58	9.04
PC4	6.19	9.60	5.25	9.49	5.79	6.36	5.64	6.65
PC5	4.78	6.40	4.74	6.69	4.19	3.67	3.35	4.55
PC6	4.14	5.32	3.40	5.13	3.27	2.76	3.02	3.87

On a continental level, the Kruskal-Wallis-Test (Table 5) shows no significance in any of the lM1 data sets (CER, p = 0.668 CRO, p = 0.250; EDJ, p = 0.267; COM, p = 0.466) and in the

CER data set of the upper molars (CER, p = 0.175). The crown outline and the combined data sets in uM1 provide significant values (CRO, p = 0.021; COM, p = 0.044), and the EDJ highly significant values (EDJ, p = 0.003). The Man-Whitney-U test (Table 6) shows that the EDJ (p = 0.001), crown outline (p = 0.004) and combined data (p = 0.007) in Asians are significantly larger than in Europeans. There is also a significant difference in size for the EDJ and crown outline between the South American and the European populations (p = 0.008 and 0.021, respectively).

Table 5 – The difference in size between geographical groups.

	lM1				uM1			
	CER	**CRO**	**EDJ**	**COM**	**CER**	**CRO**	**EDJ**	**COM**
Kruskal-Walis-test	1.519	4.109	3.951	2.551	4.962	9.693	13.915	8.116
asympt. significance	0.688	0.250	0.267	0.466	0.175	**0.021**	**0.003**	**0.044**

Table 6 – Shows the significant results of the Man-Whitney-U test (with Monte Carlo permutation n = 10.000) within the uM1 EDJ, CRO und combined data sets based on the geographical origin.

Continental groups and data set	**Significance**	**Mean Rank**
Asian vs. European EDJ	p = 0.001	20.71 / 10.94
Asian vs. European Crown outline	p = 0.004	20.29 / 11.31
Asian vs. European combined data set	p = 0.007	20.00 / 11.56
South American vs European EDJ	p = 0.008	17.33 / 9.31
South American vs. European Crown outline	p = 0.210	16.67 / 9.56

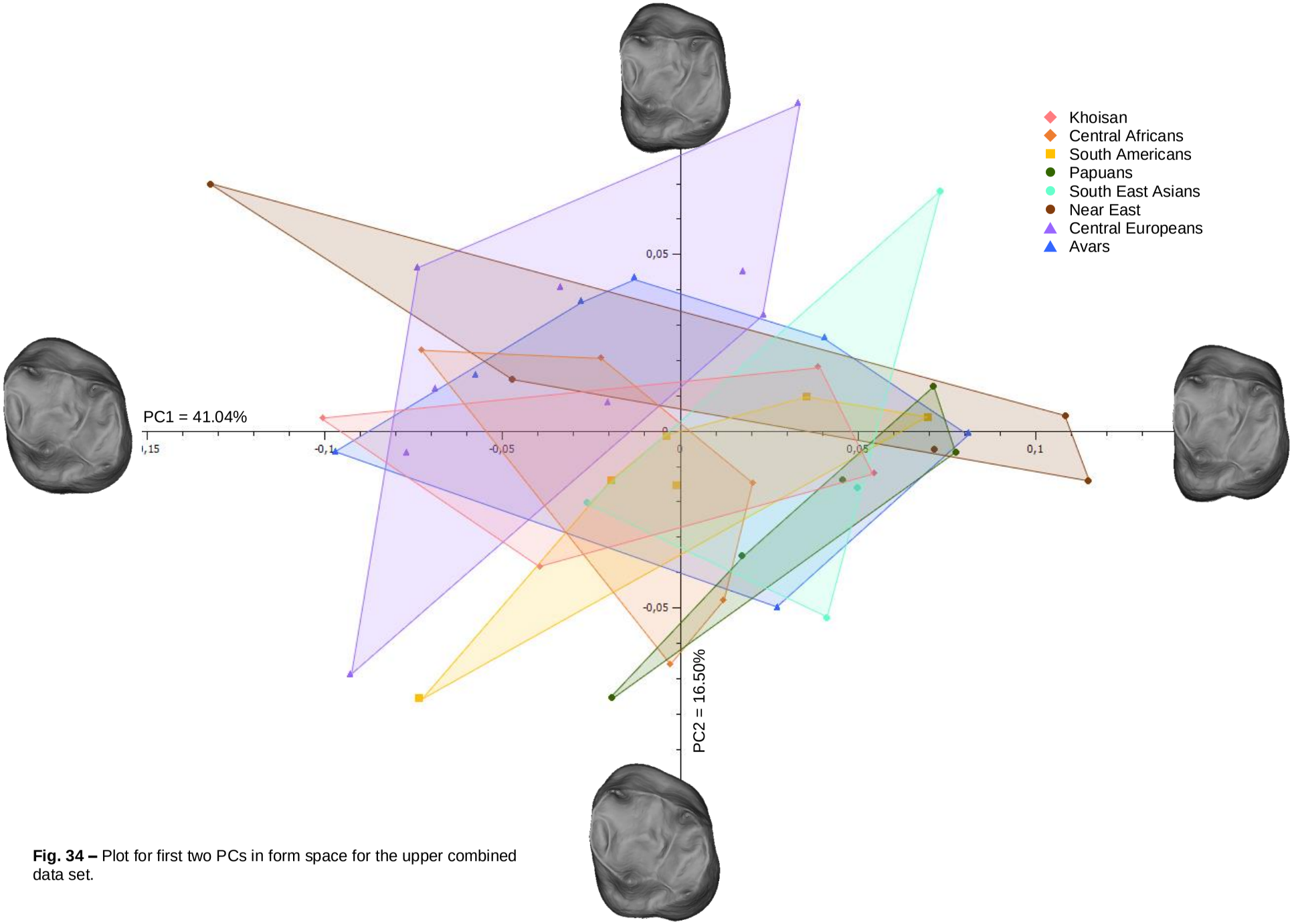

Fig. 34 – Plot for first two PCs in form space for the upper combined data set.

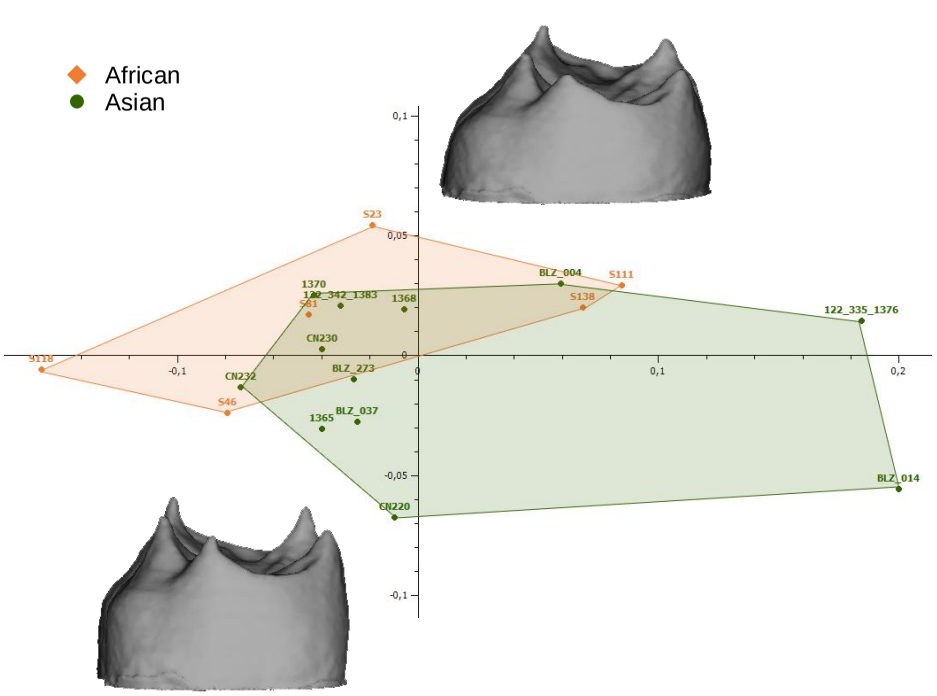

Fig. 35 – Difference in crown height between Asian and African populations.

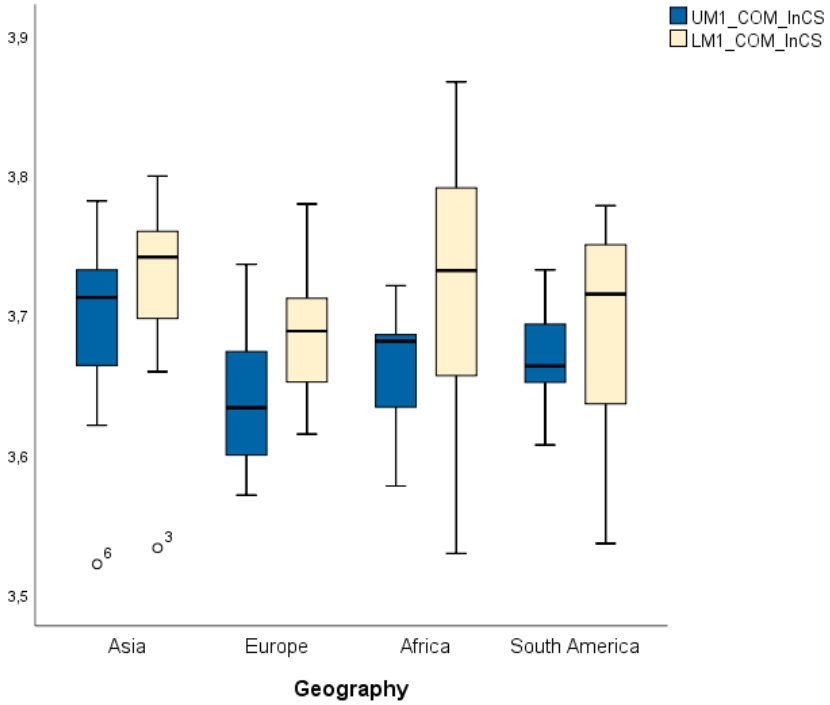

Fig. 36 – Boxplot shows the difference in upper and lower molar size between continental groups.

At ethnic level we obtained slight between-group differences in the median size, despite the small sample size. Khoisan show the largest lower M1 median values, while the largest upper M1 median values can be found within the Papuans (CER) and Bedouins (CRO, EDJ, COM) (Table 9 and Fig. 37). European consistently provide the smallest median values both in uM1 and lM1.

The KW-Test only shows significant results for the uM1 EDJ (Table 7; p = 0.027). Similar to the continental analysis, Europeans show the smallest size for both upper and lower M1s. Papuans (p = 0.001), South East Asians (p = 0.02) and South Americans (p = 0.001) have significantly larger upper EDJs than Europeans and Papuans also have significantly larger EDJs than Central Africans (Table 8; p = 0.03).

Table 7 – The difference in size between populations.

	lM1				**uM1**			
	CER	**CRO**	**EDJ**	**COM**	**CER**	**CRO**	**EDJ**	**COM**
Kruskal-Walis-test	7.590	10.987	9.466	9.423	9.142	11.685	15.805	9.806
asympt. significance	0.370	0.139	0.221	0.224	0.243	0.111	**0.027**	0.200

Table 8 – Shows the significant results of the Man-Whitney-U test (with Monte Carlo permutation n = 10.000) within the uM1 EDJ data set based on the ethnicity.

Continental groups and data set	**Significance**	**Mean Rank**
Papuan vs. European	p = 0.001	12.00 / 5.00
South East Asian vs. European	p = 0.020	10.75 / 5.33
South American vs. European	p = 0.001	12.17 / 5.22
Papuan vs. Central African	p = 0.030	7.60 / 3.40

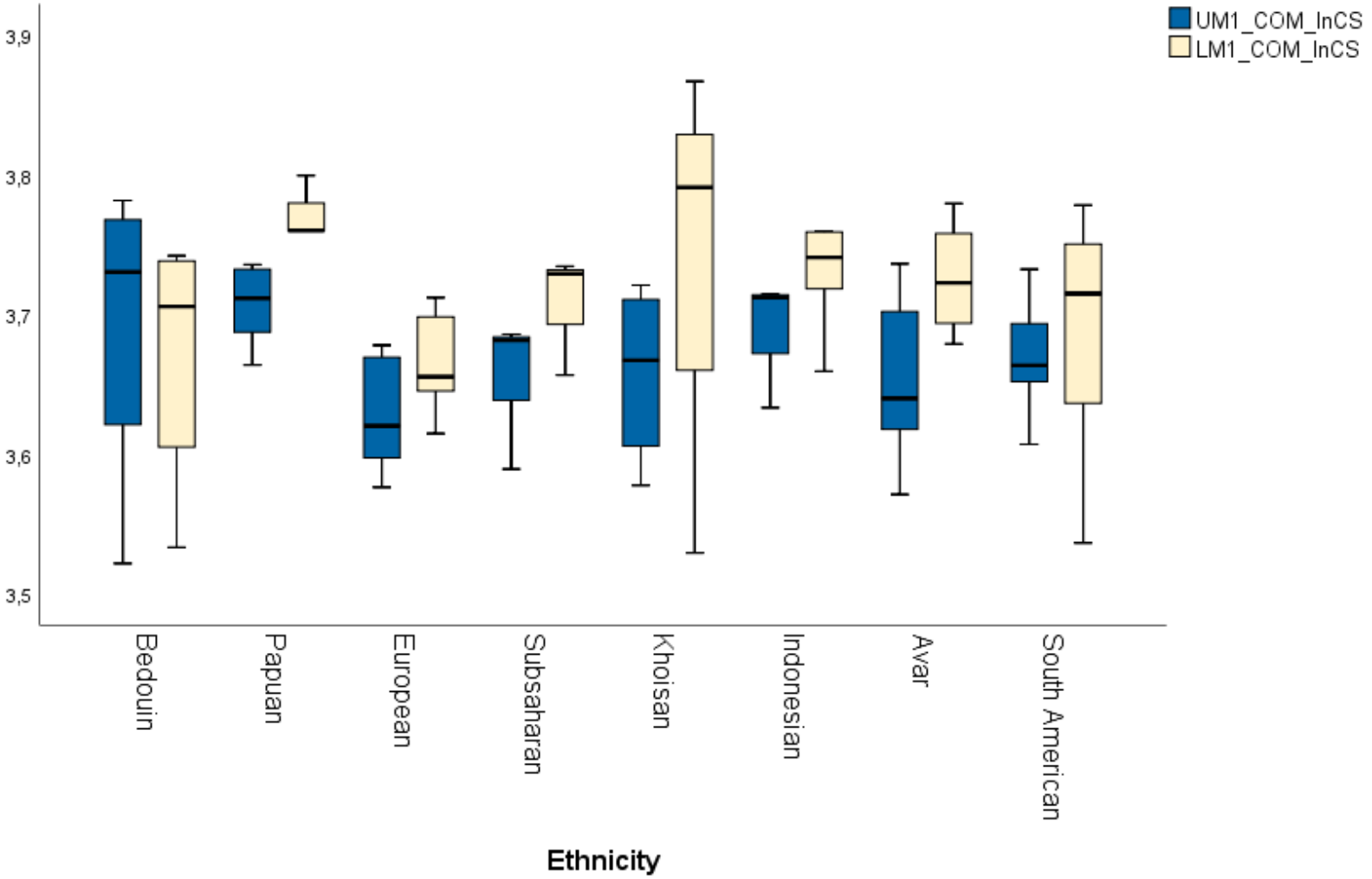

Fig. 37 – Difference in upper and lower molar size between the eight populations.

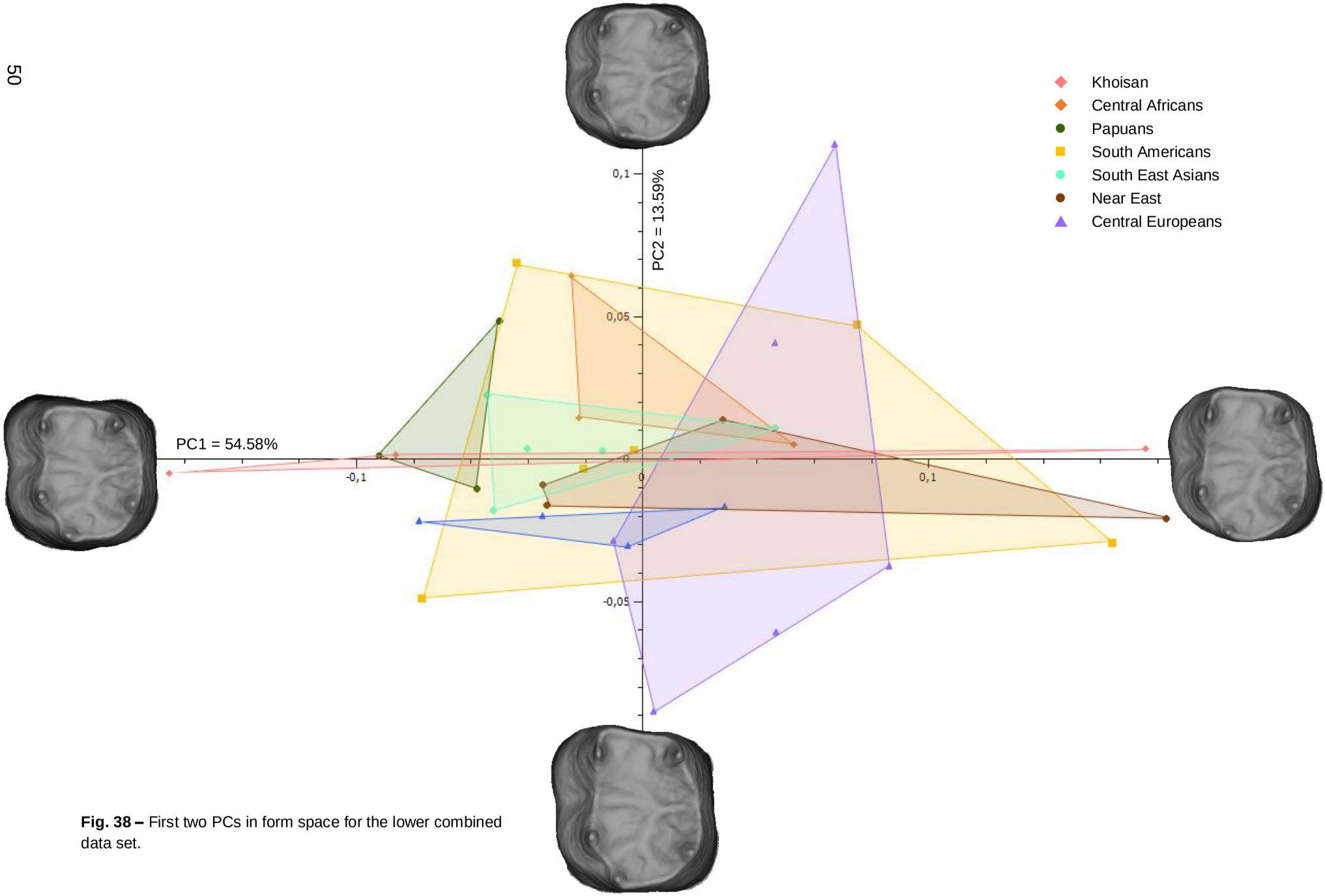

Fig. 38 – First two PCs in form space for the lower combined data set.

Table 9 – lnCS median values compared between continental groups and ethnicities. Bold numbers represent the highest and cursive numbers the lowest values per variable.

	lM1				uM1			
Group/Population	**lnCS_CER**	**lnCS_CRO**	**lnCS_EDJ**	**lnCS_COM**	**lnCS_CER**	**lnCS_CRO**	**lnCS_EDJ**	**lnCS_COM**
Asian	3.1967	3.3669	3.3287	**3.7414**	**3.2261**	**3.3654**	**3.2349**	**3.7125**
European	*3.1408*	*3.3109*	*3.2833*	*3.6885*	*3.1593*	*3.3000*	*3.1436*	*3.6337*
African	**3.2004**	**3.3790**	**3.3446**	3.7318	3.2086	3.3530	3.1847	3.6814
South Am.	3.1909	3.3201	3.3028	3.7149	3.1737	3.3560	3.2078	3.6636
Bedouin	3.1583	3.3417	3.3097	3.7057	3.2259	**3.3705**	**3.2573**	**3.7304**
Papua-Newguinea	3.2456	3.3847	3.3863	3.7600	**3.2313**	3.3604	3.2244	3.7116
European	*3.1333*	*3.2880*	*3.2647*	*3.6554*	*3.1583*	*3.2930*	*3.1408*	*3.6203*
Sub-Saharan	3.1513	3.3781	3.3122	3.7292	3.2306	3.3758	3.1834	3.6814
Khoisan	**3.2496**	**3.4072**	**3.3894**	**3.7908**	3.1820	3.3408	3.1950	3.6673
Indonesia	3.2006	3.3714	3.3145	3.7409	3.1865	3.3561	3.2128	3.7122
Avar	3.1900	3.3451	3.3256	3.7226	3.1752	3.3117	3.1446	3.6399
South Am.	3.1909	3.3201	3.3028	3.7149	3.1737	3.3560	3.2078	3.6636
Total median	3.1678	3.3365	3.3037	3.7049	3.1817	3.3361	3.1842	3.6643

Based on the individuals with known sex (m = 23, f = 15), we did not observe sexual dimorphism for size. The median sizes for both uM1s and lM1s in females are only slightly larger than in males (Table 10 and Fig. 39), but they are not significantly different (Table 11).

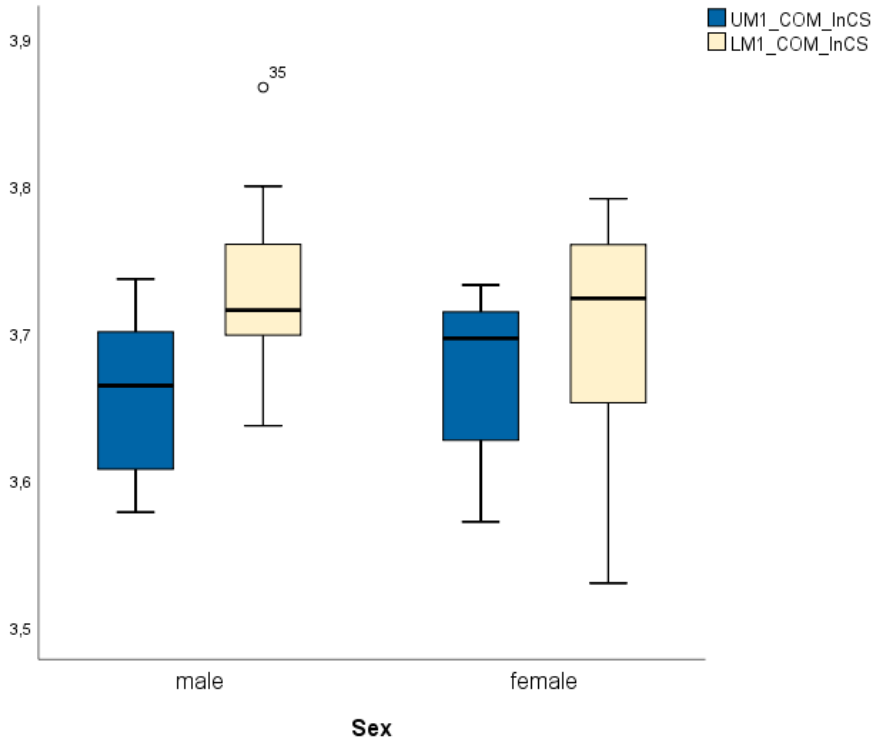

Fig. 39 – Boxplot shows the difference in in M1 median size between sexes.

Table 10 lnCS value medians by sex for all dental traits.

	lM1				uM1			
sex	**CER**	**CRO**	**EDJ**	**COM**	**CER**	**CRO**	**EDJ**	**COM**
males	3.2027	3.3354	3.2980	3.7152	3.1603	3.3285	3.1847	3.6639
females	3.1772	3.3325	3.3257	3.7232	3.1885	3.3514	3.2108	3.6961
Total mean	3.1812	3.3404	3.3043	3.7137	3.1793	3.3310	3.1843	3.6638

Table 11 – Man-Whitney-U test between M1 sizes in both sexes.

	lM1				uM1			
Sex	**CER**	**CRO**	**EDJ**	**COM**	**CER**	**CRO**	**EDJ**	**COM**
Mann-Whitney-U	45.000	62.000	56.000	91.000	77.000	86.000	57.000	91.000
Wilcoxon-W	90,000	107.000	101.000	244.000	230.000	239.000	102.000	244.000
Z	-1.134	-0.063	-0.441	-0.487	-1.107	-0.708	-0.378	-0.487
asympt. sig.	0.257	0.950	0.659	0.626	0.268	0.479	0.705	0.626

Allometry

A multiple multivariate regression of the natural logarithm of the centroid size on the combined data set showed that only a small percentage (uM1 = 4.14%, lM1 = 3.19%) of the shape variance can be explained by size. In smaller uM1 the hypocone is placed further distolingually, which leads to a compressed occlusal surface and an elongation in the paracone-hypocone axis. Therefore, smaller uM1s tend to have an ellipsoid shape. Large uM1s are squared shaped with well-developed distal horn tips. The distance between the four major tips is equally distributed (Fig. 40). The crown height is only affected slightly, whereat small molars have shorter crowns than large molars. For the lM1s, the most manifest shape variation relates to the relative proportions between the occlusal surface and the basal area. In large molars, the occlusal surface is smaller in proportion, whereas the difference between the occlusal surface and the basal area is less distinctive in small lM1s. At the same time, large lM1s have a higher crown than small ones.

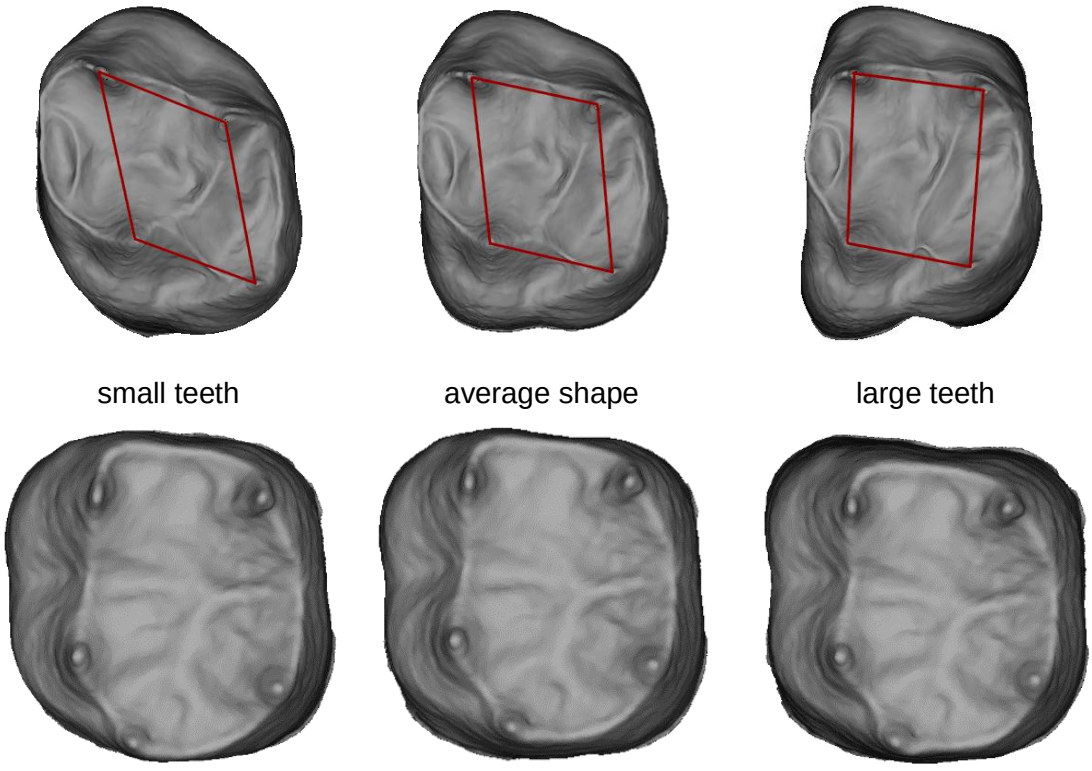

Fig. 40 – Allometric shape variation in upper and lower combined data sets. The warps are showing the extrapolations of the distribution range for the purpose of visualization.

Qualitative traits

In the uM1s, the most frequent trait is the anterior transverse ridge (ATR) (Table 19). Seventy-one percent of the 45 upper teeth show some grade of manifestation of this trait, which can be found in each ethnical group. However, only one uM1 (cat. no. 5389) of the six South American teeth shows an ATR. The second most frequent trait (63%) of this uM1 sample is the anterior accessory tubercle (AAT). The combined occurrence of a protoconule and a paraconule is the most common (27%). A stand- alone protoconule or a paraconule can be found in 18% of the sample, and 38% of the uM1 show no manifestation of AAT at all. Additionally, an enamel extension along the roots could be found only in the Indonesian uM1 2583.

The Carabelli's tubercle is the most frequent in the Near Eastern (100%) and the Central African (100%) sample (Table 19), where all individuals show at least a minimal manifestation of the trait. Three individuals (cat. no. S81, CS569, 1370) of the uM1 sample (7%) have a Carabelli tubercle classified as an ASUDAS – class 7. Papuan, Avar, South East-Asians and Khoisan teeth show less frequent tubercles and also the weakest degree of manifestation. As for the metaconule, only one-third of the sampled upper M1s possesses a metaconule with a generally low degree of expression, except for two teeth (4%) with a degree four (cat. no. CS569 and S29). For CS569 both additional cusps are prominent, while S29 only shows a well-expressed metaconule (4) and a degree 2 Carabelli's tubercle. Examples of the manifestations can be observed in Fig. 41.

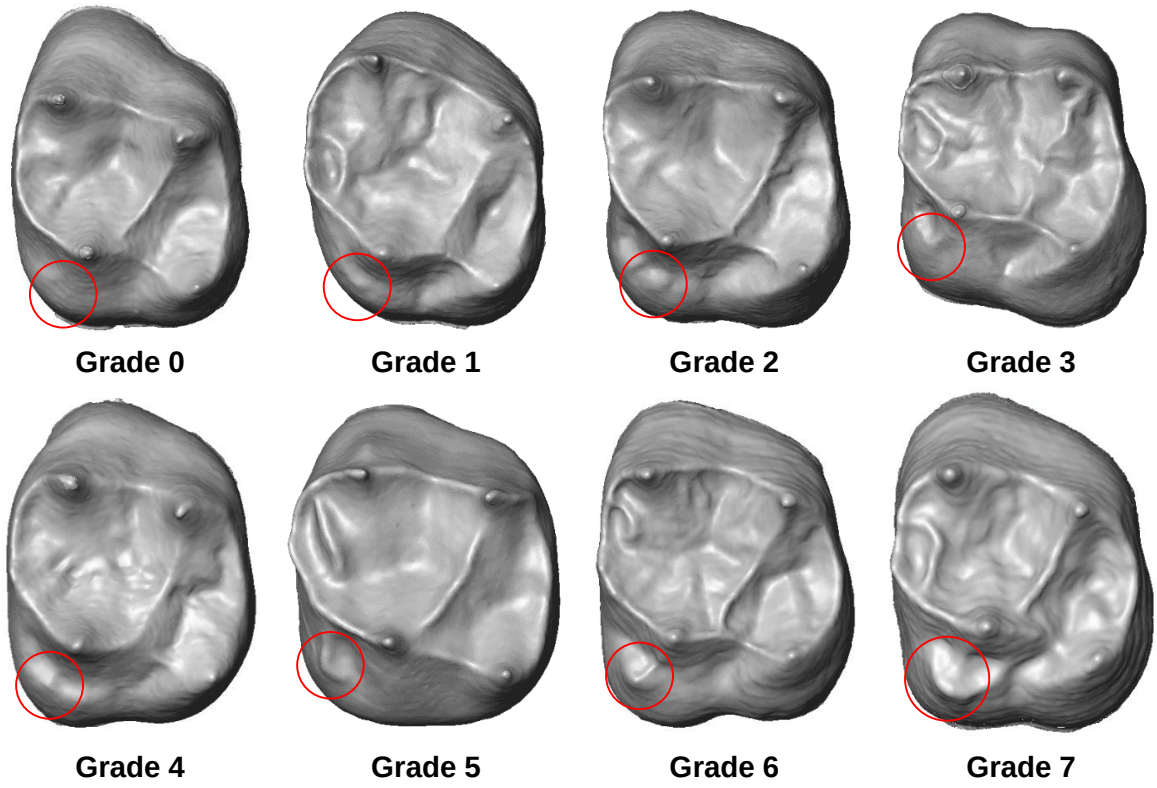

Fig. 41 – Carabelli's tubercle – manifestation grades within the sample.

The calculation of the Carabelli's trait peculiarity depending on the size of the tooth, by using the lnCS values as a size indicator, shows no significant values (Table 12). The explained variance by the model was low (6.2%).

However, the data set using the mean linear distances (units in mm, all 4 ICDs averaged into one mean) shows a significant inverted relationship between the Carabelli expression and the relative ICDs (Table 13), except for manifestation grade 6 (p = 0.052). However, the results of the remaining 4 individual ICD data sets are only partially significant, whereat the significance breakpoint seems to appear at CAR = 2 (Table 14 to 17). An exception is the protocone – paracone data set, where none of results was significant. The control approach with the merged peculiarity groups could neither provide significant values (Table 18).

Table 12 – Ordinal regression results using the lnCs value of the main horn tips/CRO lnCs. CAR = 7 serves as the reference value, therefore is missing in this table.

Grade of manifestation	Estimate	Sig.
CAR = 0	-18.059	0.088
CAR = 1	-16.732	0.112
CAR = 2	-15.955	0.129
CAR = 3	-15.141	0.149
CAR = 4	-14.992	0.153
CAR = 5	-14.442	0.168
CAR = 6	-13.882	0.186

Table 13 – Ordinal regression results using the mean linear distances / CRO area. CAR = 7 serves as the reference value, therefore is missing in this table.

Grade of manifestation	Estimate	Sig.
CAR = 0	-11.546	0.003
CAR = 1	-10.165	0.008
CAR = 2	-9.380	0.013
CAR = 3	-8.557	0.022
CAR = 4	-8.412	0.024
CAR = 5	-7.846	0.035
CAR = 6	-7.238	0.052

Table 14 – Ordinal regression results using the protocone – paracone ICD values /CRO area. CAR = 7 serves as the reference value, therefore is missing in this table.

Grade of manifestation	Estimate	Sig.
CAR = 0	-4.472	0.125
CAR = 1	-3.186	0.268
CAR = 2	-2.441	0.393
CAR = 3	-1.652	0.562
CAR = 4	-1.510	0.596
CAR = 5	-0.970	0.734
CAR = 6	-0.407	0.887

Table 15 – Ordinal regression results using the protocone – hypocone ICD values /CRO area. CAR = 7 serves as the reference value, therefore is missing in this table.

Grade of manifestation	Estimate	Sig.
CAR = 0	-6.892	0.005
CAR = 1	-5.541	0.020
CAR = 2	-4.795	0.042
CAR = 3	-4.000	0.086
CAR = 4	-3.854	0.098
CAR = 5	-3.284	0.159
CAR = 6	-2.691	0.253

Table 16 – Ordinal regression results using the metacone – hypocone ICD values /CRO area. CAR = 7 serves as the reference value, therefore is missing in this table.

Grade of manifestation	Estimate	Sig.
CAR = 0	-8.757	0.008
CAR = 1	-7.476	0.022
CAR = 2	-6.745	0.037
CAR = 3	-5.930	0.064
CAR = 4	-5.779	0.071
CAR = 5	-5.186	0.104
CAR = 6	-4.553	0.154

Table 17 – Ordinal regression results using the paracone – metacone ICD values /CRO area. CAR = 7 serves as the reference value, therefore is missing in this table.

Grade of manifestation	Estimate	Sig.
CAR = 0	-7.712	0.008
CAR = 1	-6.343	0.024
CAR = 2	-5.521	0.047
CAR = 3	-4.665	0.090
CAR = 4	-4.520	0.100
CAR = 5	-3.980	0.148
CAR = 6	-3.419	0.216

Table 18 – Ordinal regression results using the mean absolute ICD values / CRO area and the grouped Carabelli traits. High Carabelli manifestations (5-7 = "big") serves as the reference value, therefore is missing in this table.

Grade of manifestation	Estimate	Sig.
CAR = under breakpoint	-6.973	0.081
CAR = small	-5.221	0.185

In the lM1 sample, the hypoconulid is ubiquitous (in fact, its horn tip was represented by a fix landmark in the GM analysis). The anterior fovea (AF) is the next frequent trait (Table 20). Forty-three percent of the lM1 possess an AF, and five of them present additionally a complete midtrigonid crest (MC). Only the South American specimen 806 shows a distal trigonid crest, which is in fact a rare trait. The Central African and Khoisan individuals show the highest frequency of AF (67% for both groups). European, South East Asian and Avar teeth show no manifestation of a midtrigonid crest. Only 17% of the lM1 reveals an expression of a MC, most frequently found in the Papuan (33%), Central African (33%), Khoisan (33%) and South American (29%) sample. However, it has to be considered that the Papuan, Central African and Khoisan samples each have a very small sample size (n = 3). Indonesian, Avar, and Sub-Saharan teeth lack this trait completely.

Thirteen teeth with additional cusps could be found in the lM1 sample. In particular, there are seven slightly expressed entoconulids almost exclusively visible on the EDJ and six metaconulids of which one (cat. no. 5758) is well expressed. The South American lower molar 5758 also possesses a degree 2 entoconulid. All other teeth exhibit only one of the two possible additional cusps.

Table 19 – Percentage of qualitative trait manifestations in ASUDAS classes clustered by ethnicity in uM1 (NE = Near East; PAP = Papua New Guinea; EU = European; CAF = Central African; KHO = Khoisan; SEA = South-East Asian; AV = Avars; SA = South American).

Trait	Manifestation	NE (n = 5)	PAP (n = 5)	EU (n = 9)	CAF (n = 5)	KHO (n = 4)	SEA (n = 4)	AV (n = 7)	SA (n = 6)	Total (n = 40)
Carabelli	1	0.20	0.40	0.11	0.40	0.25	0.25		0.67	**0.27**
	2	0.20		0.22	0.20	0.50	0.25	0.29		**0.20**
	3	0.40		0.22	0.20			0.29		**0.16**
	4							0.14		**0.02**
	5	0.20		0.22						**0.07**
	6		0.20						0.17	**0.04**
	7				0.20		0.25	0.14		**0.07**
	not present		0.40	0.22		0.25	0.25	0.14	0.17	**0.18**
ATR	present	0.60	0.80	1.00	0.80	0.75	0.50	0.86	0.17	**0.71**
	not present	0.40	0.20		0.20	0.25	0.50	0.14	0.83	**0.29**
Metaconule	1	0.80	0.60		0.20		0.50	0.29	0.17	**0.29**
	2		0.20	0.22						**0.07**
	3									**-**
	4					0.25		0.14		**0.04**
	not present	0.20	0.20	0.78	0.80	0.75	0.50	0.57	0.83	**0.60**
AAT	protoconule	0.20		0.22	0.20	0.25		0.29	0.17	**0.18**
	paraconule	0.40		0.11	0.20		0.75	0.29		**0.18**
	proto+paraconule	0.40	0.60	0.33				0.43		**0.27**
	not present		0.40	0.33	0.60	0.75	0.25		0.83	**0.38**
Sum of traits absolute		17	14	24	12	8	10	22	8	**115**
% out of total		0.15	0.12	0.21	0.10	0.07	0.09	0.19	0.07	**1**
Trait per individual		3.4	2.8	2.7	2.4	2	2.5	3.1	1.3	**2.5**

Table 20 – Percentage of qualitative trait manifestations in ASUDAS classes clustered by ethnicity in lM1 (NE = Near East; PAP = Papua New Guinea; EU = European; CAF = Central African; KHO = Khoisan;, SEA = South-East Asian; AV = Avars; SA = South American)

Trait	Manifestation	NE (n = 4)	PAP (n = 3)	EU (n = 6)	CAF (n = 3)	KHO (n = 3)	SEA (n = 5)	AV (n = 74)	SA (n = 7)	Total (n = 35)
Midtrigonid crest	1	0.25	0.33		0.33	0.33			0.29	**0.17**
	not present	0.75	0.67	1.00	0.67	0.67	1.00	1.00	0.71	**0.83**
Anterior fovea	present	0.25	0.33	0.33	0.67	0.67	0.60	0.25	0.43	**0.43**
	not present	0.75	0.67	0.67	0.33	0.33	0.40	0.75	0.57	**0.57**
Groove pattern	+	0.75			0.33	0.33	0.60	0.25	0.57	**0.34**
	Y	0.25	1.00	1.00	0.67	0.67	0.20	0.75	0.43	**0.60**
	X									**-**
	unknown						0.20			**0.03**
Entoconulid	1		0.33	0.17					0.14	**0.09**
	2			0.17		0.33			0.29	**0.11**
	not present		0.67	0.63	1.00	0.67	1.00	1.00	0.57	**0.80**
Metaconulid	1	0.25				0.33	0.40		0.14	**0.14**
	2									**-**
	3				0.33					**0.03**
	4								0.14	**0.03**
	not present	0.75	1.00	1.00	0.67	0.67	0.60	1.00	0.71	**0.80**
Protstylid	present		0.33	0.50	0.33	0.33		0.25		**0.20**
	not present	1.00	0.67	0.50	0.67	0.67	1.00	0.75	1.00	**0.80**
Sum of traits absolute		7	7	13	8	9	9	6	17	**76**
% out of total		0.09	0.09	0.17	0.11	0.12	0.12	0.08	0.22	**1**
Trait per individual		1.7	2.3	2.2	2.7	1.8	1.8	1.5	2.4	**2.2**

The most common groove pattern is type ‘y’ which was found in 22 teeth, followed by type ‘+’ which is present in 12 individuals (Fig. 42). None of the specimens in the sample shows the pattern ‘x’ where the protoconid and the entoconid are in contact with each other. The occlusal surface of specimen 1365 was too damaged to determine its groove pattern.

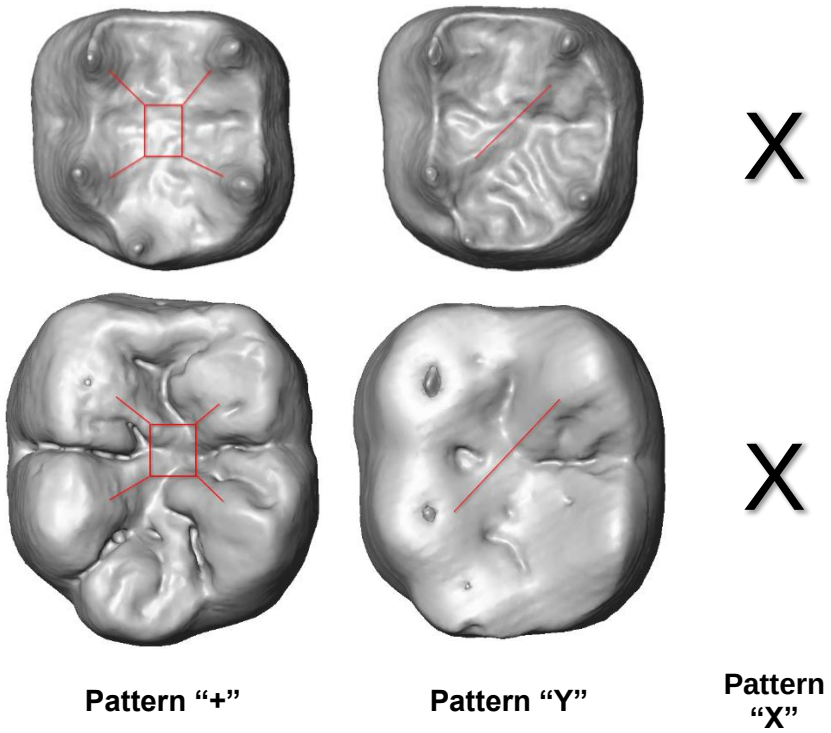

Fig. 42 – Groove patterns in lM1.

The whole sample including both upper and lower M1s, lacks a significant manifestation of a protostyl/id, and only 8 of the lM1 have a class 1 tubercle. European molars show in the upper molar data set the highest total frequency of traits (21%), while in the lower molars the highest frequency could be found in the South American group (22%). This is not surprising since they both are the relatively largest groups in their respective sample. We therefore calculated the average number of traits per individual, dividing the absolute number of traits within a population through the sample size of the population (Fig. 43). In upper molars, the highest numbers of traits per individual are represented the Near East (3.4), Avar (3.1), and the Papuan (2.8) samples. Europeans (2.7), South East Asians (2.5) and Central Africans (2.4) show intermediate scores, while Khoisan (2) and South Americans (1.3) show low manifestation of traits per individual. For the lower molars, the highest values can be found within the Khoisan (3) and Central African (2.7) samples and the lowest values in Avar (1.5), Near East (1.7) and South East Asian (1.8) groups. The average number of traits per individual is 2.5 for the uM1s and 2.2 for the lM1s.

There is an inverted relation between the quantity of traits per individual within populations for the uM1s and lM1s (Fig. 43). Groups with higher trait number in uM1s tend to have less traits per individual in the lower molars (Near East, Avars), while groups with less traits in the upper molars have a higher number of traits in the lower molars (Khoisan, Central Africans and South Americans). Populations with values close to the mean trait number show more or less the same number of traits in both upper and lower molars (European, Papuans and South East Asians).

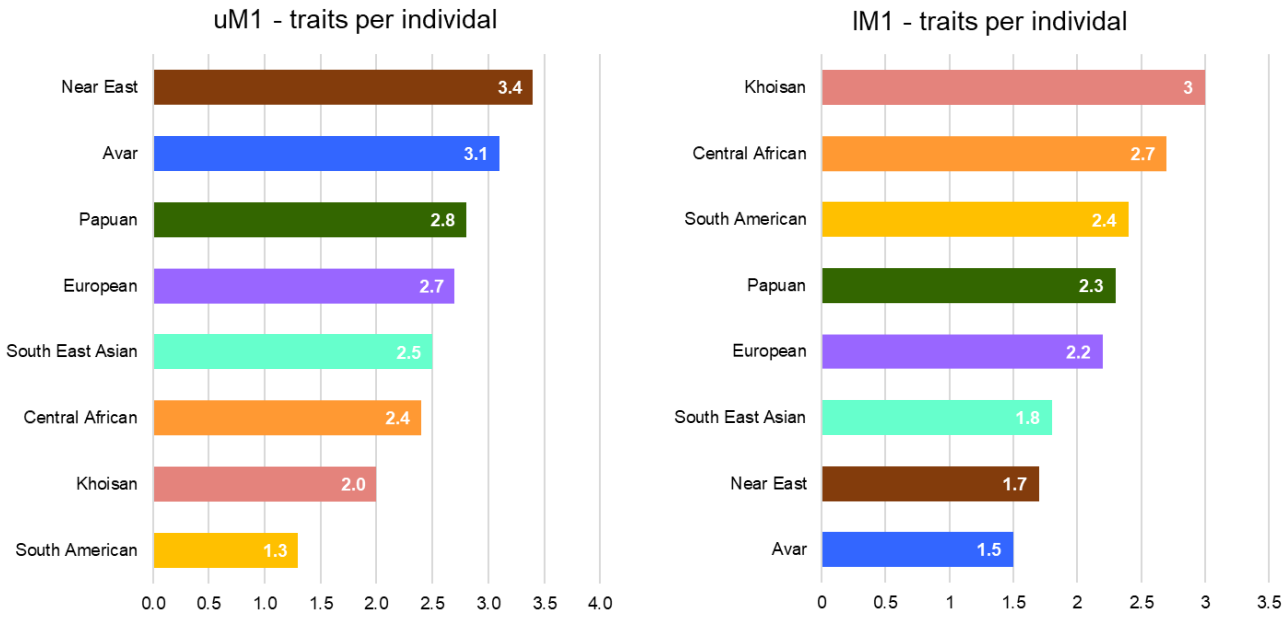

Fig. 43 – Number of traits/individual clustered by populations. Groups with great uM1 trait number have small lM1 numbers and vice versa. Groups in the middle stay relatively constant.

Owing to the small sample size, the differences in trait frequency were tested via Fisher's exact test on both ethnical and continental level. Only two of the nine present traits show a possibility of influence (Table 21). The ATR and AAT are both uM1 traits located at the mesial part of the tooth and provided significant values on both population and continental level. The metaconule shows significant differences in uM1s based on ethnicity. Interestingly, none of the lM1 traits show significant values based on ethnical grouping.

Table 21 – Probability of ethnical or geographical influence via Fisher's exact test (chi^2 crosstable).

		Fisher's exact test	
		continental level	**ethnical level**
uM1	**Carabelli**	1.000	0.808
	Anterior transverse ridge (ATR)	0.004	0.024
	Metaconule	0.038	0.181
	Anterior accessory tubercle (AAT)	0.006	0.012
lM1	**Entoconulid**	0.364	0.399
	Metaconulid	0.227	0.611
	Midtrigonid crest (MC)	0.215	0.490
	Anterior fovea	0.928	0.986
	Groove pattern	0.165	0.102

Discussion

The aim of this study was to gather morphological information about first permanent upper and lower molars (both uM1s and lM1s, respectively), and to assess their variability in terms of shape and size within modern human populations. For the analysis, 45 upper and 35 lower first molars from eight different populations were considered and examined through geometric morphometric as well as traditional analyses of the discrete traits. The shape variation in four different data sets (EDJ, cervical line, combined data and crown outline) was analyzed through quantitative methods in order to capture the morphology of the entire molar crown. Discrete traits on the enamel-dentine junction were described qualitatively.

In both uM1s and lM1s, all four landmark data sets showed a wide overlap of shape and form between the different populations and continental groups. Therefore, despite different lifestyles (e.g., agriculturalist, nomads, hunters and gatherers) and population history no morphological differences in tooth shape could be detected between the groups. Given that our study material originates only from recent modern humans, we can assume that their food was prepared extra orally before consumption, at least to a certain degree. One can argue that with greater source availability and the pre-processing of food the selective pressure on high bite forces and efficient break-down of food particles has been eased in modern humans (Wrangham et al., 1999). In modern human societies malocclusion is present at high rates and it affects 36 - 87% of the world population (Thilander, 2001; Varrela, 2006; Dhar et al., 2007; Corrêa-Faria et al., 2014). However, it is also known, that odontogenesis is strictly regulated by genetic patterning (Deter, 2009; Forshaw, 2014). The formation of a certain dental phenotype is determined by a dynamic system of interactions and folds of the inner enamel epithelium. The position, size and shape of the later cusps are dependent on influence of their associated enamel knot but can be influenced by other knots, grow rates and other heritable effects (Salazar-Ciudad and Jernvall, 2002; Polly and Mock, 2018; Ortiz et al., 2018). Therefore, the shape of the dental crown has to be determined long before its eruption, since enamel does not go through later remodelling (except by means of mechanical and chemical agents). External factors like malnutrition (hypoplasia), population history (trend in discrete traits) or food preparation (change in size and malocclusion) might have an influence on individual dental development.

The combined data set allowed us to analyze not only the occlusal surface of the molars, but also included the factor crown height. The performed analyses showed that in upper molars the shape is mostly dependent of the relation of the trigon and the talon. Small, round teeth have a relatively small (but further distally placed) hypocone compared to their trigon and a low crown, while large, rectangular teeth have a relatively large hypocone and high crown. These findings agree with the results of Gómez-Robles (2007) in uM1 and with the results of

Teplanova (2015) in uM2. For the lM1, the variation in crown height corresponds to a variation in the relative size of the occlusal area. A large occlusal surface coincides with a relatively low crown height, while a narrow shape corresponds to a high crown.

Based on the results, the distal aspect of both upper and lower molars can be considered as the most variable area. In upper molars this applies to the talon and therefore for the hypocone. The distal variation also describes the mesiodistal shift of the buccal cusps, especially for the metacone. If the metacone is mesiolingually shifted and well pronounced, the hypocone also becomes larger and placed further distally. These shape differences remind to some extent what observed in Neanderthal molars, even though the degree of variation differs. There, the metacone was shifted mesiolingually compared to anatomically modern humans and this resulted in a very large hypocone (Bailey, 2004; GómezRobles et al., 2007). This effects seem to be smaller in modern humans (Bailey, 2002; Bailey and Hublin, 2006; Benazzi et al., 2011; Weber et al., 2016; Martin et al., 2017) but was still visible in our sample.

In lower molars the distal variation mainly occurred owing to the position and peculiarity of the hypoconulid. A high pairwise correlation was found between the upper and lower molars, effecting repeatedly the distal aspects in both counterparts. A functional dentition, and therefore an optimal cusp arrangement, is necessary for effective mastication. The concept of a bilaterally balanced occlusion states that each tooth is in permanent contact with two other counterparts from the opposite dental arch (Kraus et al., 1988). While the mesial part of the first upper molars interacts with the central part of the first lower molars, the distal cusps (especially the hypocone) articulate with the point of contact area between the first and the second lower molar (Fig. 44). Therefore, the relative position of the hypocone to the trigon in uM1 seems to be strongly related to the distal reduction in lM1. Even though upper and lower M1s developed within jaws with different embryologic origin, the fact that the occlusal aspects showed high covariation is again proof of a tight genetic control during odontogenesis. This condition can be interpreted in terms of the functional need for dental pairs to occlude well for an effective mastication. In contrast to other occluding structures, such as joints, the only possibility for antagonistic teeth to adapt to each other is intercuspation and finally wear. The magnitude of shape correlation of the antagonist EDJs obviously seems to be sufficient, probably because the surfaces of upper and lower M1s do not need to be perfectly matched for effective food comminution, and wear would also compensate for miss-matches during use. The correlation between the whole crowns (combined data set) is clearly less than that between the occlusal surfaces (EDJ). The former data set includes also crown height and shape of the crown base. Minor miss-matching of tooth surface elevations, i.e. the EDJ situated below or above the occlusal plane, could however be compensated by the attachment of the tooth in the sockets of the jaw bone. This would mean that the constraints for higher shape

correlation of the whole crown could be relieved. This potential approach is yet still an open field for future research.

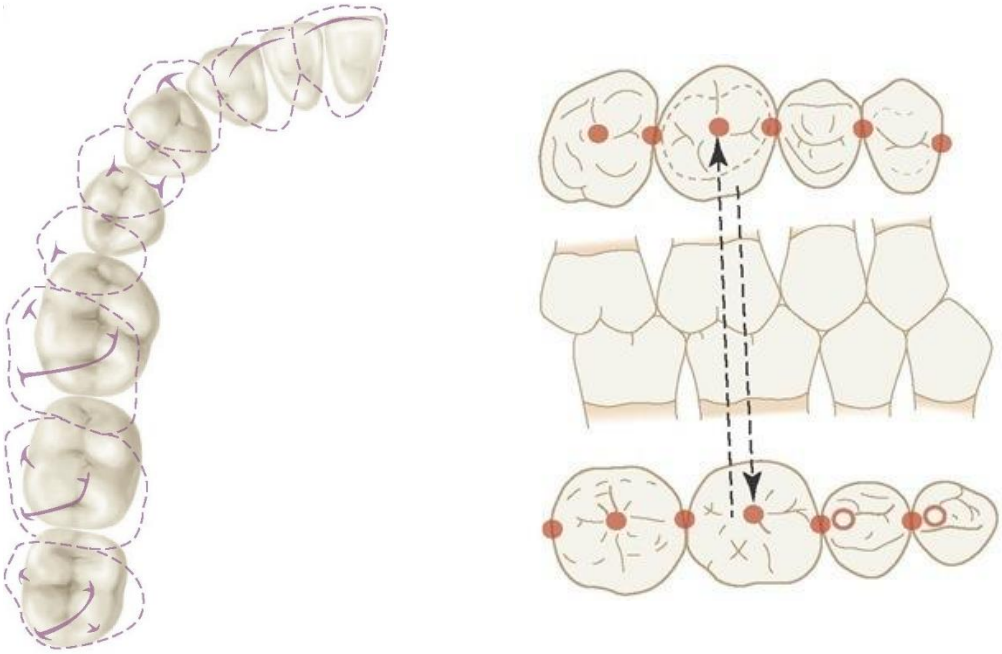

a) **b)**

Fig. 44 – a) Shows a symmetrical occlusion at the left dental arches. The lower molars are illustrated in colour; purple lines indicate the position of the upper molars; **b)** shows the cusps interaction between uM1 and lM1 // upper mesiolingual cusp (protocone) occludes in the central fossa of lM1 // lower distobuccal cusp (hypoconid) occludes in the central fossa of uM1. Source: www.what-when-how.com

The highest pairwise correlation was found after comparing the cervical to the crown outline data set within upper and lower molars separately. This outcome is in agreement with the findings by Teplanova (2015) for uM2s.

Our investigation also revealed a variation of the cervical line in lower molars. The appearance varies from hourglass-shaped to ellipsoid. A comparison of the dental model for the most extreme teeth along PC1 allowed us to link these changes of the cervical outline to the shape of the dental roots. A distinct constriction corresponded to a wide angle between the mesial and distal roots, while a less pronounced or no constriction is associated to straight roots forming an acute angle at the cervix (Fig. 45).

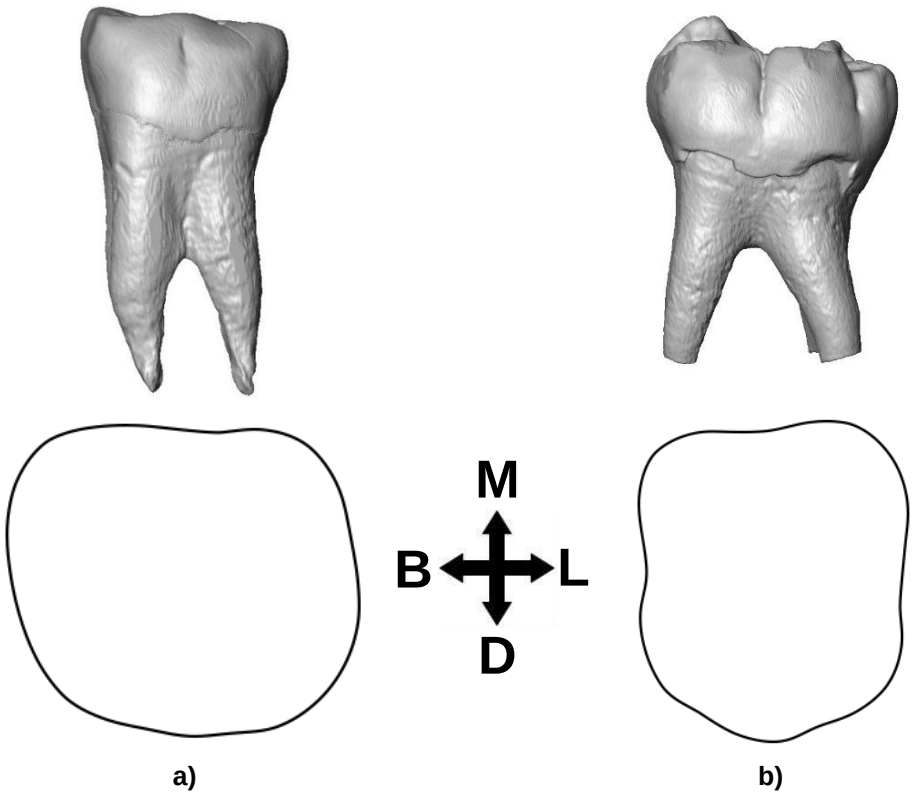

Fig. 45 – Buccal view of **a)** CS569 (no constriction) and; **b)** S118 (expressed constriction).

The first change in the absolute size of the masticatory system of *Homo* became evident 1.9 – 1.6 mya ago with *H. habilis* (McHenry and Coffing, 2000). Henceforth, the relative size of teeth changed constantly during the phylogenetic development towards modern humans. Based on the lnCS median values Asians, South Americans and Africans have bigger teeth than Europeans, and the difference is greater in the uM1 than in lM1 (Fig. 46). These findings are similar to those from other studies on major populations of the world (Hanihara and Ishida, 2005). Khoisan, Papuans and Bedouins have the largest uM1 and lM1 which is consistent with the findings by Krenn (2015) in premolars, and by Teplanova (2015) in uM2. The lnCS median results showed an odd distribution of the highest values on a continental level in lower first molars. The largest size was found within the African populations with the exception of the combined data set. At first glance this could seem incorrect, given that the combined data set is composed of the cervical outline and the EDJ data, but considering the nature of the centroid sizes it is indeed possible. The advantage of the combined data set is that it represents the whole dental crown including its height. In the case of high and narrow crowns this could results in larger centroid sizes than in the separate data sets. Our sample showed that Asian populations have higher crowns than Africans (Fig. 35). Similar results were found previously in Avar vs. European premolars (Krenn et al., 2019).

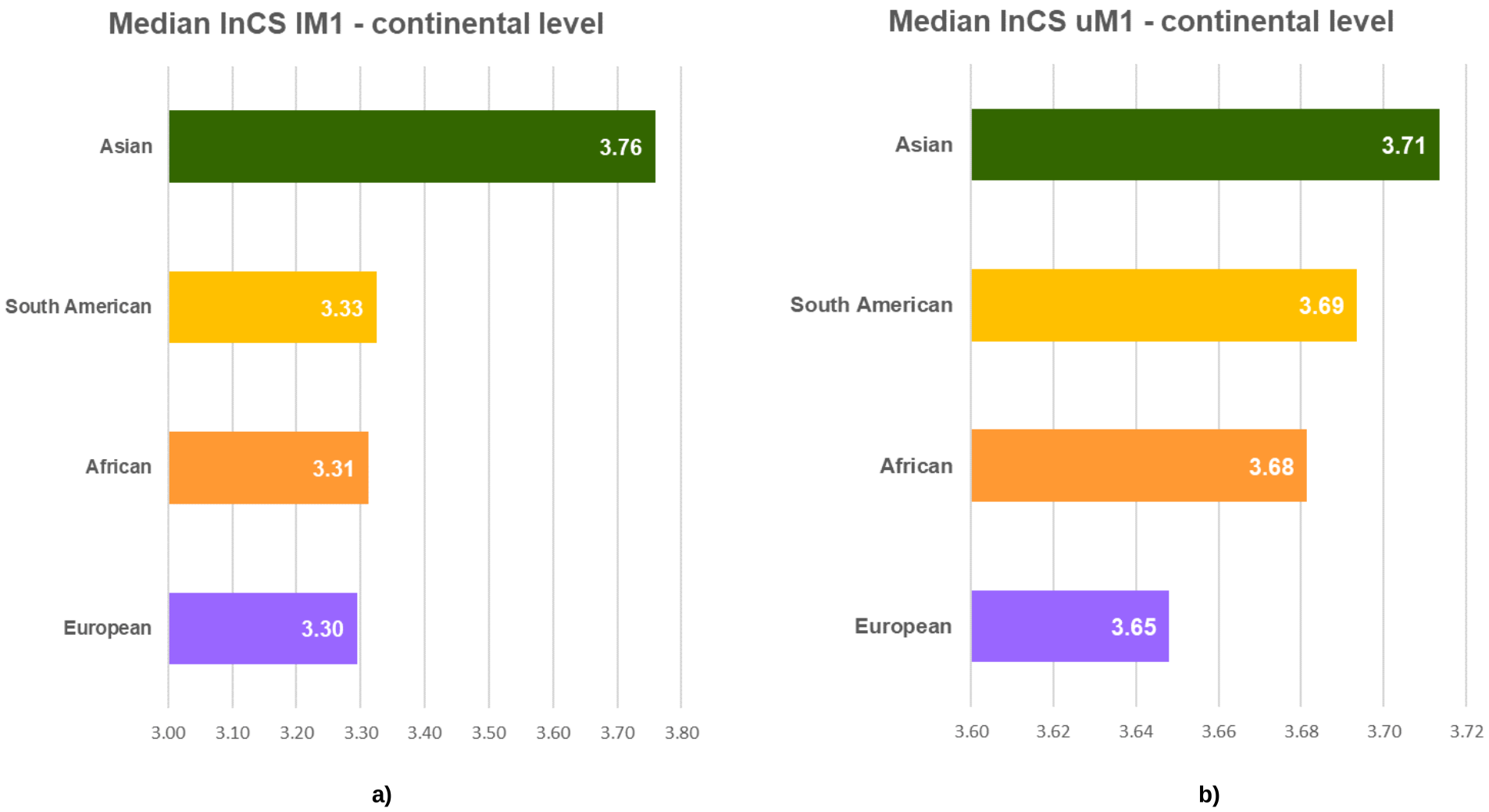

Fig. 46 – Combined data set of uM1 and lM1 pairs and their mean size difference in **a)** lM1 and; **b)** uM1 grouped by continent of origin

In addition, a striking discordance between the upper and lower M1s for the Near East and Khoisan populations was found (Fig. 33). This effect is most likely caused by the small lower molar sample size within the populations (Khoisan n = 3, Near East n = 4). Therefore, we decided to remain on a continental level with our results.

Our attempt to explain the large shape variation within populations through size showed only a very small covariation between size and shape. The allometric effect accounted only for a negligible influence on shape in both upper and lower first molars. Therefore, the effect of size on shape is minimal. These findings are consistent with Wood (1983) and Bailey (2016) who compared deciduous second molars and lM1 in Neanderthals and modern human teeth, but is not in agreement with Polychronis (2013) who found significant allometry on both the upper and lower occlusal surface.

Sexual dimorphism is strongly pronounced in mammals, especially in the anterior dentition, but is reduced in modern humans (Hillson, 1996). According to previous studies based on measurements of the crown diameters, the difference is a result of unequal composition of dentin and enamel. The X chromosome regulates only the enamel growth while the Y chromosome controls both the enamel and the dentine accretion. Alvesalo and Tammisalo (1981) showed that an additional X chromosome (e.g. 47, XXX) results in proportionally thicker enamel with no changes in the dentine thickness, while a missing sexual chromosome (45, X0) results in a thinner enamel showing no difference in the dentine production. Y chromosome aneuploides (46, XY or 47, XYY) affect both enamel and dentine (Townsend and Alvesalo, 1985). Schwartz (2005) confirmed these findings. Other studies showed only difference in dentine but not in enamel thickness (Harris and Hicks, 1998; Stroud et al., 1994, 1998) or no difference at all (Górka et al., 2015) between sexes. Our study supports Górka's findings about size difference between sexes given that no significant size difference could be found in our sample. However, the sample used in this study is too heterogenous for definite statements.

In the first half of the 20th century several studies started focusing on dental traits (Scott and Irish, 2017). Owing to the lack of virtual methods researchers applied other methods for scoring and recording dental remains. Long before standards were defined, traits were selected and described arbitrarily (Nelson, 1938; Rosenzweig and Zilberman, 1967; Bang and Hasund, 1971, 1972, 1973; Hasund and Bang, 1985). Claims were made based on small, geographically homogeneous samples, and were therefore not accurate or not applying to all modern human populations. In this regard, the Carabelli's trait is emblematic. First described by Georg Carabelli in 1787, the Carabelli's tubercle was seen as a typical trait of Europeans (Carbonell, 1960; Turner, 1967; Alvesalo et al., 1975; Scott, 1980; Marado and Campanacho, 2013). Today it is known that the tubercle is equally common in other ethnical groups (Hanihara, 2008). Harris (2007) showed that there is a connection between the grade of

expression and the tooth size in maxillary molars, where Carabelli's trait occurs more often in larger molars. Our sample, although also small but heterogenous, shows a total of 37 occurrences (82%) with different grades of expression for the various populations. Based on previous assumptions, one would assume to find a higher expression of the Carabelli's trait in populations with larger teeth. However, the highest prevalence rate was scored for Central Africans, Avars and South East Asians, while only the latter had a significantly larger uM1 median size. Papuans, possessing the largest teeth among our sample, presented only one rank-six Carabelli's tubercle (20% of intergroup formation) and two grade-one tubercles (40% of intergroup formation). All other high-degree manifestations of the Carabelli's trait are found in small- to average-sized teeth (based on the population median). These findings do not support the hypothesis that larger teeth present higher expression of the Carabelli's cusp, and are in line with what Teplanova (2015) found for uM2s.

Apparently large crown size alone does not correlate with a greater trait expression, rather does a longer period of formation during morphogenesis (Kondo and Townsend, 2006). We used Hunter's (2010) approach to test the influence of the intercuspal distances (ICD) on expression of the Carabelli's trait with two different approaches. The attempt using the calculated form space values did not produce significant results. It is worth noting that in contrast to the pilot study (Hunter et al., 2010) our first approach used the natural logarithm of Centroid Size (unit less) instead of absolute values. In contrast, using the absolute values for the analysis, the results were partly significant. The data set using the mean Intercuspal Distances divided by the area of the crown outline showed a significant, negative relationship between intercuspal distance and the Carabelli's trait expression. Therefore this data set confirms the statement of Hunter et al. (2010) that the manifestation of the Carabelli's trait and the ICD are connected: molars with small ICD show greater expressions of the Carabelli's trait, given that closely spaced enamel knots provide greater chance for forming additional knots. For the control linear data set (three, summarized Carabelli peculiarities), the lower type of expression (up to Carabelli expression 2) was significant. It is noteworthy, that Scott and Irish (2017) defined expression grade 2 as breakpoint due to difficulties in scoring lower than this threshold, especially on worn teeth.

For the remaining traits, only two among the 10 discrete traits in this work were found to differ between populations, i.e. the expression of the anterior transverse ridge (ATR) and the frequency of the anterior accessory tubercles (AAT). A possible reason for this is that AATs can be frequently found at the origin of an ATR. Marginal tubercles develop similar to the wrinkles on the occlusal surface (Kanazawa et al., 1990), therefore a joint development of AAT and ATR cannot be excluded. Kanazawa (1990) suggested that Asian groups express AAT more often than Africans or Western Eurasians but he also stated that the number of the

tubercles is highly variable ranging from zero to four tubercles. Our sample showed similar tendencies: in accordance with Kanazawa's results (1990) South East Asians have a high percentage of trait expression (75%) and Africans (CAF = 40%, KHO = 25%) rather low ones. However, contrary to Kanazawa et al. (1990), the Bedouin and Avar samples showed 100% trait manifestation and our second Asian sample (Papuans) only 60%. Therefore, more data is required before valid statements considering geographic variation can be made.

Conclusions

All findings of this study are part of a more comprehensive project of the Department of Evolutionary Anthropology, University of Vienna. This master thesis follows a previously established, non-invasive protocol and investigates shape variation of the first permanent molars of the upper and lower jaw.

By means of geometric morphometric methods, we could show that there is no significant shape difference in first molars between modern human populations, neither on an ethnical or continental level. The variation in shape and form is high within each population and the different populations overlap greatly. Gross molar morphology varies mostly between high and narrow or low and broad. Regardless of the great overlap of gross shape between populations, the distal region of both uM1s and lM1s is the most variable within the first molar crowns. In contrast to traditional literature, where only outlines are used for size determination, we applied the natural logarithm of centroid size of the whole 3D data set. This approach made it possible to obtain different signals regarding size than reported earlier. A difference in size was only found in uM1, but not in lM1. This former result is in agreement with previous findings that Europeans possess smaller teeth than Africans and Asians. The allometric effects measured were negligible (~4%) and a significant difference between the sexes could not be confirmed. A high pairwise correlation of the occlusal surface (r_1=0.85 for the EDJ) and the dental crown (r_1= 0.61 for the combined dataset) was revealed between the uM1 and lM1 shape variables. These results reflect the high morphological integration of the molars, and of their occlusal aspect in particular, which in turn can be explained with a strong genetic control during odontogenesis. Few of the discrete traits considered (the anterior transverse ridge and the anterior accessory tubercles) provided population-specific frequencies. Additionally, we replicated the results of Hunter et al. (2010) on the positive correlation between the intercuspal distances and Carabelli's cusp manifestation, but only using absolute measurements in millimetres and not form space data Our investigation also revealed that the shape of the cervical outline (hourglass shaped vs. oval) is dependent on the configuration of the root system (widely spread vs. close or fused roots, respectively), which can be of use in case the roots are not preserved.

Using GM methods made the visualisation of minimal shape differences possible. All our data support the interpretation that dental shape is strictly regulated during odontogenesis - this assures uM1 and lM1 working together efficiently. Concluding we can say, that assigning a single molar to a certain population based only on the M1s shape and form or on its dental traits is not possible. The results also indicate that in comparative studies of hominoid molars the choice of the modern human sample would have no effect.

Acknowledgement

First, I would like to thank my thesis advisor Univ.-Prof. Dr. Gerhard Weber at the Department of Evolutionary Anthropology, University of Vienna for his supervision and his patience during the “genesis” of this study. Special gratitude I want to express to Dr. Cinzia Fornai who tirelessly supported me from the start till the end and helped me whenever I ran into trouble with my research or my writing. Likewise, my gratitude goes to Viktoria Krenn, Msc. who introduced me to the stunning world of the human dentition and helped me with valuable input, whenever needed. My sincere thanks also go to Mag. Martin Dockner (Vienna µCT Lab) for his technical support and a friendly ear. I thank Gerlinde Gruber (Center of Anatomy and Cell Biology – Medical University, Vienna), Maria Teschler-Nicola, Karin Wiltschke-Schrotta, Sabine Eggers and Eduard Winter (Natural History Museum Vienna) as well as Israel Hershkovitz (Department of Anatomy and Anthropology, Sackler Faculty of Medicine, Tel Aviv University) for access to materials. My appreciation goes to Katarina Matiasek, who provided background information on the collections. Many thanks go to my fellow office and lunch mates Lisa Buchegger, Msc. and Nina Oberklammer, Bsc. for the interesting discussions and for all the fun we had in the last years.

I am grateful for the encouragement of my superiors and colleagues at Learnchamp - without their support this thesis would not have been possible.

Last but not least, I would like to thank my family and friends for their continuous support, especially my parents, who made my scientific journey possible. This thesis is dedicated to them for giving me the opportunity of a great education and for their tireless support throughout my life.

Thank you! Danke! Grazie! Köszönöm!

Literature

Alvesalo, L., and Tammisalo, E. (1981). Enamel thickness of 45,X females' permanent teeth. Am. J. Hum. Genet. *33*, 464–469.

Alvesalo, L., Nuutila, M., and Portin, P. (1975). The cusp of Carabelli: Occurrence in first upper molars and evaluation of its heritability. Acta Odontol. Scand. *33*, 191–197.

Ash, M.M., Nelson, S.J., and Ash, M.M. (2003). Dental anatomy, physiology, and occlusion (Philadelphia: W.B. Saunders).

Bailey, S.E. (2002). A closer look at Neanderthal postcanine dental morphology: The mandibular dentition. Anat. Rec. *269*, 148–156.

Bailey, S.E. (2004). A morphometric analysis of maxillary molar crowns of Middle-Late Pleistocene hominins. J. Hum. Evol. *47*, 183–198.

Bailey, S.E., and Hublin, J.J. (2006). Did Neanderthals make the Châtelperronian assemblage from La Grotte du Renne (Arcy-sur-Cure, France)? In Neanderthals Revisited: New Approaches and Perspectives, J.-J. Hublin, K. Harvati, and T. Harrison, eds. (Dordrecht: Springer Netherlands), pp. 191–209.

Bailey, S.E., Skinner, M.M., and Hublin, J.-J. (2011). What lies beneath? An evaluation of lower molar trigonid crest patterns based on both dentine and enamel expression. Am. J. Phys. Anthropol. *145*, 505–518.

Bailey, S.E., Benazzi, S., Buti, L., and Hublin, J.-J. (2016). Allometry, merism, and tooth shape of the lower second deciduous molar and first permanent molar: Allometry, Merism, and Tooth Shape of the DM_2 AND M_1. Am. J. Phys. Anthropol. *159*, 93–105.

Bang, G., and Hasund, A. (1971). Morphologic characteristics of the Alaskan Eskimo dentition. I. Shovel-shape of incisors. Am. J. Phys. Anthropol. *35*, 43–47.

Bang, G., and Hasund, A. (1972). Morphologic characteristics of the Alaskan Eskimo dentition. II. Carabelli's Cusp. Am. J. Phys. Anthropol. *37*, 35–39.

Bang, G., and Hasund, A. (1973). Morphologic characteristics of the Alaskan Eskimo dentition. III. Number of cusps on the upper permanent molars. Am. J. Phys. Anthropol. *38*, 721–725.

Bartling, W.C., and Schleyer, T.K. (2003). An application of Geospatial Information System (GIS) technology to anatomic dental charting. AMIA Annu. Symp. Proc. AMIA Symp. 786.

Bei, M. (2009). Molecular genetics of tooth development. Curr. Opin. Genet. Dev. *19*, 504–510.

Benazzi, S., Coquerelle, M., Fiorenza, L., Bookstein, F., Katina, S., and Kullmer, O. (2011). Comparison of dental measurement systems for taxonomic assignment of first molars. Am. J. Phys. Anthropol. *144*, 342–354.

Benazzi, S., Fornai, C., Buti, L., Toussaint, M., Mallegni, F., Ricci, S., Gruppioni, G., Weber, G.W., Condemi, S., and Ronchitelli, A. (2012). Cervical and crown outline analysis of worn

Neanderthal and modern human lower second deciduous molars. Am. J. Phys. Anthropol. *149*, 537–546.

Benazzi, S., Panetta, D., Fornai, C., Toussaint, M., Gruppioni, G., and Hublin, J.-J. (2014). Technical Note: Guidelines for the digital computation of 2D and 3D enamel thickness in hominoid teeth: Guidelines for Digital Enamel Thickness Analysis. Am. J. Phys. Anthropol. *153*, 305–313.

Bernal, V. (2007). Size and shape analysis of human molars: Comparing traditional and geometric morphometric techniques. HOMO *58*, 279–296.

Bookstein, F.L. (1992). Morphometric tools for landmark data: Geometry and biology (Cambridge: Cambridge University Press).

Bookstein, F.L. (1997). Landmark methods for forms without landmarks: morphometrics of group differences in outline shape. Med. Image Anal. *1*, 225–243.

Brook, A.H., Griffin, R.C., Townsend, G., Levisianos, Y., Russell, J., and Smith, R.N. (2009). Variability and patterning in permanent tooth size of four human ethnic groups. Arch. Oral Biol. *54*, S79–S85.

Buchegger, L. (2015). Variation of outer and inner crown morphology in upper premolars. Masterarbeit. Universität Wien.

Butler, P.M. (1956). The ontogeny of molar pattern. In Biological Reviews, (Cambridge), pp. 30–70.

Carbonell, V.M. (1960). The Tubercle of Carabelli in the Kish Dentition, Mesopotamia, 3000 B.C. J. Dent. Res. *39*, 124–128.

Carter, K., Worthington, S., and Smith, T.M. (2014). News and views: Non-metric dental traits and hominin phylogeny. J. Hum. Evol. *69*, 123–128.

Clement, A.F., Hillson, S.W., and Aiello, L.C. (2012). Tooth wear, Neanderthal facial morphology and the anterior dental loading hypothesis. J. Hum. Evol. *62*, 367–376.

Corrêa-Faria, P., Ramos-Jorge, M.L., Martins-Júnior, P.A., Vieira-Andrade, R.G., and Marques, L.S. (2014). Malocclusion in preschool children: prevalence and determinant factors. Eur. Arch. Paediatr. Dent. *15*, 89–96.

Dahlberg, A.A. (1963). ANALYSIS OF THE AMERICAN INDIAN DENTITION. In Dental Anthropology, (Elsevier), pp. 149–177.

Dahlberg, A.A. (1971). Dental morphology and evolution (Chicago: University of Chicago Press).

Delezene, L.K., Zolnierz, M.S., Teaford, M.F., Kimbel, W.H., Grine, F.E., and Ungar, P.S. (2013). Premolar microwear and tooth use in Australopithecus afarensis. J. Hum. Evol. *65*, 282–293.

Deter, C.A. (2009). Gradients of occlusal wear in hunter-gatherers and agriculturalists. Am. J. Phys. Anthropol. *138*, 247–254.

Dhar, V., Jain, A., Van Dyke, T., and Kohli, A. (2007). Prevalence of gingival diseases, malocclusion and fluorosis in school-going children of rural areas in Udaipur district. J. Indian Soc. Pedod. Prev. Dent. *25*, 103.

Fiorin, E., Ibáñez-Gimeno, P., Cadafalch, J., and Malgosa, A. (2017). The study of dental occlusion in ancient skeletal remains from Mallorca (Spain): A new approach based on dental clinical practice. HOMO *68*, 157–166.

Fornai, C., Bookstein, F.L., and Weber, G.W. (2015). Variability of Australopithecus second maxillary molars from Sterkfontein Member 4. J. Hum. Evol. *85*, 181–192.

Forshaw, R. (2014). Dental indicators of ancient dietary patterns: dental analysis in archaeology. Br. Dent. J. *216*, 529–535.

Gaewkhiew, P., Sabbah, W., and Bernabé, E. (2017). Does tooth loss affect dietary intake and nutritional status? A systematic review of longitudinal studies. J. Dent. *67*, 1–8.

Gingerich, P.D. (1974). Size Variability of the Teeth in Living Mammals and the Diagnosis of Closely Related Sympatric Fossil Species. J. Paleontol. *48*, 895–903.

Gómez-Robles, A., Martinón-Torres, M., Bermúdez de Castro, J.M., Margvelashvili, A., Bastir, M., Arsuaga, J.L., Pérez-Pérez, A., Estebaranz, F., and Martínez, L.M. (2007). A geometric morphometric analysis of hominin upper first molar shape. J. Hum. Evol. *53*, 272–285.

Górka, K., Romero, A., and Pérez-Pérez, A. (2015). First molar size and wear within and among modern hunter-gatherers and agricultural populations. HOMO *66*, 299–315.

Gower, J.C. (1975). Generalized procrustes analysis. Psychometrika *40*, 33–51.

Handt, O., Richards, M., Trommsdorff, M., Kilger, C., Simanainen, J., Georgiev, O., Bauer, K., Stone, A., Hedges, R., Schaffner, W., et al. (1994). Molecular genetic analyses of the Tyrolean Ice Man. Science *264*, 1775–1778.

Hanihara, T. (2008). Morphological variation of major human populations based on nonmetric dental traits. Am. J. Phys. Anthropol. *136*, 169–182.

Hanihara, T., and Ishida, H. (2005). Metric dental variation of major human populations. Am. J. Phys. Anthropol. *128*, 287–298.

Harris, E.F. (2007). Carabelli's trait and tooth size of human maxillary first molars. Am. J. Phys. Anthropol. *132*, 238–246.

Harris, E.F., and Hicks, J.D. (1998). A radiographic assessment of enamel thickness in human maxillary incisors. Arch. Oral Biol. *43*, 825–831.

Hasund, A., and Bang, G. (1985). Morphologic characteristics of the Alaskan Eskimo dentition: IV. Cusp number and groove patterns of mandibular molars. Am. J. Phys. Anthropol. *67*, 65–69.

Hershkovitz, I., Weber, G.W., Quam, R., Duval, M., Grün, R., Kinsley, L., Ayalon, A., Bar-Matthews, M., Valladas, H., Mercier, N., et al. (2018). The earliest modern humans outside Africa. Science *359*, 456–459.

Hillson, S. (1996). Dental Anthropology (Cambridge: Cambridge University Press).

Hunter, J.P., and Jernvall, J. (1995). The hypocone as a key innovation in mammalian evolution. Proc. Natl. Acad. Sci. *92*, 10718–10722.

Hunter, J.P., Guatelli-Steinberg, D., Weston, T.C., Durner, R., and Betsinger, T.K. (2010). Model of Tooth Morphogenesis Predicts Carabelli Cusp Expression, Size, and Symmetry in Humans. PLoS ONE *5*, e11844.

Jernvall, J. (2000). Linking development with generation of novelty in mammalian teeth. Proc. Natl. Acad. Sci. *97*, 2641–2645.

Jernvall, J., and Thesleff, I. (2000). Reiterative signaling and patterning during mammalian tooth morphogenesis. Mech. Dev. *92*, 19–29.

Kanazawa, E., Sekikawa, M., and Ozaki, T. (1990). A quantitative investigation of irregular cuspules in human maxillary permanent molars. Am. J. Phys. Anthropol. *83*, 173–180.

Kodama, Y., Harinath, D., Mihara-Tomiyama, N., Tominaga, N., Ide, Y., Nakahara, T., Maeda, M., Igarashi, M., D'Armiento, J., Chada, K., et al. (2019). Hmga2 regulation of tooth formation and association with Sox2 and Nanog expression. Biochem. Biophys. Res. Commun. *509*, 1008–1014.

Kondo, S., and Townsend, G.C. (2006). Associations between Carabelli trait and cusp areas in human permanent maxillary first molars. Am. J. Phys. Anthropol. *129*, 196–203.

Kondo, S., Townsend, G.C., and Yamada, H. (2005). Sexual dimorphism of cusp dimensions in human maxillary molars. Am. J. Phys. Anthropol. *128*, 870–877.

Korenhof, C.A.W. (1982). Evolutionary trends of the inner enamel anatomy of deciduous molars from Sangiran (Java, Indonesia). In Teeth: Form, Function and Evolution., (New York: Columbia University Press), pp. 3550–365.

Kraus, B.S., Jordan, R.E., and Abrams, L. (1988). Dental anatomy and occlusion: a study of the masticatory system (Toronto; Philadelphia: B.C. Decker).

Krenn, V. (2015). Variation of 3D outer and inner crown morphology of lower premolars in modern humans. Masterarbeit. Universität Wien.

Krenn, V.A., Fornai, C., Wurm, L., Bookstein, F.L., Haeusler, M., and Weber, G.W. (2019). Variation of 3D outer and inner crown morphology in modern human mandibular premolars. Am. J. Phys. Anthropol.

Mahoney, P. (2006). Microwear and morphology: Functional relationships between human dental microwear and the mandible. J. Hum. Evol. *50*, 452–459.

Mahoney, P., Schmidt, C.W., Deter, C., Remy, A., Slavin, P., Johns, S.E., Miszkiewicz, J.J., and Nystrom, P. (2016). Deciduous enamel 3D microwear texture analysis as an indicator of childhood diet in medieval Canterbury, England. J. Archaeol. Sci. *66*, 128–136.

Marado, L.M., and Campanacho, V. (2013). Carabelli's trait: Definition and review of a commonly used dental non- metric variable.

Martin, L. (1985). Significance of enamel thickness in hominoid evolution. Nature *314*, 260.

Martin, R.M.G., Hublin, J.-J., Gunz, P., and Skinner, M.M. (2017). The morphology of the enamel–dentine junction in Neanderthal molars: Gross morphology, non-metric traits, and temporal trends. J. Hum. Evol. *103*, 20–44.

Martínez de Pinillos, M., Martinón-Torres, M., Skinner, M.M., Arsuaga, J.L., Gracia-Téllez, A., Martínez, I., Martín-Francés, L., and Bermúdez de Castro, J.M. (2014). Trigonid crests expression in Atapuerca-Sima de los Huesos lower molars: Internal and external morphological expression and evolutionary inferences. Comptes Rendus Palevol *13*, 205–221.

McHenry, H.M., and Coffing, K. (2000). *Australopithecus* to *Homo* : Transformations in Body and Mind. Annu. Rev. Anthropol. *29*, 125–146.

Mitteroecker, P., and Gunz, P. (2009). Advances in Geometric Morphometrics. Evol. Biol. *36*, 235–247.

Molnar, S. (1971). Human tooth wear, tooth function and cultural variability. Am. J. Phys. Anthropol. *34*, 175–189.

Moorrees, C.F.A., and Chadha, J.M. (1962). Crown Diameters of Corresponding Tooth Groups in the Deciduous and Permanent Dentition. J. Dent. Res. *41*, 466–470.

Morita, W. (2016). Morphological comparison of the enamel–dentine junction and outer enamel surface of molars using a micro-computed tomography technique. J. Oral Biosci. *58*, 95–99.

Morita, W., Yano, W., Nagaoka, T., Abe, M., Ohshima, H., and Nakatsukasa, M. (2014). Patterns of morphological variation in enamel-dentin junction and outer enamel surface of human molars. J. Anat. *224*, 669–680.

Moynihan, P., Thomason, M., Walls, A., Gray-Donald, K., Morais, J.A., Ghanem, H., Wollin, S., Ellis, J., Steele, J., Lund, J., et al. (2009). Researching the impact of oral health on diet and nutritional status: Methodological issues. J. Dent. *37*, 237–249.

Nager, G. (1960). Der Vergleich zwischen dem räumlichen Verhalten des Dentin-kronenreliefs und dem Schmelzrelief der Zahnkrone. Cells Tissues Organs *42*, 226–250.

Nelson, C.T. (1938). The teeth of the Indians of Pecos Pueblo. Am. J. Phys. Anthropol. *23*, 261–293.

Olejniczak, A.J., Gilbert, C.C., Martin, L.B., Smith, T.M., Ulhaas, L., and Grine, F.E. (2007). Morphology of the enamel-dentine junction in sections of anthropoid primate maxillary molars. J. Hum. Evol. *53*, 292–301.

Ortiz, A., Skinner, M.M., Bailey, S.E., and Hublin, J.-J. (2012). Carabelli's trait revisited: An examination of mesiolingual features at the enamel–dentine junction and enamel surface of Pan and Homo sapiens upper molars. J. Hum. Evol. *63*, 586–596.

Ortiz, A., Bailey, S.E., Schwartz, G.T., Hublin, J.-J., and Skinner, M.M. (2018). Evo-devo models of tooth development and the origin of hominoid molar diversity. Sci. Adv. *4*, eaar2334.

Pääbo, S., Poinar, H., Serre, D., Jaenicke-Després, V., Hebler, J., Rohland, N., Kuch, M., Krause, J., Vigilant, L., and Hofreiter, M. (2004). Genetic Analyses from Ancient DNA. Annu. Rev. Genet. *38*, 645–679.

Palci, A., and Lee, M.S.Y. (2019). Geometric morphometrics, homology and cladistics: review and recommendations. Cladistics *35*, 230–242.

Panda, B., Dhanu Radha, V., Chidambaram, S., Arindam, M., Thilagavathi, R., Manikandan, S., Thivya, C., Ramanathan, A.L., and Ganesh, N. (2019). Fluoride Contamination in Groundwater—A GIS and Geostatistics Reappraisal. In GIS and Geostatistical Techniques for Groundwater Science, (Elsevier), pp. 309–322.

Pereira, S.M., Ambrosano, G.M.B., Cortellazzi, K.L., Tagliaferro, E.P.S., Vettorazzi, C.A., Ferraz, S.F.B., Meneghim, M.C., and Pereira, A.C. (2010). Geographic Information Systems (GIS) in Assessing Dental Health. Int. J. Environ. Res. Public. Health *7*, 2423–2436.

Peterson, A., Abella, E.F., Grine, F.E., Teaford, M.F., and Ungar, P.S. (2018). Microwear textures of Australopithecus africanus and Paranthropus robustus molars in relation to paleoenvironment and diet. J. Hum. Evol. *119*, 42–63.

Plomp, E., von Holstein, I.C.C., Koornneef, J.M., Smeets, R.J., Baart, J.A., Forouzanfar, T., and Davies, G.R. (2019). Evaluation of neodymium isotope analysis of human dental enamel as a provenance indicator using 1013 Ω amplifiers (TIMS). Sci. Justice.

Polly, P.D., and Mock, O.B. (2018). Heritability: the link between development and the microevolution of molar tooth form. Hist. Biol. *30*, 53–63.

Polychronis, G., Christou, P., Mavragani, M., and Halazonetis, D.J. (2013). Geometric morphometric 3D shape analysis and covariation of human mandibular and maxillary first molars: Human First Molar 3D Shape Analysis and Covariation. Am. J. Phys. Anthropol. n/a-n/a.

Rohlf, F.J., and Slice, D. (1990). Extensions of the Procrustes Method for the Optimal Superimposition of Landmarks. Syst. Zool. *39*, 40.

Rosenzweig, K.A., and Zilberman, Y. (1967). Dental morphology of Jews from Yemen and Cochin. Am. J. Phys. Anthropol. *26*, 15–21.

Salazar-Ciudad, I., and Jernvall, J. (2002). A gene network model accounting for development and evolution of mammalian teeth. Proc. Natl. Acad. Sci. *99*, 8116–8120.

Schwartz, G.T., and Dean, M.C. (2005). Sexual dimorphism in modern human permanent teeth. Am. J. Phys. Anthropol. *128*, 312–317.

Schwartz, G.T., Thackeray, J.F., Reid, C., and van Reenan, J.. (1998). Enamel thickness and the topography of the enamel–dentine junction in South African Plio-Pleistocene hominids with special reference to the Carabelli trait. J. Hum. Evol. *35*, 523–542.

Scott, G.R. (1980). Population variation of Carabelli's trait. Hum. Biol. 63–78.

Scott, G.R., and Irish, J.D. (2017). Human tooth crown and root morphology: the Arizona State University dental anthropology system.

Scott, G.R., and Turner, C.G. (1997). The anthropology of modern human teeth: Dental morphology and its variation in recent human populations (Cambridge: Cambridge University Press).

Skinner, M.M., Gunz, P., Wood, B.A., and Hublin, J.-J. (2008a). Enamel-dentine junction (EDJ) morphology distinguishes the lower molars of Australopithecus africanus and Paranthropus robustus. J. Hum. Evol. *55*, 979–988.

Skinner, M.M., Wood, B.A., Boesch, C., Olejniczak, A.J., Rosas, A., Smith, T.M., and Hublin, J.-J. (2008b). Dental trait expression at the enamel-dentine junction of lower molars in extant and fossil hominoids. J. Hum. Evol. *54*, 173–186.

Skinner, M.M., Wood, B.A., and Hublin, J.-J. (2009). Protostylid expression at the enamel-dentine junction and enamel surface of mandibular molars of Paranthropus robustus and Australopithecus africanus. J. Hum. Evol. *56*, 76–85.

Skinner, M.M., Alemseged, Z., Gaunitz, C., and Hublin, J.-J. (2015). Enamel thickness trends in Plio-Pleistocene hominin mandibular molars. J. Hum. Evol. *85*, 35–45.

Slice, D.E. (2005). Modern Morphometrics in Physical Anthropology.

Slice, D.E., Bookstein, F.L., Rohlf, F.J., and Marcus, L.F. (1996). Appendix I. A glossary for geometric morphometrics. In Advances in Morphometrics, (New York: Plenum Press), pp. 531 –551.

Smith, T.M., Olejniczak, A.J., Zermeno, J.P., Tafforeau, P., Skinner, M.M., Hoffmann, A., Radovčić, J., Toussaint, M., Kruszynski, R., Menter, C., et al. (2012). Variation in enamel thickness within the genus Homo. J. Hum. Evol. *62*, 395–411.

Spoor, C.F., Zonneveld, F.W., and Macho, G.A. (1993). Linear measurements of cortical bone and dental enamel by computed tomography: Applications and problems. Am. J. Phys. Anthropol. *91*, 469–484.

Stahl, W. (1968). Search for natural variations in calcium isotope abundances. Earth Planet. Sci. Lett. *5*, 171–174.

Stroud, J.L., Buschang, P.H., and Goaz, P.W. (1994). Sexual dimorphism in mesiodistal dentin and enamel thickness. Dentomaxillofacial Radiol. *23*, 169–171.

Stroud, J.L., English, J., and Buschang, P.H. (1998). Enamel thickness of the posterior dentition: Its implications for nonextraction treatment. Angle Orthod. *68*, 141–146.

Teplanova, D. (2015). Geometric morphometric analyses of modern human upper second molars. Masterarbeit. Universität Wien.

Thesleff, I., and Sharpe, P. (1997). Signalling networks regulating dental development. Mech. Dev. *67*, 111–123.

Thilander, B. (2001). Prevalence of malocclusion and orthodontic treatment need in children and adolescents in Bogota, Colombia. An epidemiological study related to different stages of dental development. Eur. J. Orthod. *23*, 153–168.

Townsend, G., and Alvesalo, L. (1985). Tooth size in 47, XYY males: evidence for a direct effect of the Y chromosome on growth. Aust. Dent. J. *30*, 268–272.

Townsend, G., Richards, L., Hughes, T., Pinkerton, S., and Schwerdt, W. (2003). The value of twins in dental research. Aust. Dent. J. *48*, 82–88.

Townsend, G., Harris, E.F., Lesot, H., Clauss, F., and Brook, A. (2009). Morphogenetic fields within the human dentition: A new, clinically relevant synthesis of an old concept. Arch. Oral Biol. *54*, S34–S44.

Tucker, A.S., and Sharpe, P.T. (1999). Molecular Genetics of Tooth Morphogenesis and Patterning: The Right Shape in the Right Place. J. Dent. Res. *78*, 826–834.

Turner, C.G. (1967). Dental Genetics and Microevolution in Prehistoric and Living Koniag Eskimo. J. Dent. Res. *46*, 911–917.

Turner, C.G., Nichol, C.R., and Scott, G.R. (1991). Scoring procedures for key morphological traits of the permanent dentition: the Arizona State University Dental Anthropology system. In Advances in Dental Anthropology., (New York: Wiley-Liss.), pp. 13–31.

Varrela, J. (2006). Masticatory Function and Malocclusion: A Clinical Perspective. Semin. Orthod. *12*, 102–109.

Walker, A., Hoeck, H., and Perez, L. (1978). Microwear of mammalian teeth as an indicator of diet. Science *201*, 908–910.

Weber, G.W., and Bookstein, F.L. (2011). Virtual anthropology: a guide to a new interdisciplinary field (New York: Springer).

Weber, G.W., Fornai, C., Gopher, A., Barkai, R., Sarig, R., and Hershkovitz, I. (2016). The Qesem Cave hominin material (part 1): A morphometric analysis of the mandibular premolars and molar. Quat. Int. *398*, 159–174.

Weiss, M.L., and Mann, A.E. (1985). Human biology and behavior: an anthropological perspective (Boston; Toronto: Little, Brown).

Wood, B.A., and Abbott, S.A. (1983). Analysis of the dental morphology of Plio-pleistocene hominids. I. Mandibular molars: crown area measurements and morphological traits. J. Anat. *136*, 197–219.

Wood, B.A., and Zuckerman, L. (1981). Tooth Size and Shape and their Relevance to Studies of Hominid Evolution [and Discussion]. Philos. Trans. R. Soc. B Biol. Sci. *292*, 65–76.

Wrangham, R.W., Jones, J.H., Laden, G., Pilbeam, D., and Conklin-Brittain, N. (1999). The Raw and the Stolen: Cooking and the Ecology of Human Origins. Curr. Anthropol. *40*, 567–594.

Yoshimura, H., Honjo, M., Mashiyama, Y., Kaneyama, K., Segami, N., Sato, J., Sugai, T., Kato, N., and Onoda, N. (2008). Multiple tooth-losses during development suppress age-dependent emergence of oscillatory neural activities in the oral somatosensory cortex. Brain Res. *1224*, 37–42.

Zanolli, C., Pan, L., Dumoncel, J., Kullmer, O., Kundrát, M., Liu, W., Macchiarelli, R., Mancini, L., Schrenk, F., and Tuniz, C. (2018). Inner tooth morphology of Homo erectus from Zhoukoudian. New evidence from an old collection housed at Uppsala University, Sweden. J. Hum. Evol. *116*, 1–13.

(1998). The Cambridge encyclopedia of human growth and development (Cambridge, UK ; New York, NY, USA: Cambridge University Press).

Attachment

ESHE'19 poster abstract submission

Morphological assessment of modern human upper and lower first molars

Human first permanent molars are well studied, but comprehensive investigations that elucidate 3D crown morphology variation of geographically diverse populations are lacking. The aim of the present study is to provide quantitative and qualitative data from upper and lower first molar crowns (uM1s and lM1s, respectively) for the understanding of human dental shape and size variation. Studying the outer enamel surface (OES) can be limited by various factors such as abrasion or damage. The enamel-dentin-junction (EDJ) is less affected by those factors and shows a high correspondence of features with the OES. Following previously established, non-invasive protocols [1],[2], we focused both on the EDJ and the OES. This study combines 3D imaging techniques and geometric morphometric methods [3], and compares the outcome of the morphometric analyses with the results of the analysis of discrete traits scored on the EDJ.

A total of 80 molar crowns (45 uM1s and 35 lM1s) were examined. The sample consisted of populations with different geographical origin and subsistence background: Sub-Saharan Africans, Southeast Asians, Bedouins, Avars, South Americans, and Central Europeans. 3D image data were obtained at the Vienna µCT Lab, Austria. Four sets of landmarks were considered: EDJ occlusal surface, cervical outline, crown outline, and a dataset combining the EDJ surface with the cervical outline which represented the dentinal crown most comprehensively. Multivariate statistics were used to assess shape variance, covariance, and allometry. The discrete traits were assessed based on the Arizona State University Dental System [4].

The landmark-based analyses showed that in both upper and lower first molars, morphology did not differ significantly between modern human group. Shape and form variation were generally high within each population, and the different populations overlapped widely. First molar crown gross morphology varied between narrow and high, and broad and low. The most distal regions of both uM1s and lM1s were more variable than the mesial regions. Molar size variation (here represented by both 2D and 3D landmark configurations) confirmed previous findings, namely Europeans possess smaller teeth than Africans and Asians. The allometric effects measured were negligible (~4%). Similarly, we did not find an indication of molar shape sexual dimorphism. Our investigation revealed that the appearance of the cervical line

(hourglass-shaped vs. oval) depended on the configuration of the root system (widely separated vs. close or fused roots, respectively). A high pairwise correlation of the occlusal surface (r_1=0.85 for the EDJ) and dentinal crown (r_1= 0.61 for the combined dataset) were revealed between the uM1 and lM1 shape variables. These results reflect the high morphological integration of upper and lower molars, and of their occlusal aspects in particular, which in turn can be explained by a strong genetic control during odontogenesis. Few of the discrete traits considered (the anterior transverse ridge and the anterior accessory tubercles) provided population-specific frequencies. Additionally, we replicated the results of Hunter et al. [5] on the positive correlation between the intercuspal distances and Carabelli's cusp degree of expression.

In conclusion, M1s shape and form do not make it possible to attribute an individual tooth to its own population. This also means that in any comparative analyses of hominoid molars, the choice of the modern human sample would have no influence. Our results do not support a relevant effect of gene drift or diet on molar shape.

[1] Benazzi, S., Fornai, C., Buti, L., Toussaint, M., Mallegni, F., Ricci, S., Gruppioni, G., Weber, G.W., Condemi, S., and Ronchitelli, A. (2012). Cervical and crown outline analysis of worn Neanderthal and modern human lower second deciduous molars. American Journal of Physical Anthropology 149, 537–546 DOI: 10.1002/ajpa.22155"10.1002/ajpa.22155.

[2] Weber, G.W., Fornai, C., Gopher, A., Barkai, R., Sarig, R., and Hershkovitz, I. (2016). The Qesem Cave hominin material (part 1): A morphometric analysis of the mandibular premolars and molar. Quaternary International 398, 159–174. DOI: 10.1016/j.quaint.2015.11.102.

[3] Weber, G.W., and Bookstein, F.L. (2011). Virtual anthropology: A guide to a new interdisciplinary field (New York: Springer) ISBN 978-3-211-48647-4.

[4] Turner, C.G., Nichol, C.R., and Scott, G.R. (1991). Scoring procedures for key morphological traits of the permanent dentition: The Arizona State University Dental Anthropology system. Advances in Dental Anthropology., (New York: Wiley-Liss.), pp. 13–31. ISBN: 978-0-471-56839-1.

[5] Hunter, J.P., Guatelli-Steinberg, D., Weston, T.C., Durner, R., and Betsinger, T.K. (2010). Model of Tooth Morphogenesis Predicts Carabelli Cusp Expression, Size, and Symmetry in Humans. PLoS ONE 5, e11844.

Acknowledgements:

We thank Gerlinde Gruber (Medical University of Vienna), Maria Teschler-Nicola and Eduard Winter (Natural History Museum Vienna), Department of Anatomy and Anthropology (Sackler Faculty of Medicine, Tel Aviv University) for access to materials. C. Fornai was financially

supported by the Swiss National Science Foundation grant no. 31003A 176319. We are grateful to Martin Dockner (Vienna Micro-CT Lab) for his technical support, Viktoria Krenn and Lisa Wurm for collaboration during data acquisition.

Authors:

Vanda Halász
Department of Evolutionary Anthropology, University of Vienna, Austria

Cinzia Fornai
Institute Evolutionary Medicine, University of Zurich, Switzerland
Department of Evolutionary Anthropology, University of Vienna, Austria

Gerhard Weber
Department of Evolutionary Anthropology, University of Vienna, Austria
Core Facility for Micro-Computed Tomography, University of Vienna, Austria